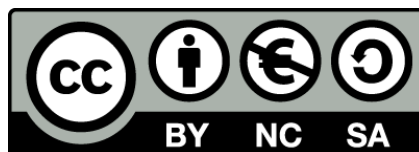




UNIVERSITAT_{DE}
BARCELONA

Microscopic analysis of rotating Black Holes

Alessandro Maccarrone Heredia



Aquesta tesi doctoral està subjecta a la llicència **Reconeixement- NoComercial – Compartirlqual 4.0. Espanya de Creative Commons.**

Esta tesis doctoral está sujeta a la licencia **Reconocimiento - NoComercial – Compartirlqual 4.0. España de Creative Commons.**

This doctoral thesis is licensed under the **Creative Commons Attribution-NonCommercial-ShareAlike 4.0. Spain License.**

Microscopic analysis of rotating Black Holes

Memòria presentada per optar al títol de doctor per

Alessandro Maccarrone Heredia

*Departament de Física Fonamental i
Institut de Ciències del Cosmos, Universitat de Barcelona,
Martí i Franquès 1, E-08028 Barcelona, Spain*

Programa de doctorat de Física Avançada de la Universitat de Barcelona
Bienni 2003-05

Dirigida i tutoritzada pel Prof. **Roberto Alejandro Emparan García de Salazar**

A zio Ilio

Contents

1	Resum de la tesi en català	1
2	Introduction	5
2.1	General relativity and black holes	5
2.1.1	The Schwarzschild metric	6
2.1.2	Charged black holes	8
2.1.3	Rotating black holes	10
2.1.4	Ergosphere and superradiance	11
2.2	Extra dimensions	12
2.2.1	Black holes in $D > 4$	12
2.2.2	Kaluza-Klein theory	14
2.3	Black holes and string theory	17
2.3.1	The D1-D5-P system	17
2.3.2	Dualities	20
2.4	Structure of the thesis	20
3	Rotating Kaluza-Klein Black Holes	22
3.1	Extremal Kaluza-Klein black holes	23
3.2	Microscopic model of rotating D0-D6 black holes	24
3.2.1	Rotating zero-temperature configurations in the $(4,0)$ -SCFT	25
3.2.2	Microscopics of D0-D6	26
3.2.3	Discussion	28
3.3	Ergospheres and Superradiance	30
3.3.1	Qualitative microscopics	30
3.3.2	4D vs 5D perspectives	31
4	Microscopic Theory of Black Hole Superradiance	33
4.1	Microphysics of cold ergoregions	34
4.1.1	Qualitative microscopic origin of the ergoregion	35

4.1.2	Microscopic derivation of the superradiant frequency bound	37
4.1.3	Four-dimensional black holes	40
4.1.4	Other systems with ergoregion	41
4.1.5	No superradiant emission of linear momentum	42
4.1.6	Superradiant amplification, extremal and non-extremal	43
4.2	Emission rates: supergravity analysis	44
4.2.1	The D1-D5-P family of black holes	45
4.2.2	Absorption cross section and emission rate	48
4.2.3	Superradiant emission rate from the ergo-cold black hole	54
4.3	Microscopic description	55
4.3.1	The dual CFT state	55
4.3.2	Emission rate and absorption cross section	56
5	Conclusions	60
A	Myers-Perry from Kaluza-Klein: General case	63
A.1	Limiting procedure	63
A.2	Relations between physical parameters	65
A.3	The two extremal limits	67
B	Ergospheres and superradiance in extremal KK-Black Holes	69
B.1	$Q \neq 0, J = 0$ extremal black hole	70
B.2	$Q = 0, J \neq 0$ extremal black hole	72
B.3	$Q \neq 0, J \neq 0$, fastly rotating extremal black hole	73
C	The near-horizon signature of superradiance	74
C.1	Near-horizon geometry	74
C.2	The Bardeen-Horowitz signature of superradiance	76

Acknowledgements

Ho pensato tante volte al momento in cui avrei scritto la pagina dei ringraziamenti della mia tesi dottorale. Sono passati ormai quasi otto anni da quando ho smesso di lavorare all'università. In tutto questo tempo ho provato diverse volte a concludere il mio lavoro, ma non è stato facile trovarne il tempo né, tanto meno, la convinzione che ce l'avrei fatta. Per fortuna, ho avuto persone intorno a me, che mi hanno sempre incoraggiato e che mi hanno aiutato a trovare delle piccole oasi di calma nel viavai quotidiano. È soprattutto grazie a loro che oggi posso cominciare a scrivere questo capitolo. Il fatto che siano passati tanti anni fa sí che questo momento s'intinga di solennità. Oltre ad essere il punto finale della mia ricerca intorno ai buchi neri con rotazione, questo è pure un punto d'inflessione vitale, un lasciare indietro una tappa che è rimasta aperta troppo a lungo. Probabilmente per questo motivo, in questo capitolo dei ringraziamenti vorrei andare oltre il riferimento stretto alla mia ricerca.

No puedo no empezar dándote las gracias a ti, Roberto. En primer lugar, por haberme dirigido la tesis. Gracias también por tu paciencia y por haber respetado mis ritmos de trabajo mucho más de lo que habría sido razonable. También por haberme respondido con un "piénsatelo" cuando hace un par de años te escribí para decirte que tiraba la toalla definitivamente. También guardo un recuerdo muy agradable de una tarde que nos pasamos intercambiando correos electrónicos mientras íbamos comprendiendo la relación entre las dos soluciones extremales de KK y sus correspondientes límites de Myers-Perry. Es uno de los momentos en que me he sentido más inmerso en el mundo de la investigación, con el que nunca he acabado de tener una relación tranquila. En un ámbito como el nuestro, tan abstracto y técnico, ha sido un placer trabajar con alguien capaz de poner siempre en primer plano la física del asunto, procurando ofrecer en todo momento una imagen intuitiva del objeto de estudio, sin perderse en excesivos formalismos.

Oscar, thanks for a fruitful collaboration and for your friendship. I remember that I was excited when Roberto told me that the guy whose papers I have been studying in order to understand superradiance, was going to be the new postdoc in our department. It was very nice to share with you a couple of meetings in Granada and Valencia.

Thanks to Tomeu Fiol, Marco Caldarelli, Alessio Celi, Josep Maria Pons, Jorge Russo, Jaume Garriga and all the people in the String Journal Club, for sharing you knowledge and for interesting discussions.

Gràcies Enric, per haver-me ensenyat Relativitat Especial i Relativitat General durant la carrera i per haver despertat el meu interès en aquest camp de la física en el qual s'emmarca aquesta tesi.

Grazie Alessandro per avermi invitato a Valencia a dare il mio primo vero e proprio seminario. Grazie pure per avermi dato delle indicazioni sull'assenza di superradianza fermionica. Purtroppo, alla fine non sono riuscito a provare a studiare questo fenomeno.

Josep, a tu també t'he de donar les gràcies. Va ser una llàstima no poder acabar la tesi

amb tu. Però has estat probablement el professor que, durant la carrera i després, més m'ha marcat. M'has ensenyat el *swing* de la física, el mateix que jo ara intento que descobreixin els meus alumnes. I també m'has fet conèixer altres meravelles com la tonyina amb cigrons, el Dim Sum o les cuques voladores de Princeton.

Gràcies als meus germans de tesi i de despatx, Pau, Majo, Joan i Guillem. Pau, recordo el dia en què parlant amb tu al despatx va sorgir la idea de relacionar la condició de superradiància amb l'energia de Fermi. Guillem, gràcies per repetir-me tantes vegades que la meva feina et semblava molt interessant. Joan, gràcies per haver-me donat tantes pistes, conscients i inconscients, sobre com rematar la tesi.

Un agraïment també a tota la gent que paga els seus impostos, gràcies als quals vaig poder gaudir d'una beca del MEC per a la Formació del Professorat Universitari. Thanks to Michael Wise for the translation of the introduction. Gràcies a l'Hotel Roca d'Alp, per haver-me ofert un espai i moltes tasses de cafè per completar els últims detalls de la tesi.

Els meus anys de carrera i de doctorat no s'entenen sense la meva participació en l'AEP i en els CJC. Per a mi han estat una escola de formació i de compromís social. M'alegra compartir encara moments i discussions amb algunes de les persones que hi vaig conèixer, l'Adri, la Neus, el Juan, el Gerard, el Julián, la Laia, l'Eulàlia, l'Antoni, l'Andreu, etc.

Gràcies Mireia per haver-me acompanyat durant l'etapa del doctorat amb les crisis i dubtes successius i per haver testimoniat els assajos de seminaris i presentacions, que per a tu havien de resultar incomprensibles.

Gràcies Laia pels moments compartits durant la carrera, per les hores d'estudi junts i pels formularis preparats de matinada a poques hores de l'examen.

El meu pas per Martí i Franquès, m'ha deixat dos regals insubstituïbles: el coneixement de la física i la colla dels "físics". Hem compartit estudis, escapades a Castelldefels, viatges a París i a Menorca, nits de Karaoke, matins a Sitges, felicitat xinesa i un llarg etcètera d'anècdotes. Gràcies als que hi sou sempre el 26 de desembre i el 4 de gener, Alberto, Jorge, Laura, Martí, Josep. També als que ara pràcticament no veig, Isaac, Vicente, Jordi. I a les "físiques adoptades", Julia, Liz, Anna, Camino, Sílvia, gràcies per la vostra paciència amb el nostre humor peculiar.

Gràcies Carles per les converses sempre estimulants, pel teu raonament tranquil, profund i escèptic, per les discussions de física a les aules d'estudi i per haver lloat sempre els meus apunts.

Gràcies Marta, per ser una de les amigues més importants que tinc. Per les reunions ímprovísades a la planta 3 per discutir de coses que poc tenien a veure amb la física, per haver-me fet descobrir una illa que ara és part de la meva identitat, per haver comptat amb mi en moments difícils i per haver-me fet sentir sempre a casa, en la teva companyia.

Gràcies als *amigos*, per compartir neguits, reflexions, il·lusions, idees i cançons, des de fa molts anys. Gràcies Dani per ser tan illenc i haver-me'n fet una mica a mi, per haver-me dit un dia que jo era com un gat, que cau sempre dret, i que per això estaves convençut que tot i les

dificultats acabaria la tesi. No saps quantes vegades m'ho he repetit durant aquests anys i com d'important ha estat perquè finalment me n'hagi sortit. Funo, crec que els dos recordem amb carinyo els nostres "becaris al Sol", que ens van ajudar a portar amb més optimisme els moments d'avorriment acadèmic. Em vaig perdre la celebració de la teva tesi, així que espero que aquest cop, puguem fer un *2 en 1*. Roger, gràcies per ser un referent de rigor i vocació intel·lectual i per compartir experiències i inquietuds de la paternitat.

Gràcies també als amics i amigues que he conegut en la meva etapa postuniversitària, que heu contribuït també al meu creixement professional i que m'heu animat a acabar la tesi. Al German, la Raquel, la Montse, el Toni i la resta de companys de Digital-Text. Gràcies al "millor de Gràcia". Gràcies a tot el professorat de Casp. Gràcies Helena, Maria Josep i Sílvia per haver confiat en mi. Maria gràcies per haver-me ajudat a realitzar-me professionalment i per la nostra admiració mútua, Àlex gràcies per ser doctor perquè això m'obligava a ser-ho jo també, Montse Vilela, gràcies per fer-me sentir útil i ensenyar-me a ser més organitzat, Albert, gràcies per mostrar-me que moltes vegades "no hi ha tema", Oriol, gràcies per la teva preocupació constant pels altres, Montse Florenciano, grazie mille per avermi aiutato con la traduzione, e grazie dei caffè, le pizze e tutte le conversazioni sulla "nostra scuola". Gràcies molt especialment a tots els nois i noies que heu passat per les meves classes i que m'heu fet gaudir i emocionar-me fent de profe.

Grazie alle maestre, professori e professoressa che ho incontrato nella Scuola Statale Italiana di Barcellona. Grazie Maria Luisa Giua, per avere posto le basi della mia formazione personale, grazie professoressa Lozzi e professor Renzetti per avermi fatto interessare alla fisica e alla matematica. Grazie professoressa Aversa, per essere stata il mio più importante punto di riferimento intellettuale. Grazie professor Bertini per averci trattati sempre da alunni maturi e per averci proposto attività sconcertanti. Grazie Giampiero per essere stato il mio primo amico-professore.

Grazie Luca per essere il mio più caro amico, per "I Ragazzi della via Paal", la banda, l'Adagio d'Albinoni, "Los Vacíos", la musica, da De Andrè a Loquillo, per essere stato il primo compagno di casa insieme a Gabriele (grazie anche a lui) e per essere diventato lo "zio Luca" insieme a Laia. Sei stato e sei un grandissimo punto di riferimento e il testimone degli episodi più importanti di tutti questi anni.

Grazie Simone per essere anche tu il mio più caro amico, nonostante la distanza, il tempo e il calcio. Grazie per avermi insegnato lo stoicismo e per aver voluto sempre e soltanto che io stessi bene, anche se "non parlo mai con te". E grazie soprattutto per non aver voluto presentare la tua tesi prima che io presentassi la mia.

A tutta la mia famiglia di Roma, di Barcellona e di Badalona, grazie, gracias, gràcies.

Gràcies Mercè per haver-me ajudat a tenir temps i tranquil·litat per acabar aquesta feina, per la teva força quasi inescotable. Gràcies Anton pel mateix i per haver-me demostrat que es pot fer front a les pitjors dificultats sense perdre el somriure. M'alegro molt d'haver tingut la sort de conèixer-te.

Grazie Vincenzo e Tiziana per avermi trattato come un amico da molto giovane, per avere ispirato molte mie idee e per essere stati un punto di riferimento, soprattutto nella mia adolescenza.

Grazie zia Pupa, per le estati a Lavinio, insieme ai nonni, per avermi fatto amare i libri e la lettura, per "Il Signore degli Anelli" che alla fine non ho mai letto e per avermi regalato "L'Antologia di Spoon River" nella primavera del 1994.

Grazie Stefano per ricordarmi quant'è importante che il tuo lavoro ti renda felice e per avermi perdonato quell'iscrizione a Statistica. Grazie Daniela per essere sorella, zia, compagna ed amica, per avermi fatto imparare la logica formale in un giorno e per aver avuto fiducia in me nei momenti difficili. Gràcies Gerard per haver esdevingut de seguida de la família.

Mamá, gracias por haberme regalado horas para poderme dedicar a rematar la faena, por haberle enviado a todo el mundo un mensaje al saber que acabaría la tesis y por haberme enseñado a ser autónomo y a responsabilizarme de mis asuntos desde muy pequeño. Grazie papà per avermi regalato la colonna sonora di tutta una vita, per tutti i riferimenti culturali italiani e per la tua fiducia in me. A entrambi, grazie per avermi consentito di crescere fra l'amore e la sicurezza, entrambi fondamentali per avere tanti interessi e tanta sete di conoscenza.

Annucia, gràcies per moltíssimes coses, per les dues estrelles que hem portat a aquest món, per les converses de Skype, per *Anna e Marco*, per la Font del gat, per Sitges. Gràcies per haver-me regalat hores i hores per poder acabar aquesta tesi, per contagiarme una mica del teu esperit lluitador i tenaç, però, sobretot, gràcies per no deixar-me "perdre el temps" amb migdiades, per poder-lo dedicar a coses més importants.

Gian e Martina grazie semplicemente di esistere e di dare un senso alla mia vita. Se sono riuscito a finire questa tesi è soprattutto perché voglio che vi sentiate orgogliosi di vostro papà.

Dulcis in fundo, grazie zio Ilio. Tu mi hai insegnato i primi concetti di fisica, protoni, elettroni e neutroni, mi hai fatto riflettere sulla fisica quantistica e la realtà oggettiva, ma, soprattutto mi hai contagiato la tua passione per la fisica. E non solo. Mi hai fatto amare anche il latino e la Divina Commedia. Sei stato una colonna essenziale della mia maturazione intellettuale e lo hai fatto sempre mosso dal tuo amore di zio e di padrino. Ci rivedremo in Paradiso.

*Supereró le correnti gravitazionali
lo spazio e la luce per non farti invecchiare*
Franco Battiato

Chapter 1

Resum de la tesi en català

Aquesta tesi s'emmarca en l'estudi de la gravetat, que, de les quatre interaccions fonamentals és probablement la més evident en la nostra vida quotidiana. La relativitat general d'Einstein situa l'origen i l'efecte del camp gravitatori en la pròpia estructura de l'espai-temps. Les seves equacions relacionen un cert tensor construït a partir de la mètrica de l'espai-temps amb el contingut d'energia de la regió sota estudi. Aquesta teoria ofereix una descripció molt satisfactòria de gran part dels fenòmens clàssics coneguts. En canvi, no és possible construir una versió quàntica de la relativitat general que sigui renormalitzable, és a dir que sigui finita a qualsevol ordre de pertorbació.

Una de les solucions més característiques de les equacions d'Einstein són els forats negres: objectes on la gravetat és tan intensa que fins i tot la llum queda atrapada dins del que s'anomena *horitzó d'esdeveniments*. Un forat negre és el que Fermi hauria anomenat "l'àtom d'hidrogen" de la Relativitat General, és a dir, un sistema prou senzill per estudiar-lo analíticament, però prou complex per reflectir el caràcter no lineal de la teoria.

Un forat negre pot correspondre a l'estat final de l'evolució d'una estrella molt massiva. Segons la relativitat general, un cop format, es manté igual per sempre, o, com a molt, segueix augmentant la seva massa com a conseqüència de l'acreció de matèria externa. Tanmateix, la cosa canvia si es considera una teoria semiclàssica en què es quaten camps en un espai-temps corbat clàssic. En aquest cas, un forat negre emet radiació tèrmica (radiació de Hawking) i la seva massa disminueix. Per tant, si els forats negres són objectes tèrmics, és possible assignar-los una temperatura (temperatura de Hawking) i una entropia (entropia de Bekenstein-Hawking).

En general, l'entropia d'un sistema es pot interpretar estadísticament com una mesura del nombre de microestats compatibles amb un estat macroscòpic. Per tant, una de les qüestions que hauria de resoldre una teoria quàntica de la gravetat és l'origen microscòpic de l'entropia de forats negres. Això s'ha aconseguit, per a determinades solucions, en el marc de la teoria de cordes.

En efecte, en el límit de baixes energies d'aquesta teoria, es recuperen les equacions de supergravetat, generalització de la Relativitat General, que inclou també altres tipus de camps. Això fa pensar que la teoria de cordes pot oferir una descripció quàntica satisfactòria de la gravetat.

Aquesta és una de les motivacions per estudiar forats negres en $D > 4$, atès que la teoria de cordes requereix la introducció de dimensions addicionals per a la seva consistència.

Determinades solucions de forat negre es poden relacionar amb estats pertorbatius de la teoria de cordes. Normalment es tracta de forats negres carregats, per als quals és possible identificar els estats de cordes corresponents. Aquests estats inclouen Dp -branes, objectes p -dimensionals on se situen els extrems de les cordes obertes i que actuen com a font de les càrregues. Un cop identificada la configuració de cordes, es poden comptar els estats microscòpics compatibles amb les càrregues del forat negre i avaluar-ne així l'entropia.

Cal tenir present, que aquesta correspondència relaciona estats amb acoblament fort (forats negres) i estats amb acoblament feble (estats pertorbatius de cordes). En principi, no hi ha cap garantia que el nombre d'estats i altres magnituds físiques es mantinguin constants en passar d'un règim a l'altre. Existeixen però determinades solucions amb un alt grau de simetria, per a les quals l'entropia no es renormalitza en passar d'acoblament feble a acoblament fort. Això passa, per exemple, en els forats negres supersimètrics (BPS). En aquests casos, és possible reproduir microscòpicament l'entropia de Bekenstein-Hawking.

Una de les limitacions del procediment anterior és que els forats negres realistes no tenen càrrega. Aquest fet dificulta identificar els estats de cordes corresponents. Tanmateix, hi ha casos com la solució extremal de Kerr en què l'entropia té una forma molt simple, que no depèn de la constant d'acoblament, $S = 2\pi J$. Això fa pensar que ha de ser possible reproduir-la exactament mitjançant un comptatge d'estats microscòpics.

Un dels reptes actuals és, per tant, reproduir microscòpicament l'entropia de forats negres neutres. El capítol 3 de la tesi se situa precisament en aquesta línia de recerca. En ell, considerem forats negres de Kaluza-Klein (KK). Des del punt de vista 4-dimensional, aquestes solucions tenen càrrega elèctrica i magnètica, però, en canvi, són neutres quan es *puja* a 5 dimensions.

Els forats negres de KK, es poden interpretar com a estats lligats de $D0$ i $D6$ branes, de la teoria de cordes tipus IIA. A través d'una sèrie de dualitats no trivials podem *mapejar* aquests estats a un sistema de 4 càrregues, on se sap com comptar el nombre de microestats. Aquest procediment ja s'havia utilitzat prèviament per a un dels límits extrems dels forats negres de KK, el de rotació lenta. Nosaltres, estenem aquesta anàlisi a la solució extremal amb rotació ràpida. Cal remarcar que aquest forat negre té una velocitat angular de l'horitzó diferent de zero i, per tant, s'assembla més a la solució extremal de Kerr, que el de rotació lenta. Amb el nostre estudi, aconseguim reproduir l'entropia de Bekenstein-Hawking, però no la massa, atès que aquesta queda renormalitzada en passar d'acoblament feble a acoblament fort.

Si en el forat negre de KK fem tendir el radi de la dimensió compacta a infinit (límit de descompactificació), recuperem la solució de Myers i Perry (MP), generalització del forat negre de Kerr en $D > 5$. Aquest límit ja s'havia obtingut prèviament per al cas extremal amb rotació lenta, però nosaltres mostrem com realitzar-lo en el cas general. D'aquesta manera, comprovem

que el càlcul microscòpic reproduïx també l'entropia d'un forat negre de MP extremal qualsevol.

Quan treballem amb forats negres amb rotació, apareixen nous fenòmens, que ens poden ajudar a entendre millor la teoria microscòpica. Aquest és el cas de la superradiància. En solucions en què l'horitzó té una certa velocitat angular, Ω_H , com ara en la de Kerr, el vector de killing temporal pot esdevenir tipus espai en una certa regió que s'estén fora de l'horitzó. La superfície que tanca aquesta regió rep el nom d'*ergosfera*. Es pot demostrar que en aquest cas, una ona que impacti amb el forat negre pot sortir reflectida amb una energia superior a la inicial. Això només passa per a modes amb moment angular, m , diferent de 0 i l'energia dels quals satisfaci la fita $\omega < m\Omega_H$. Aquest mecanisme permet extreure simultàniament energia i moment angular d'un forat negre.

La superradiància és un procés clàssic d'emissió estimulada, que, com hem vist, només es pot produir en forats negres en què l'horitzó té una certa velocitat angular. Té associat un procés anàleg d'emissió espontània, de caràcter quàntic, molt semblant a la radiació de Hawking. De fet, en el cas general d'un forat negre rotant, l'emissió tèrmica i la superradiant són simplement dos aspectes d'un mateix fenomen. En canvi, en forats negres extremals, amb $T = 0$, no hi ha efectes tèrmics i l'única emissió possible és la superradiància. Aquest és el fet que motiva el nostre interès per l'estudi microscòpic de forats negres extremals amb rotació, atès que poden ajudar a entendre millor el fenomen de la superradiància i la naturalesa de l'ergosfera.

En els forats negres de KK tenim dos casos extremals amb moment angular: el de rotació lenta i el de rotació ràpida. Només en el segon cas, l'horitzó té una certa velocitat angular i, per tant, apareix el fenomen de la superradiància. La comparació dels estats microscòpics corresponents a aquestes dues solucions ens permet explicar-ne la diferència de comportament.

Com hem dit abans, aquests forats negres corresponen microscòpicament a estats lligats de D0 i D6 branes, que es poden relacionar mitjançant dualitats amb un sistema de 4 càrregues. Aquest sistema es pot descriure amb una teoria de camps conforme supersimètrica (4,0)-SCFT, amb dos sectors de quiralitat, dels quals només un és supersimètric. La radiació de Hawking es pot entendre com l'emissió d'una corda tancada després de la col·lisió de dues excitacions amb quiralitat oposada.

Podem utilitzar aquesta mateixa imatge per entendre la diferència qualitativa dels dos forats negres extremals. En el cas de rotació lenta, només tenim excitacions en un dels dos sectors i, per tant, no hi ha cap tipus d'emissió. En canvi, en el cas de rotació ràpida sí tenim els dos sectors excitats i això explica la presència de superradiància. En aquest cas, el sector supersimètric consta només d'excitacions fermiòniques que omplen un mar de Fermi. Això és el que provoca que la temperatura global del sistema sigui nul·la. A més, aquestes excitacions són portadores d'una càrrega de tipus SU(2), anomenada càrrega R . Això és el que proporciona el moment angular al forat negre i el que explica el fet que la radiació emesa tingui necessàriament un cert moment angular.

En el capítol 4 estudiem amb detall aquesta descripció microscòpica del fenomen de la superradiància. Per fer-ho, resulta més convenient considerar els forats negres 5-dimensionals amb 3 càrregues D1-D5-P, amb moment angular. Aquests forats negres es poden descriure de forma directe en termes d'una teoria de camps sobre una corda efectiva, sense necessitat d'aplicar cap dualitat. A més, com hem dit abans, la superradiància només es produeix per a modes amb una energia inferior a un cert valor. De cara a reproduir microscòpicament aquesta fita, és, doncs, important que les energies no quedin renormalitzades en passar d'acoblament feble a acoblament fort, com passava amb el sistema D0D6 extremal de rotació ràpida. En canvi, això no passa en el sistema D1D5P, que té una geometria a prop de l'horitzó de tipus AdS₃ (BTZ). La simetria conforme d'aquesta geometria garanteix que les energies no es renormalitzin.

De nou, prenem en consideració dos tipus de solucions extremals amb moment angular: la solució supersimètrica (BPS), que no presenta ergosfera i la solució extremal no supersimètrica amb horitzó rotant, que sí en presenta. Ens referim a aquesta solució com a *ergo-cold*.

La dinàmica dels estats lligats de D1 i D5-branes es pot descriure amb una teoria de camps conforme 1+1-dimensional al llarg de la seva direcció comuna. Aquesta teoria no és quiral, de manera que conté dos sectors supersimètrics.

La solució BPS correspon a excitar només un d'aquests dos sectors. Les excitacions fermiòniques són les que, una vegada més, proporcionen el moment angular. En no tenir els dos sectors poblats, aquest forat negre no presenta cap mena d'emissió espontània. En canvi, la solució *ergo-cold* sí que té els dos sectors excitats, però un d'ells només conté excitacions fermiòniques que omplen un mar de Fermi. Per això, el forat negre corresponent sí presenta una ergosfera i pot emetre radiació superradiant.

La situació és anàloga a la dels dos límits extremals del sistema D0D6. En aquest cas però, es pot realitzar un estudi més quantitatiu, que permet interpretar el fenomen de la superradiància com una conseqüència de l'estadística de Fermi-Dirac. La fita superior de l'energia de les emissions superradiants està relacionada amb el fet que les excitacions fermiòniques d'un dels sectors es troben totes per sota del nivell de Fermi.

Després d'oferir una imatge senzilla i intuïtiva d'aquesta interpretació de la superradiància, computem els ritmes d'emissió des de la solució de supergravetat corresponent al forat negre i des de la teoria de camps conforme que descriu el règim pertorbatiu de teoria de cordes i en discutim la concordància.

El treball contingut en aquesta tesi ha donat lloc a dues publicacions [1, 2].

Chapter 2

Introduction

2.1 General relativity and black holes

Of the four fundamental interactions, gravity is without doubt the most evident in our everyday lives. It is responsible for phenomena as apparently diverse as the weight of physical objects and the tides on Earth or the movement of celestial bodies in space.

Even though it is the weakest of the four interactions, it is the dominant force on the largest scale, due to the fact that, macroscopically speaking, matter is neutral with respect to the other three forces, whereas Everything that has mass or energy experiences or generates gravity.

In secondary education, when students first study physics, they learn that all bodies fall with the same acceleration. This property is explained by the fact that the magnitude that measures the resistance of an object to being accelerated (inertial mass) and that which measures the gravitational *charge* (gravitational mass) coincide:

$$G \frac{mM}{r^2} = ma \quad \rightarrow \quad a = G \frac{M}{r^2}. \quad (2.1.1)$$

The same idea forms the basis of Einstein's equivalence principle, which can be stated in the following way: [3,4] *The movement of a body subjected to a gravitational field is physically indistinguishable to that of an accelerated body in flat spacetime.*

This universal characteristic is what urged Einstein to transfer the properties of the gravitational field to the structure of spacetime.

His theory of general relativity can be summarised in the following way:

1. Mass and energy are the characteristics of the physical system that allow gravity to be generated and felt. That is to say, they are the gravitational *charge*
2. Gravity is a manifestation of the curvature of spacetime. Its structure *tells* matter how to move

3. The geometry of spacetime is not static. Mass and energy cause changes in its structure, according to Einstein's equations:

$$G_{\mu\nu} = \frac{8\pi G}{c^4} T_{\mu\nu}, \quad (2.1.2)$$

where $G_{\mu\nu}$ is Einstein's tensor, which depends on the geometry of the spacetime and $T_{\mu\nu}$ is the stress-energy tensor.

There is an important nuance to take into account. Not only matter and radiation have energy. The curvature of spacetime also has energy, so that in a certain way it affects itself. This is the root of the strongly non-linear character of Einstein's equations, which manifests itself, for example, in the solutions of black holes.

There is a third aspect to gravity, which makes it especially interesting to study: its *capricious* nature. The appearance of special relativity meant that everything that was known about physics up to that point needed to be revised, in order to adapt it to the new theory. Electromagnetism, formalized as Maxwell's equations, was already compatible. In fact, it was inconsistencies between these equations and Newtonian mechanics that motivated Einstein's work. It was the theory of gravity that needed to be rethought and it was this that gave birth to general relativity.

The other revolution in physics in the 20th century was quantum mechanics. This also transformed the way in which known physical phenomena were interpreted. At the moment, electromagnetism, the weak interaction and the strong interaction all have a very satisfactory quantum description within the framework of the Standard Model. However, we do not yet have a complete quantum description of gravity. The quantum version of Einstein's equations gives rise to a non-renormalizable theory, which, therefore, is uncontrollable at high energies. As we shall see later, string theory is one attempt to respond to this challenge.

Due to these reasons, this line of research promises to provide us with a better understanding of how our universe works.

2.1.1 The Schwarzschild metric

Einstein's equations provide us with a metric to describe the development of the universe on the largest scale. They also predict the existence of gravitational waves, which have not yet been detected. But some of the most evocative solutions obtained, not only for physicists, but also for art, literature and cinema, are those which give rise to black holes. Black holes are what Fermi would call *the hydrogen atom of general relativity*, that is to say, a problem sufficiently simple to deal with analytically, but sufficiently complex to show the non-linear character of the theory.

Beyond the images of science fiction, a black hole is an object of gravitational attraction so intense that not even light can escape from it. In fact, even Newtonian physics can predict the existence of something similar. From the law of universal gravitation, we can calculate the *escape*

velocity:

$$v_e = \sqrt{\frac{2GM}{r}}, \quad (2.1.3)$$

where M is the mass of the object and r is its radius.

This magnitude indicates with which minimum velocity we would have to launch a body from the surface of that object so that it would be able to reach infinity, that is to say, so that it could free itself of the gravitational field. If the object has a very large mass concentrated in a very small radius, the escape velocity may be greater than the velocity of light. In this case, an observer far from the object would not even be able to see it and we could say that we are dealing with a kind of black hole, or more specifically, a *black star*. For this to happen, the radius must be lower than a certain minimum value, which depends on the mass:

$$R_S = \frac{2GM}{c^2}. \quad (2.1.4)$$

This radius goes by the name of the Schwarzschild radius and, as we shall see, it appears in the context of the solution of Einstein's equations that has the same name. However, black holes which appear within the framework of general relativity have more exotic properties than these *black stars*, as we shall see below.

Shortly after Einstein published his definitive formulation of general relativity, the German physicist Karl Schwarzschild published the first exact vacuum solution to his equations ($T_{\mu\nu} = 0$) [5]:

$$ds^2 = - \left(1 - \frac{2M}{r}\right) dt^2 + \left(1 - \frac{2M}{r}\right)^{-1} dr^2 + r^2 d\Omega^2, \quad (2.1.5)$$

where natural units have been used with $G = c = 1$ and M represents the total mass of the system in these units.

Here we are dealing with a static solution with spherical symmetry, which serves to describe the exterior of a star with these same properties. As can be seen, the metric diverges when $r = 2M$ and when $r = 0$.

In general relativity, when a metric diverges it can be for two different reasons. The first is when some invariant (scalar) built upon Riemann's tensor, such as Ricci's scalar or Riemann's tensor squared, also diverges. In this case, we are dealing with a singularity of *curvature*, which needs new physics to be understood. If the curvature is finite, then the singularity of the metric is a product of an inappropriate choice of coordinates, which can be resolved by changing to another system. In the case of Schwarzschild's solution, the curvature only diverges at $r = 0$.

As such, we can choose a coordinate system so that the metric does not diverge at $r = 2M$. In doing so, another fact is observed [6]: in the region $r < 2M$, photons that should move radially outward, actually move to decreasing values of r . This indicates that even light remains trapped inside the surface $r = 2M$, which goes by the name of the *event horizon*. This is what allows us to interpret Schwarzschild's solution as a black hole.

Actually, in ordinary stars, the horizon would be located within their interior, where this metric is not valid as this region is not a vacuum. However, during collapse, very massive stars can reduce their radius to a value which is practically zero. There is therefore a moment when all of the matter becomes concentrated within the horizon and we can say that a black hole has formed.

If we return to SI units, we can see that the radius of the horizon is $r = 2GM/c^2$, that is the Schwarzschild radius that we have already found in the classical context (2.1.4). The interpretation now is considerably different. In the Newtonian case, we had objects which were incapable of escaping to infinity. In the context of general relativity light cannot even cross the horizon, and so there is no longer a causal relationship between the interior and the exterior. What happens inside cannot influence what happens outside.

The star will continue collapsing until it is completely concentrated at the centre of the hole, $r = 0$, where, as we have said, Schwarzschild's solution diverges. This is a sign that a new theory is needed to understand what is really happening in this singularity. In the context of general relativity, from now on, the black hole will remain the same forever, at least not decreasing in size, and possibly growing due to accretion of external matter.

Things change when we take into account quantum effects. Previously we said that general relativity cannot be quantized in a consistent way in all energy ranges, but quantum theories can be studied in a classical gravitational environment. Stephen Hawking discovered [7] that when quantum effects are taken into account near a black hole, certain phenomena appear which are prohibited from a classical point of view. In particular, black holes emit black-body radiation. This behaviour allows us to associate a temperature to them

$$T = \frac{\hbar\kappa}{2\pi}, \quad (2.1.6)$$

where, κ is a property of the event horizon, known as *surface gravity*.

Likewise, Jacob D. Bekenstein argued [8] that a black hole can also be assigned an entropy, which depends on the area of the horizon $A_H = 4\pi R_s^2$

$$S = \frac{A_H}{4G\hbar}. \quad (2.1.7)$$

It can be shown [9] that with these properties, black holes are consistent with the zeroth law, the first law and the second law of thermodynamics.

However, if we assign an entropy to black holes, we need to be able to interpret this in terms of the degeneration of microstates. This is one of the problems that a quantum description of gravity needs to face.

2.1.2 Charged black holes

A black hole can have an electric or magnetic charge. If so, it couples both to the gravitational field and to the electromagnetic field. In this case, we have to consider the following Einstein-Maxwell

equations that describe an electromagnetic field in curved space:

$$G_{\mu\nu} = 8\pi \left(F_{\mu\rho} F_{\nu}{}^{\rho} - \frac{1}{4} g_{\mu\nu} F^2 \right), \quad (2.1.8)$$

$$\partial_{\mu} (\sqrt{-g} F^{\mu\nu}) = 0. \quad (2.1.9)$$

The term on the right in the first set of equations is the energy-momentum tensor of the electromagnetic field. The second set consists of Maxwell's equations in curved spacetime.

The static black hole solution corresponding to these equations was found by Reissner and Nordström [10] and has the following form:

$$ds^2 = - \left(1 - \frac{2M}{r} + \frac{Q^2}{r^2} \right) dt^2 + \left(1 - \frac{2M}{r} + \frac{Q^2}{r^2} \right)^{-1} dr^2 + r^2 d\Omega^2, \quad (2.1.10)$$

where M is still the mass and the parameter Q is the charge. The components of the tensor $F_{\mu\nu}$ that do not vanish depend on whether the charge is electric or magnetic.

For weak fields, we have

$$-g_{tt} \simeq 1 + 2\Phi_N, \quad (2.1.11)$$

where Φ_N is the Newtonian potential. We can then see that the electromagnetic field produces a gravitational repulsion, as shown by the term $+Q^2/r^2$. This is not an effect of the electromagnetic interaction, since it forms part of the metric, and, hence, also acts on neutral particles.

Again, the curvature diverges only at $r = 0$, which corresponds to a singularity. As we are dealing with a static metric, in order to detect the presence of horizons, we can search for the zeros of g_{tt}

$$g_{tt} = 0 \quad \Rightarrow \quad r = r_{\pm} = M \pm \sqrt{M^2 - Q^2}. \quad (2.1.12)$$

Depending on the relationship between the parameters M and Q , we can distinguish three cases:

- $M < |Q|$: There is no horizon and $r = 0$ is a naked singularity.
- $M > |Q|$: There are two horizons: the inner horizon at $r = r_-$ and the outer horizon at $r = r_+$.
- $M = |Q|$: This is the extreme limit of the previous case. It represents the maximum charge that a black hole of mass M can have. In this case, $r_+ = r_-$ and so the spacetime has only one degenerate horizon. The metric can be written in the following way:

$$ds^2 = - \left(1 - \frac{Q}{r} \right)^2 dt^2 + \left(1 - \frac{Q}{r} \right)^{-2} dr^2 + r^2 d\Omega^2. \quad (2.1.13)$$

All points with $r > r_+$ are at an infinite proper distance from the external event horizon. However, timelike trajectories may reach this horizon in a finite time and null trajectories in a finite affine parameter.

It is convenient to change coordinates: $\rho = r - Q$, so that the solution (2.1.13) becomes:

$$ds^2 = -\frac{1}{H^2}dt^2 + H^2(d\rho^2 + \rho^2 d\Omega), \quad (2.1.14)$$

where

$$H = 1 + \frac{Q}{\rho}. \quad (2.1.15)$$

With these new coordinates, the horizon is found at $\rho = 0$ which is not a point since it corresponds to the sphere $r = Q$ with the singularity found at $\rho = -Q$. The spacetime described by this solution is asymptotically flat. It can be shown that the near-horizon metric is:

$$ds^2 = Q^2 \left[-\tilde{\rho}^2 d\tilde{t}^2 + \frac{d\tilde{\rho}^2}{\tilde{\rho}^2} + d\Omega^2 \right], \quad (2.1.16)$$

where $t = \tilde{Q}^2/\epsilon$, $\rho = \epsilon\tilde{\rho}$ and $\epsilon \rightarrow 0$.

As we can see, this geometry is the product of a 2-sphere, S^2 , and bi-dimensional space of negative constant curvature AdS_2 .

2.1.3 Rotating black holes

Macroscopic black holes that we can find in our universe must rotate. The generalization of the Schwarzschild solution, with non-vanishing angular momentum, is Kerr's solution [11]:

$$ds^2 = -\left(1 - \frac{2Mr}{\Sigma}\right) dt^2 - \frac{4Mar \sin^2 \theta}{\Sigma} dt d\phi + \frac{\Sigma}{\Delta} dr^2 + \Sigma d\theta^2 + \left[\frac{(r^2 + a^2)^2 - \Delta a^2 \sin^2 \theta}{\Sigma} \right] \sin^2 \theta d\phi^2, \quad (2.1.17)$$

where

$$\Sigma = r^2 + a^2 \cos^2 \theta, \quad \Delta = r^2 - 2Mr + a^2. \quad (2.1.18)$$

M is the mass, while the parameter a is related to the angular momentum $J = Ma$. In the case of $a = 0$, we recover Schwarzschild's solution.

One important difference between this solution and the previous solutions is that crossed terms are present, $g_{t\phi} \neq 0$. This reflects the fact that this is a rotating spacetime and means that a local observer at rest will have a certain angular velocity from the point of view of an observer situated at infinity.

The components of the metric diverge when $\Sigma = 0$ or when $\Delta = 0$. Only in the first case, do we have a curvature singularity, which can be found at $r = 0$ and $\theta = 0$. An appropriate choice of coordinates shows that this singularity has the form of a ring.

Analogous to the Reissner-Nordström case, $\Delta = 0$ is a singularity associated with choice of coordinates. The function Δ vanishes when $r = r_{\pm} = M \pm \sqrt{M^2 - a^2}$. Again, we can distinguish three cases:

- $M < |a|$: There are no horizons, the ring singularity is null and there are closed timelike curves at all points in space.
- $M < |a|$: There is an inner horizon at r_- and an outer horizon at r_+ , which hides the singularity in its interior.
- $M = |a|$: The angular momentum is $J = M^2$, which is the maximum that a black hole of mass M can have. The two horizons coincide at $r = M$.

2.1.4 Ergosphere and superradiance

The Kerr solution with $M \geq a$, shows a new feature *outside* the black hole. The vector $\partial/\partial t$ becomes spacelike when $r^2 - 2Mr + a^2 \cos^2 \theta < 0$. This region is outside of the external horizon and is enclosed by a surface known as *ergosphere*. In this region, all observers are dragged by the rotation of spacetime, not only those that are locally at rest.

The Killing vector that becomes null over the external horizon is:

$$\chi^\mu = (\partial/\partial t)^\mu + \Omega_H (\partial/\partial \phi)^\mu, \quad (2.1.19)$$

where $\Omega_H = a/2Mr_+$ is the angular velocity of the horizon.

Penrose showed [12] that energy can be extracted from a rotating black hole, due to the presence of the ergosphere. Qualitatively the idea is as follows. Suppose that a particle found inside the ergosphere has a certain energy E . If it decays into two particles, the energy will be conserved $E = E^{(1)} + E^{(2)}$. Suppose as well that one of these particles falls towards the black hole and crosses the horizon and the other moves off towards infinity. Since the Killing vector $\partial/\partial t$ becomes spacelike inside the ergosphere, in this region there are geodesics with negative energy. If the particle that crosses the horizon has negative energy, the particle that moves outwards must have a higher energy than the original particle: $E^{(2)} > E$. The extra energy must be extracted from the black hole, so that its mass and angular momentum are reduced.

The same process takes place in the case of field scattering [13, 14]. We can consider, for example, a scalar field. Due to the symmetries of the Kerr metric, this field will have the form $\phi = f(r, \theta) e^{-i\omega t} e^{im\phi}$. Let us consider the conserved current

$$J_\mu = i(\phi^* \nabla_\mu \phi - \phi \nabla_\mu \phi^*). \quad (2.1.20)$$

Its flux through the horizon is

$$J_\mu \chi^\mu = (\omega - m\Omega_H) |\phi|^2, \quad (2.1.21)$$

where χ^μ is the Killing vector tangential to the horizon, defined in (2.1.19). This flux is negative for modes that satisfy

$$\omega < m\Omega_H. \quad (2.1.22)$$

Therefore all these modes are reflected with a greater energy than the incident energy and so have extracted energy from the black hole. This phenomenon goes by the name of *superradiance*. It is worth noting that, unlike Hawking radiation, this process is completely classical and only requires that the horizon of the black hole has a certain angular velocity.

2.2 Extra dimensions

There are several reasons for studying general relativity and its black holes in more than four dimensions. The first has to do with the fact that general relativity appears as a low energy limit when studying string theory and this theory requires the introduction of additional dimensions in order to be consistent.

A second reason is that gravitational models predict extra dimensions on the TeV scale and this may open the possibility of detecting small black holes in future particle accelerators. These black holes would occupy more than four dimensions. However, at the moment, results from the LHC would appear to discard this possibility.

There is a third more ambitious reason. General relativity may have applications beyond astrophysics or cosmology. It can be considered a widely applicable theoretical tool, such as quantum field theory. Indeed, there are some strongly coupled non-gravitational systems, which allow a semiclassical description with diffeomorphism invariance, and which can be studied with the aid of general relativity or its generalisations. We are talking of the whole spectrum of correspondences of the type AdS/CFT according to which certain gravitational objects can be related through dualities to excitations of a conformal field theory that *lives* at the spacetime boundary. In this context black holes with more than four dimensions often appear.

2.2.1 Black holes in $D > 4$

The generalisation of Schwarzschild's solution in greater dimensions, known as the Schwarzschild-Tangherlini solution, is easy to obtain [15]. Only decay rate of the components of the metric needs to be modified:

$$ds^2 = - \left(1 - \frac{\mu}{r^n} \right) dt^2 + \frac{dr^2}{1 - \frac{\mu}{r^n}} + r^2 d\Omega_{n+1}, \quad (2.2.23)$$

where $n = D - 3$ and $d\Omega_{n+1}$ is the differential of the solid angle in $n + 1$ dimensions. The parameter μ is proportional to the mass and determines the solution in a unique way. This black hole has a horizon at $r = r_0 \equiv \mu^{1/n}$, which has the topology of an $(n + 1)$ -sphere. This means that qualitatively there is little new with respect to the case of $D = 4$.

When we consider rotating black holes, things change significantly. In 1986 Myers and Perry [16] found a generalisation of the Kerr metric which describes rotating black holes in any dimension

$D > 4$. The explicit form of this solution for $D = 5$ is:

$$ds^2 = -dt^2 + \frac{\mu}{\Sigma} (dt - a \sin^2 \theta d\psi - b \cos^2 \theta d\phi)^2 + \Sigma \left(\frac{d\rho^2}{\Delta} + d\theta^2 \right) + (\rho^2 + a^2) \sin^2 \theta d\psi^2 + (\rho^2 + b^2) \cos^2 \theta d\phi^2, \quad (2.2.24)$$

with

$$\Sigma = \rho^2 + a^2 \cos^2 \theta + b^2 \sin^2 \theta \quad (2.2.25)$$

$$\Delta = \frac{(\rho^2 + a^2)(\rho^2 + b^2) - \mu\rho^2}{\rho^2}. \quad (2.2.26)$$

The parameter μ is again related to the mass and a and b to the angular momenta J_1 and J_2 . As we can see, in this case, the black hole can rotate in two independent planes. In general, the Myers and Perry solution takes into account the fact that in D dimensions rotations in $[\frac{D-1}{2}]$ different planes can be produced. The horizon of these black holes also takes the shape of a sphere.

Surprisingly, there are many other black holes in $D \geq 5$ that are vacuum (neutral) solutions to Einstein's equations. In 2001, Emparan and Reall found a solution for a black ring in five dimensions [17], the first example of a non-spherical asymptotically flat black hole, since in this case, the topology is $S^2 \times S^1$.

The appearance of this new solution also demonstrated that the *no hair* theorem is not verified in greater dimensions. In four dimensions, once the mass M and the angular momentum J have been specified there is only one compatible vacuum asymptotically flat black hole which is the Kerr black hole. However, in five dimensions, for a certain range of parameters, there are two different black rings and a Myers and Perry black hole with the same values of M and J . Later, many other five-dimensional solutions appeared (black saturns, black rings with two independent rotations, etc.) [18]

In $D \geq 6$, the number of topologies of black holes is expected to increase. Even though there are not yet analytical solutions that describe these objects, there does exist a formalism for constructing them in an approximate way known as *blackfold* approach. [19]

In $D > 4$ *black objects* with non-compact topologies can also be constructed. We only need to take into account that the direct product of two Ricci flat metrics is Ricci flat too. We can, therefore, construct solutions adding an arbitrary number of plane dimensions to Schwarzschild's solution:

$$ds_{(D)}^2 = ds^2(\text{Schw}_{(D-p)}) + d\mathbf{x}_{(p)}^2. \quad (2.2.27)$$

This solution is called a neutral black p -brane and the topology of its horizon is:

$$S^{D-p-2} \times \mathbb{R}^p. \quad (2.2.28)$$

For instance, in five dimensions, we can construct a black string, adding a plane dimension to a Schwarzschild four-dimensional black hole.

$$ds_{(5)}^2 = ds^2(\text{Schw}_{(4)}) + dy^2. \quad (2.2.29)$$

Often, for example in the context of string theory, extra dimensions are considered to be compact. In the previous example this is equivalent to identifying $y \sim y + 2\pi R$. Then the topology of the horizon becomes $S^2 \times S^1$. The difference with respect to the solution for a black ring is that in that case, we would have a horizon with exactly the same topology, but located in a five dimensional asymptotically flat spacetime, whereas we now have a black string wrapping one of the dimensions, which is compact.

2.2.2 Kaluza-Klein theory

Another reason for introducing additional dimensions is to try to describe different types of interactions in a unified manner. Let us consider for example a $D = 5$ spacetime where one of the dimensions, y , is rolled into a circle of radius r_5 , that is, a space time with a topology asymptotically $\mathbb{R}^4 \times S^1$. This is what is known as Kaluza-Klein theory. [20]

If the metric does not depend on the coordinate y , it can be interpreted as a four-dimensional spacetime, coupled to an electromagnetic field and a scalar field. To look at it in detail, we start with a five-dimensional metric of the form:

$$ds^2 = e^{-4\phi/\sqrt{3}}(dy + 2A_\mu dx^\mu)^2 + e^{2\phi/\sqrt{3}}g_{\mu\nu}dx^\mu dx^\nu. \quad (2.2.30)$$

If we introduce this *ansatz* to the Einstein-Hilbert action in five dimensions and integrate the compact coordinate, we obtain an effective action in four dimensions with additional non-gravitational terms.

$$\begin{aligned} S &= \frac{1}{16\pi G_5} \int dy d^4x \sqrt{-g} {}^5R \\ &= \frac{1}{16\pi G_4} \int d^4x \sqrt{-g} \left[R - 2(\nabla\phi)^2 - e^{-2\sqrt{3}\phi} F^2 \right], \end{aligned} \quad (2.2.31)$$

where $F_{\mu\nu} = 2\nabla_{[\mu} A_{\nu]}$ and $G_4 = G_5/2\pi r_5$.

Therefore, the terms A_μ and ϕ of the metric (2.2.30) can be interpreted respectively as an electromagnetic vector potential and a scalar field, from a four-dimensional point of view.

The simplest black hole solution in this theory is the black string described by (2.2.29). In this case, the electromagnetic and scalar fields in $D = 4$ are null and we come back to a Schwarzschild black hole.

But starting from this metric, there is a simple way of generating new charged solutions [21]. If we apply a *boost* throughout the compact dimension, the crossed component g_{ty} will appear, which gives rise to the *gauge* field in four dimensions. This suggests that we can interpret the momentum along the y coordinate as an electric charge from a four-dimensional point of view.

In more detail, under the transformation

$$\begin{aligned} t &= \tilde{t} \cosh \alpha - \tilde{y} \sinh \alpha, \\ y &= \tilde{y} \cosh \alpha - \tilde{t} \sinh \alpha, \end{aligned} \quad (2.2.32)$$

the solution (2.2.29) becomes

$$ds_{(5)}^2 = - \left(1 - \frac{2m \cosh^2 \alpha}{r} \right) d\tilde{t}^2 + \left(1 + \frac{2m \sinh^2 \alpha}{r} \right) d\tilde{y}^2 - \frac{4m \cosh \alpha \sinh \alpha}{r} d\tilde{t} d\tilde{y} + \left(1 - \frac{2m}{r} \right)^{-1} dr^2 + r^2 d\Omega^2. \quad (2.2.33)$$

If we reorganise the components to give this metric the form (2.2.30), we obtain the fields in the effective description of $D = 4$:

$$e^{-4\phi/\sqrt{3}} = 1 + \frac{q}{r}, \quad (2.2.34)$$

$$A_t = - \frac{\sqrt{q(q+2m)}}{2(r+q)}, \quad (2.2.35)$$

$$ds_{(4)}^2 = -f(r)dt^2 + \frac{dr^2}{f(r)} + R(r)^2 d\Omega^2, \quad (2.2.36)$$

with

$$f(r) = \frac{r-2m}{[r^2+qr]^{1/2}}, \quad R^2(r) = r[r^2+qr]^{1/2}, \quad (2.2.37)$$

where we have introduced the parameter $q = 2m \sinh^2 \alpha$ and simplified the notation by removing the tildes.

The vector potential (2.2.35), indicates that the solution is electrically charged. It is not the Reissner-Nordström solution (2.1.10) though, since in this case a scalar field also appears in the theory. In fact, the horizon is still found at $r = 2m$ and the singularity at $r = 0$ as in the case of the Schwarzschild solution.

The mass and charge of this black hole is:

$$G_4 M = \frac{q}{4} + m, \quad Q^2 = \frac{q(q+2m)}{4}. \quad (2.2.38)$$

When $q = 0$ the charge disappears and we come back to Schwarzschild's solution, while in the limit $\alpha \rightarrow \infty$, $m \rightarrow 0$, with q fixed, we obtain the extremal $Q = 2G_4 M$ case.

From the electric solution, we can obtain a magnetic solution applying a duality transformation over the electromagnetic field of the type:

$${}^*F_{\mu\nu} = \frac{1}{2} e^{-2\sqrt{3}\phi} \epsilon_{\mu\nu}{}^{\rho\sigma} F_{\rho\sigma}. \quad (2.2.39)$$

The equations of motion that are derived from the action (2.2.31) are invariant under the simultaneous transformation $F \rightarrow {}^*F$, $\phi \rightarrow -\phi$. Therefore, the four-dimensional metric (2.2.36) also serves to describe a black hole with magnetic charge.

To emphasise the change from electric charge to magnetic charge, we change the parameter q to p , that is, now, $p = 2m \sinh^2 \alpha$. The magnetic charge is then:

$$P = \frac{p(p + 2m)}{4}, \quad (2.2.40)$$

and the new non-gravitational fields can be described as:

$$e^{4\phi/\sqrt{3}} = 1 + \frac{p + 2m}{r}, \quad (2.2.41)$$

$$A_\phi = P(1 - \cos \theta). \quad (2.2.42)$$

Now, we can return to the description in $D = 5$ and analyse what type of solution we are dealing with. Remembering that the five-dimensional metric must take the form (2.2.30), we obtain:

$$\begin{aligned} ds_{(5)}^2 &= \left(1 + \frac{p}{r}\right)^{-1} [dy + 2P(1 - \cos \theta)d\phi]^2 \\ &\quad - \left(1 - \frac{2m}{r}\right) dt^2 + \frac{\left(1 + \frac{p}{r}\right)}{\left(1 - \frac{2m}{r}\right)} dr^2 + r^2 \left(1 + \frac{p}{r}\right) d\Omega^2. \end{aligned} \quad (2.2.43)$$

This spacetime still has a horizon at $r = 2m$ and a singularity at $r = 0$. As we can see, there now appear crossed terms $y - \phi$. In order to understand the meaning of these components, we will consider the extremal case $\alpha \rightarrow \infty$, $m \rightarrow 0$, with p fixed.

$$ds_{(5)}^2 = \left(1 + \frac{p}{r}\right)^{-1} [dy + 2P(1 - \cos \theta)d\phi]^2 - dt^2 + \left(1 + \frac{p}{r}\right) dr^2 + r^2 \left(1 + \frac{p}{r}\right) d\Omega^2, \quad (2.2.44)$$

where now $P = p^2/4$.

In this case, the horizon disappears and we apparently have a naked singularity at $r = 0$. However, if we introduce the new coordinates:

$$\chi \equiv y/2P, \quad \rho \equiv 2\sqrt{pr}, \quad (2.2.45)$$

close to $r = 0$, the spatial part of (2.2.44) can be written as:

$$d\rho^2 + \frac{\rho^2}{4} \{[d\chi + (1 - \cos \theta)d\phi]^2 + d\theta^2 + \sin^2 \theta d\phi^2\}. \quad (2.2.46)$$

If the period of χ is 4π , the part between square brackets, corresponds to a 3-sphere, expressed as a Hopf bundle. Therefore, the metric (2.2.44) is regular at $\rho = 0$ or $r = 0$ if the compact dimension y as a period equal to $8\pi P$. That is to say, the four-dimensional magnetic charge P fixes the period of the Kaluza-Klein circle. This choice is also necessary to avoid the appearance of Dirac strings.

The solution (2.2.44) goes by the name of *Kaluza-Klein monopole* [22]. Its spatial part corresponds to the self-dual Euclidean Taub-Nut geometry, which is characterised by behaving like \mathbb{R}^4

close to $r = 0$ and as $\mathbb{R}^3 \times S^1$ close to infinity. [23] The magnetic charge, P , identifies with the *nut* N charge and defines the class of the solution, fixing the periodicity of the compact dimension $y \sim y + 8\pi N$.

It is worth stating that in the extremal case, the four-dimensional solution (2.2.36) is singular. However, we have seen that the corresponding five-dimensional solution can be regular. This is an example of how the introduction of extra dimensions can help to resolve singularities.

2.3 Black holes and string theory

String theory is often presented as a quantum theory of gravity [24, 25]. There are many reasons why this is so.

The first reason is that in the fundamental state of the spectrum of closed strings, a mode without mass and with spin 2 appears, which is interpreted as graviton. In the second place, in the limit of low energies of string theory, supergravity is obtained, a generalisation of general relativity which incorporates other types of fields. Therefore, string theory should serve for understanding some of the open questions concerning black holes, such as the statistical origin of their entropy. And, in fact, it is in this area that string theory has achieved its most important success.

Supergravity solutions exist that represent charged black holes, which can be related to certain string configurations [26]. In the perturbation regime it is possible to count the number of microstates that are compatible with the charges of the system and reproduce in this way the entropy of the corresponding black holes [27].

This procedure raises a difficulty: black holes appear in the strongly coupled regime, while the perturbation treatment consists precisely of considering the string coupling constant g_s , to be small. It is not clear that, in passing from one regime to the other, the physical magnitudes do not get renormalized. In other words, in general, there is no guarantee that the number of microstates counted in the perturbation calculation coincides with the number of microstates of the black hole.

There do exist though certain solutions with a high amount of symmetry, where physical magnitudes, such as entropy, do not depend on the coupling constant. This is the case of supersymmetric solutions (BPS) and other extremal solutions, in which the Hawking temperature is null, but which nevertheless, have a horizon of finite area. In these cases we can be sure that microscopic counting reproduces the macroscopic entropy [28].

2.3.1 The D1-D5-P system

We can see how this procedure works in a specific example. Consider the D1-D5-P black hole, which is solution of type IIB supergravity in five-dimensions. The supersymmetric case (BPS)

has the following form [26]:

$$ds_{(5)}^2 = -\frac{1}{(H_1 H_5 H_p)^{2/3}} dt^2 + (H_1 H_5 H_p)^{2/3} (dr^2 + r^2 d\Omega_{(3)}), \quad (2.3.47)$$

where

$$H_i = 1 + \frac{q_i}{r^2}. \quad (2.3.48)$$

This black hole has three charges, corresponding to 3 $U(1)$ gauge fields, which are proportional respectively to the parameters q_i . It has a very similar structure to the extremal Reissner and Nordström black hole (2.1.14). The horizon is found at $r = 0$ and it has an area of

$$\mathcal{A}_H = 2\pi^2 \sqrt{q_1 q_5 q_p}. \quad (2.3.49)$$

Therefore, the Bekenstein-Hawking entropy is

$$S_{BH} = \frac{\mathcal{A}_H}{4G_5} = \frac{\pi^2}{2G_5} \sqrt{q_1 q_5 q_p}. \quad (2.3.50)$$

The solution (2.3.47) can be converted into a black string type solution, if we add an extra dimensions compactified along a circle, $z \sim z + 2\pi R$ in an analogous way to the case of (2.2.29)

$$ds_{(6)}^2 = \frac{H_p}{H_1^{3/4} H_5^{1/4}} (dz + (1 - H_p^{-1}) dt)^2 - \frac{1}{H_p H_1^{3/4} H_5^{1/4}} dt^2 - H_1^{1/4} H_5^{3/4} (dr^2 + r^2 d\Omega_{(3)}). \quad (2.3.51)$$

In this case, we are not dealing with a static solution, as there are crossed terms. The string has momentum throughout the compact dimension. Inspecting the term g_{tz} , we can see that this momentum is proportional to the parameter q_p , that is to say, that from a five-dimensional point of view it is interpreted as a charge associated with a gauge field $U(1)$, becoming momentum when we move up to 6 dimensions, as is usual in Kaluza-Klein type theories (Section 2.2.2).

The entropy is in this case

$$S_{BH} = \frac{\mathcal{A}_H^{\text{string}}}{4G_6}. \quad (2.3.52)$$

If we take into account the relationship $G_6 = 2\pi R G_5$, we can see that this coincides with the five-dimensional case

$$S_{BH} = \frac{\mathcal{A}_H^{(5)} \cdot 2\pi R}{4 \cdot 2\pi R G_5} = \frac{\mathcal{A}_H^{(5)}}{4G_5}. \quad (2.3.53)$$

Moving from the black hole in 5D to the black string in 6D shows that the momentum P in the direction of the string has to be quantised in units of the radius of the compact dimension R . Taking into account that this momentum is related to the parameter q_p , allows us to obtain the following quantisation rule:

$$q_p = \frac{4G_5}{\pi} P = \frac{4G_5}{\pi} \frac{N_p}{R}, \quad (2.3.54)$$

where N_p is the whole number of units of momentum.

The three charges can be interchanged, through duality transformations. Therefore, it can be shown in an analogous way that the charges q_1 and q_5 are also quantised:

$$q_{1,5} = \sqrt{\frac{4G_5 R}{\pi}} N_{1,5}. \quad (2.3.55)$$

If we substitute the quantisation rules (2.3.54) and (2.3.55) into the entropy expression (2.3.50), we get:

$$S_{BH} = 2\pi \sqrt{N_1 N_5 N_p}. \quad (2.3.56)$$

It is important to notice that neither the gravitational constant nor the radius of the string nor any other continuous parameter appears in this expression. This is what guarantees that the entropy does not change with G .

We can imagine starting with this black hole and reducing the strength of the coupling constant, without varying N_i . Consequently, the radius of the horizon also decreases until it becomes smaller than the length of the string. At this point, the system is more accurately described as a perturbative state of string theory. In order to know exactly what state we are dealing with, we need to look for states that have the same charges.

In string theory, the charged objects which source *gauge* fields in the supergravity solution are Dp -branes, p -dimensional objects upon which open strings can end.

In the case of the (2.3.47) black hole the microscopic perturbative description consists of a bound state of N_5 $D5$ -branes and N_1 $D1$ -branes sharing a common direction. Throughout this direction there is a net momentum N_p/R , corresponding to the movement of the excitations of the open strings that end on the branes.

It can be shown that this system is equivalent to an effective string of radius $R_{\text{ef}} = N_1 N_5 R$ over which bosonic and fermionic excitations can travel [29]. These supply the momentum and energy and can be described by 1+1-dimensional field theory. If we consider that these oscillations follow a thermal distribution, a statistical calculation allows us to reproduce the entropy of the black hole (2.3.56). [27]

At this point, a few things need to be cleared up. The BPS solution corresponds to a fundamental state of zero temperature. How is it possible, then, that we can describe it in terms of thermal excitations? The key point is that the string excitations can have two opposite chiralities.

Supposing that we have a non-BPS state, with two chiral sectors thermally excited, with temperatures of $T_{L,R}$. If we assume that there is very little interaction between them, we have $S = S_L + S_R$, $E = P_L + P_R$ and $P = P_L - P_R$, where $P_{L,R} = N_{L,R}/R$. Given that $T_{L,R}^{-1} = (\partial S_{L,R}/\partial P_{L,R}) = 2(\partial S_{L,R}/\partial E)_P$ then, the total temperature, which verifies $T^{-1} = (\partial S/\partial E)_P$ can be expressed as

$$T^{-1} = \frac{1}{2}(T_L^{-1} + T_R^{-1}). \quad (2.3.57)$$

Therefore, if one of the two sectors is not thermally excited ($T_L = 0$ or $T_R = 0$), the total temperature will be zero, but the entropy will not vanish. This is the case of the BPS solution.

The interpretation in terms of two sectors also gives a microscopic explanation for Hawking radiation. In a non-extremal system, two excitations travelling in opposite directions may collide and emit a closed string towards the exterior. Obviously, in systems that only have one of the two sectors excited, this process is not possible.

To close this section, we need to add that rotating black holes can also be described using this model. The rotation is then provided by the R charge carried by fermionic oscillations.

2.3.2 Dualities

The reproduction of the black hole entropy from string theory has a limitation: the types of black holes to which it can be applied are very different from the simpler and more realistic Schwarzschild and Kerr solutions. The black hole (2.3.47) has three charges and is supersymmetric. As we have seen, the charges help to identify the corresponding microscopic state and the supersymmetry guarantees that the number of microstates does not change when modifying the strength of the coupling.

There are ways of overcoming these limitations. One of these is to reduce or increase dimensions: charged black holes in a certain dimensionality, can become neutral when they are uplifted to higher dimensions. We have already seen, that the charge P in (2.3.47) becomes momentum when we move to $D = 6$.

Another strategy consists in applying a series of duality transformations that allow us to map solutions between different string theories [25].

- The **T duality** consists in changing the radius of compactification R for its inverse $1/R$. In this way, momentum in the compactified direction becomes winding number, and vice versa. This allows us to relate, for example, solutions in theories IIA and IIB.
- The **S duality** relates strongly coupled solutions with weakly coupled solutions, by the substitution $g \rightarrow 1/g$. In particular, theory IIB is self-dual with respect to this transformation. Therefore, S duality allows us to relate different solutions of this same theory.
- The **U duality** can be considered as a larger group of dualities that combine the previous two dualities.

2.4 Structure of the thesis

The main objective of this thesis is to understand from a microscopic point of view some of the characteristic phenomena of rotating black holes.

We will concentrate on extremal rotating black holes that are not supersymmetric. These kinds of solutions are the most appropriate for our purpose. Unlike supersymmetric black holes they have an ergosphere and so they can produce superradiance. However, given that they have zero temperature this phenomenon does not get mixed with Hawking radiation of purely thermal origin. At the same time, these extremal geometries also conserve the number of microstates passing from strong coupling to weak coupling.

The first part of the thesis focuses on the microscopic study of the entropy of rotating Kaluza-Klein black holes. This family of solutions gives two extremal limits: *slowly rotating* and *fastly rotating*. In [30] the entropy has already been reproduced in the first case. Here, we will extend this calculation to the fastly rotating extremal limit. At the same time, we will show how the phenomenon of superradiance can be explained in an analogous way to Hawking radiation, as the collision of two excitations, giving rise to the emission of a closed string, which in this case carries an angular momentum.

In the second part, we will focus on this microscopic interpretation of superradiance with a more quantitative treatment. In this case, we will consider the non-supersymmetric extremal solution of the rotating D1-D5-P system. From its microscopic description, we shall reproduce the superradiance condition of type (2.1.22) and show that it can be understood as a consequence of Fermi-Dirac statistics. We shall also evaluate the superradiant emission rates from the macroscopic and microscopic point of view and analyse concordance.

The order in which the content is presented is aimed at facilitating understanding. First, fundamental ideas will be explained in an intuitive way, and later, technical details will be provided, some of which are to be found in the appendix.

Chapter 3

Rotating Kaluza-Klein Black Holes

Rotating black holes with maximal angular momentum provide an interesting setting for the investigation of black hole microphysics. Consider the intriguingly simple form of the entropy of the extremal Kerr black hole,

$$S = 2\pi|J|. \tag{3.0.1}$$

Since the angular momentum J is naturally quantized, it strongly suggests that some kind of sum over states should reproduce it. In addition, the absence of Newton's constant in (3.0.1) gives hope that the counting might be performed at small gravitational coupling and then reliably extrapolated to the strong coupling regime where the black hole lies. Identifying the microscopic system behind (3.0.1) remains an open problem in string theory. This motivates the study of analogous solutions, such as the extremal Myers-Perry (MP) black hole rotating in two independent planes in five dimensions [16], whose entropy

$$S = 2\pi\sqrt{|J_1 J_2|}, \tag{3.0.2}$$

is closely similar to (3.0.1), and also of other black holes sharing some of the features of the Kerr solution.

A microscopic model for the extremal 5D MP black hole (orbifolded along a certain direction) has been presented, reproducing exactly the entropy (3.0.2) [30]. The model is based on a connection between the MP solutions and Kaluza-Klein black holes: if we place an MP black hole at the tip of a Taub-NUT geometry we recover a Kaluza-Klein black hole. Since Kaluza-Klein black holes are naturally embedded in Type IIA string theory as solutions with D0 and D6 charges, ref. [30] used the analysis of D0-D6 bound states in [31] to derive a microscopic model for (3.0.2).

Kaluza-Klein black holes are also of interest by themselves. In the generic dyonic case they are never supersymmetric, nor are in general close to any supersymmetric state. The entropy of the extremal solutions—with degenerate horizons of zero temperature—depends, like (3.0.1), only on integer-quantized charges, and not on the coupling or other moduli. There are two branches

of extremal black holes, depending on whether their angular momentum is below or above a certain bound [32, 33]. Ref. [30] developed the statistical description of KK black holes in the slow-rotation regime. In this chapter we extend the analysis to show that the entropy of fastly-rotating KK black holes can also be accurately reproduced. This is of interest for several reasons. Unlike the slowly-rotating KK black holes, whose horizons are static, the fastly-rotating black holes have non-zero horizon angular velocity, possess ergospheres and exhibit superradiance, so they are qualitatively much closer to the Kerr black hole. In fact, as J grows large with fixed charges, the KK black holes asymptotically approach the Kerr solution. So one may hope for hints for a statistical model of (3.0.1).

One feature that we find, and which we argue can be expected for the extremal Kerr black hole too, is that the microscopic calculations exactly match the entropy but *not the mass* of the fastly rotating black hole. As we will see, this fits well with the macroscopic analyses of [34–36] in the context of the attractor mechanism. Our study also gives a clear indication of how extremal rotating black holes with superradiant ergospheres are distinguished microscopically from those that cannot superradiate.

We show in full generality how Myers-Perry black holes are obtained as a limit of Kaluza-Klein black holes, and discuss the slow and fast rotation regimes and superradiance in this context.

3.1 Extremal Kaluza-Klein black holes

Refs. [32] and [33] independently constructed the solutions for general Kaluza-Klein dyonic rotating black holes, which we give in appendix A. For more details we refer to these papers and to ref. [37], which contains insightful remarks on their properties. Here we briefly summarize the most relevant features.

The solutions are characterized by four physical parameters: mass M , angular momentum J , and electric and magnetic charges Q and P . For solutions with a regular horizon, the mass always satisfies

$$2G_4M \geq \left(Q^{2/3} + P^{2/3}\right)^{3/2}. \quad (3.1.1)$$

The extremal limit, defined as the limit of degenerate, zero-temperature horizon, can be achieved in two ways, giving two distinct branches of solutions:

- **Slow rotation:** $G_4|J| < |PQ|$. The mass

$$2G_4M = \left(Q^{2/3} + P^{2/3}\right)^{3/2} \quad (3.1.2)$$

saturates the bound (3.1.1) *independently of J* . The angular velocity of the horizon vanishes, and there is no ergosphere. The entropy is

$$S = 2\pi \sqrt{\frac{P^2Q^2}{G_4^2} - J^2}. \quad (3.1.3)$$

- **Fast rotation:** $G_4|J| > |PQ|$. The entropy

$$S = 2\pi\sqrt{J^2 - \frac{P^2Q^2}{G_4^2}} \quad (3.1.4)$$

is the natural continuation of (3.1.3), but the mass is strictly above the value (3.1.2) and, for fixed Q and P , it grows monotonically with $|J|$. The angular velocity of the horizon is non-zero, and there is an ergosphere.

The extremal horizon disappears and becomes a naked singularity at the dividing value $G_4|J| = |PQ|$.

Kaluza-Klein black holes are naturally embedded in Type IIA string theory by taking a product with T^6 . The KK gauge potential is then identified with the RR 1-form potential (so the KK circle is identified with the M theory direction). Q and P correspond to D0 and D6 charges, quantized as

$$Q = \frac{g}{4V_6}N_0, \quad P = \frac{g}{4}N_6, \quad (3.1.5)$$

where N_0 and N_6 are the number of D0 and D6 branes, g is the string coupling, and the volume of T^6 is $(2\pi)^6V_6$. We work in string units, so $G_4 = g^2/8V_6$.

The mass bound (3.1.2) becomes

$$M = \frac{1}{g} \left(N_0^{2/3} + (N_6V_6)^{2/3} \right)^{3/2}, \quad (3.1.6)$$

and the entropies (3.1.3) and (3.1.4) become

$$S = 2\pi\sqrt{\frac{N_0^2N_6^2}{4} - J^2}, \quad (3.1.7)$$

and

$$S = 2\pi\sqrt{J^2 - \frac{N_0^2N_6^2}{4}}, \quad (3.1.8)$$

respectively. In analogy with (3.0.1), these entropies are independent of g , V_6 and any other T^6 moduli.

3.2 Microscopic model of rotating D0-D6 black holes

The microscopic description of two-charge D0-D6 systems requires that we recall first some aspects of four-charge configurations in Type II string theory compactified on T^6 (or M theory on T^7), in particular when rotation in the non-compact directions is present.

3.2.1 Rotating zero-temperature configurations in the (4, 0)-SCFT

Consider brane intersections with four charges N_1, N_2, N_3, N_4 , in a regime where the dynamics of low energy modes localized at the intersection is described in terms of a chiral (4, 0)-supersymmetric CFT [38–40]. We shall be somewhat unspecific about what the N_i stand for. The statistical entropy counting is most easily performed when $N_{1,2,3}$ denote wrapping numbers of M5 branes, and N_4 denotes momentum units along the (smoothed) intersection [39]. However, the U-dual frame where the N_i correspond to four stacks of D3 branes intersecting over a point [41] will be more useful later. Like in [30], the modular invariance of the entropy and angular momentum makes it natural to assume that the degrees of freedom responsible for them are localized at the point-like intersection.

To recover the SCFT we take the number of antibranes of the 1,2,3 kind to be suppressed, but we allow for both branes (or momentum) and antibranes (or oppositely moving momentum) of type 4. To leading order with $N_{1,2,3} \gg 1$, the central charge for both left- and right-moving sectors is $c = 6N_1N_2N_3$, and $L_0 - \bar{L}_0 = N_4$. Supersymmetric configurations have the left-moving sector in its supersymmetric ground state, $\bar{L}_0 = N_L = 0$ [38]. We are, however, interested in exciting the left sector, thus breaking all supersymmetries. The reason is that spacetime rotation requires exciting the fermions in this sector. Their $SU(2)$ R-charge acts on spacetime as $SO(3)$ rotation, so a macroscopic angular momentum J results from the coherent polarization of these fermions. This projection also reduces the available phase space, so the effective oscillator number entering the entropy formula is $\tilde{N}_L = N_L - 6J^2/c = N_L - J^2/N_1N_2N_3$. Then [40]

$$S = 2\pi\sqrt{\frac{c}{6}} \left(\sqrt{\tilde{N}_L} + \sqrt{N_R} \right) = 2\pi \left(\sqrt{N_1N_2N_3N_L - J^2} + \sqrt{N_1N_2N_3N_R} \right). \quad (3.2.1)$$

Under the assumption that the constituents interact only very weakly, the total mass of the system is

$$M = M_1N_1 + M_2N_2 + M_3N_3 + M_4(N_R + N_L). \quad (3.2.2)$$

Here M_i are the masses of a unit of each single constituent.

Zero-temperature states must have oscillator distributions such that either the left or right ‘temperatures’, T_L or T_R , vanish. For a state with $J \neq 0$, this results into two distinct possibilities:

- $T_R = 0$

Set $N_R = 0$ and $N_L > \frac{J^2}{N_1N_2N_3} \geq 0$, so $N_4 = -N_L < 0$. The left-moving sector gives rise to both the angular momentum,

$$J^2 < N_1N_2N_3|N_4|, \quad (3.2.3)$$

and the entropy,

$$S = 2\pi\sqrt{N_1N_2N_3|N_4| - J^2}. \quad (3.2.4)$$

Hence the mass

$$M = M_1 N_1 + M_2 N_2 + M_3 N_3 + M_4 |N_4|, \quad (3.2.5)$$

is fixed by the charges N_i independently of J .

- $T_L = 0$

Set $N_R > 0$, $N_L = \frac{J^2}{N_1 N_2 N_3}$, so $N_4 = N_R - \frac{J^2}{N_1 N_2 N_3}$. The fermions in the left sector fill up to the Fermi level, so T_L is effectively zero. *Both* sectors are excited, and in principle N_4 can be either positive, negative, or zero. However, if we require that the right sector be only slightly excited, $N_R \ll N_L$, then $N_4 < 0$. The left movers provide the angular momentum

$$J^2 = N_1 N_2 N_3 N_L > N_1 N_2 N_3 |N_4|, \quad (3.2.6)$$

and the right movers the entropy,

$$S = 2\pi \sqrt{N_1 N_2 N_3 N_R} = 2\pi \sqrt{J^2 - N_1 N_2 N_3 |N_4|}. \quad (3.2.7)$$

From (3.2.2) we find the mass

$$\begin{aligned} M &= M_1 N_1 + M_2 N_2 + M_3 N_3 + M_4 \left(N_4 + 2 \frac{J^2}{N_1 N_2 N_3} \right) \\ &= M_1 N_1 + M_2 N_2 + M_3 N_3 + M_4 |N_4| + 2M_4 \left(\frac{J^2}{N_1 N_2 N_3} - |N_4| \right) \end{aligned} \quad (3.2.8)$$

is strictly above (3.2.5).

This CFT describes the four-dimensional black holes of [42] ([40]). The restriction to small N_R , so that $\frac{J^2}{N_1 N_2 N_3} - |N_4|$ is small, is required for the validity of the CFT description. Indeed, it is only in this regime that the supergravity solutions have a locally-AdS₃ near-horizon geometry. However, the entropy of the extremal $T_L = 0$ black holes appears to be correctly reproduced for arbitrary values of the parameters. We will comment more on this in Section 3.2.3.

3.2.2 Microscopics of D0-D6

According to [31], a system of N_0 D0 branes bound to N_6 D6 branes wrapped on T^6 is T-dual to a non-supersymmetric intersection of four stacks of D3 branes. One of the stacks has reversed orientation relative to the supersymmetric case. This is similar to the configurations of the previous section with $N_4 < 0$ (the susy-breaking case), but there is one important difference: the D3 branes wrap now non-minimal rational directions k/l in each T^2 within $T^6 = T^2 \times T^2 \times T^2$. The number N of D3 branes is the same in each stack, and

$$N_0 = 4k^3 N, \quad N_6 = 4l^3 N \quad (3.2.9)$$

(so $N_{0,6}$ are necessarily multiples of four).

The main assumption of the model, supported by modular invariance, is that the entropy of the low energy excitations at the D3 brane intersection is a local property of the intersection and is independent of whether the branes wrap the torus along minimal or along non-minimal rational cycles. Then we can import the entropy calculations from the previous section by setting

$$N_1 = N_2 = N_3 = |N_4| = N. \quad (3.2.10)$$

Crucially, we must also take into account that the *number* of intersection points in the torus *does* depend on how the branes are wrapped: there are $2kl$ intersections in each T^2 , and so a total of $(2kl)^3$ in T^6 . Since the Hilbert space at each intersection is independent of the other intersections, the total entropy is $(2kl)^3$ times the entropy from a single intersection point. The angular momentum is also multiplied by this same factor. Since the total entropy is maximized by distributing J evenly over all intersections, each one carries $J_0 = J/(2kl)^3$.

In order to obtain the masses for the D3-brane configuration we note that if the volume of minimal 3-cycles in T^6 is V_3 , then each of the 3-branes has volume $(k^2 + l^2)^{3/2} V_3$, so their individual masses are

$$M_{D3} = (k^2 + l^2)^{3/2} \frac{V_3}{g}, \quad (3.2.11)$$

for branes in any of the four stacks.

In this set up, we find that the two different extremal rotating D0-D6 systems of Section 3.1 map to each of the two zero-temperature rotating intersecting D3-brane systems of Section 3.2.1:

- **Slow rotation.** This was the regime studied in [30]. The CFT at the intersection has the right sector in its ground state, with entropy per intersection given by (3.2.4). So, for the D0-D6 system,

$$S_{branes} = (2kl)^3 \times 2\pi \sqrt{N^4 - J_0^2} = 2\pi \sqrt{\frac{N_0^2 N_6^2}{4} - J^2}, \quad (3.2.12)$$

in exact agreement with (3.1.7). The mass also matches exactly. Putting N 3-branes with mass (3.2.11) in each of the four stacks, the total mass is

$$M_{branes} = 4NM_{D3} = \frac{V_3}{g} \left(N_0^{2/3} + N_6^{2/3} \right)^{3/2}. \quad (3.2.13)$$

After T-duality in the three appropriate torus directions, the agreement with the mass of the slow-rotation D0-D6 black hole (3.1.6), is exact.

- **Fast rotation.** We naturally assign to each intersection a state in the fastly-rotating regime of the CFT, *i.e.*, $T_L = 0$. Then, using the entropy formula (3.2.7),

$$S_{branes} = (2kl)^3 \times 2\pi \sqrt{J_0^2 - N^4} = 2\pi \sqrt{J^2 - \frac{N_0^2 N_6^2}{4}} \quad (3.2.14)$$

we recover the correct value for the D0-D6 black hole (3.1.8).

The agreement, however, does not extend to the mass in this case. Consider values of $|J|$ slightly above $N_0 N_6/2$, so there is only a small mass $\delta M > 0$ above (3.1.6),

$$M = \frac{V_3}{g} \left(N_0^{2/3} + N_6^{2/3} \right)^{3/2} + \delta M. \quad (3.2.15)$$

We compute first δM within the microscopic brane model. Recall that the mass is simply proportional to the volume of branes of each kind, so we use (3.2.11) in (3.2.8). δM comes from the last term in (3.2.8), and we find¹

$$\begin{aligned} \delta M_{branes} &= \frac{V_3}{g} (k^2 + l^2)^{3/2} \times 2 \left(\frac{J_0^2}{N^3} - N \right) \\ &= \frac{V_3}{g} \frac{\left(N_0^{2/3} + N_6^{2/3} \right)^{3/2}}{2} \left(\frac{4J^2}{(N_0 N_6)^2} - 1 \right). \end{aligned} \quad (3.2.16)$$

On the other hand, the ADM mass of the black hole gives, after T-duality, and to leading order in $(J^2 - (N_0 N_6)^2/4)$,

$$\delta M_{bh} = \frac{V_3}{g} \frac{(N_0 N_6)^{2/3}}{2 \left(N_0^{2/3} + N_6^{2/3} \right)^{1/2}} \left(\frac{4J^2}{(N_0 N_6)^2} - 1 \right). \quad (3.2.17)$$

So

$$\frac{\delta M_{branes}}{\delta M_{bh}} = \left[\left(\frac{N_0}{N_6} \right)^{1/3} + \left(\frac{N_6}{N_0} \right)^{1/3} \right]^2. \quad (3.2.18)$$

The discrepancy in the masses is naturally attributed to a mass renormalization as the gravitational coupling is increased. Observe that $\delta M_{branes} > \delta M_{bh}$, which is as expected since gravitational binding should reduce the energy. In the next section we discuss further why this renormalization occurs for fast but not for slow rotation.

Following the last comments in Section 3.2.1, in principle it would seem possible to extend the agreement of the entropies to arbitrarily large values of $J^2/N_0^2 N_6^2$, but in these cases the use of the CFT seems largely unjustified. The mass renormalizations get of course much larger.

3.2.3 Discussion

We have shown that it is possible to successfully extend the microscopic model of KK black holes in [30] to cover the regime of fast rotation, with horizons that rotate with non-vanishing angular velocity and therefore are more similar to the Kerr black hole. There exist other similar instances where the entropy is also correctly reproduced: extremal four-charge type II black holes also have

¹Note that we saturate $N_L = J_0^2/N^3$ at each intersection, which is smaller than J^2/N^3 .

slow and fast rotation regimes which are correctly captured by the CFT of Section 3.2.1, and there are analogous three-charge five-dimensional black holes with these properties which can be described in the (4, 4)-SCFT of the D1-D5 system [40, 42]. However, in these cases not only the entropy but also the mass is accurately reproduced by the microscopic model, both at slow and at fast rotation (at least for rotation slightly above the divide). This agreement is understood, within the context of AdS/CFT duality, as being due to the existence of a locally AdS₃ (BTZ) geometry near the horizon [43, 44]. In contrast, extremal KK black holes do not have in general AdS₃ symmetry near the horizon (only in the singular case $|PQ| = G_4|J|$), so perhaps we should be surprised by the fact that the entropy does come out correctly.

Actually, our results are in perfect agreement with the recent macroscopic studies in [34–36], which argue that the $SL(2, \mathbb{R}) \times U(1)$ symmetry near the horizon of four-dimensional extremal rotating black holes, charged as well as neutral, ensures that the macroscopic value for the entropy can be extrapolated to weak coupling. Extremal KK black holes do possess this near-horizon symmetry (and their MP limits too [45]). Hence, if a microscopic model is identified, its entropy should exactly match the macroscopic value. In this section we have provided this microscopic model and confirmed the agreement of entropies.

Ref. [34] finds that the scalar field, and indeed the whole solution, for slowly rotating KK black holes is attracted to a completely fixed form near the horizon, so not only the entropy but also the mass is fixed—in agreement with the microscopic calculation in [30]. However, for fastly rotating extremal KK black holes there exist flat directions in the effective potential for the scalar near the horizon, with the effect that only the entropy is attracted to a fixed value. Other quantities, like the mass, are not guaranteed to be fixed. We have found that in fact *they are not*. Thus we conclude that the attractor mechanism correctly predicts which quantities will match at weak and strong coupling, and which ones will, generically, be renormalized.

Extremal fastly-rotating four-charge black holes with $J^2 \gg N_1 N_2 N_3 |N_4|$, and KK black holes with $J^2 \gg N_0^2 N_6^2$, do have only $SL(2, \mathbb{R}) \times U(1)$ near-horizon symmetry. In principle these black holes can approach arbitrarily closely to the extremal Kerr solution. Their entropies, but not their masses, agree with naive CFT formulas, although one is far from the regime where any application of the CFT is justified. So, even if this may not be the correct description, it seems likely that a microscopic model for the extremal Kerr solution, which also has near-horizon symmetry $SL(2, \mathbb{R}) \times U(1)$ [45], should be able to pin down exactly the entropy (3.0.1), but not the mass of the black hole. Obtaining the exact entropy of non-extremal vacuum black holes, like Schwarzschild, will require taking into account mass renormalization effects.

3.3 Ergospheres and Superradiance

3.3.1 Qualitative microscopics

The statistical description above gives some clear hints of what is the microscopic distinction between extremal rotating black holes with or without ergospheres, and how superradiance arises from the microscopic theory

Recall first how Hawking radiation appears microscopically. In the 2D CFT, non-extremal, finite-temperature states occur when the effective temperature of the excitations in both left and right sectors is non-zero, with the total system at temperature $T_H^{-1} = (T_L^{-1} + T_R^{-1})/2$. So if we couple the CFT to closed strings that propagate out to the asymptotically flat bulk, then left- and right-moving open string excitations can combine into a closed string, resulting into Hawking radiation at temperature T_H . If rotation is present, superradiance effects will mix in. However, when one of the sectors is at zero temperature, *i.e.*, at extremality, Hawking radiation cannot occur. Above we have described two distinct rotating zero-temperature systems. In the first possibility the right-moving sector remains unexcited. So, in the absence of open string excitations of one chirality, there cannot be any closed string emission—neither Hawking emission nor superradiance. This is as it should be, since these states describe extremal black holes without ergospheres.

In contrast, extremal black holes with a superradiating ergosphere correspond to states with both left- and right-moving excitations. The emission of (non-thermal) closed strings, from the combination of left- and right-moving open string excitations, seems possible now. Moreover, since the left-moving excitations have spin, the emitted closed string will necessarily carry angular momentum away from the black hole. So it is natural to expect that this process describes superradiance.

This picture applies not only to Kaluza-Klein black holes but also to the four-charge 4D and three-charge 5D black holes, for which there also exist extremal rotating states with and without ergospheres.

In order to work out the details of this correspondence, it seems more convenient to consider D1-D5-P black holes. Indeed, they have a straightforward description in terms of an effective string along the D1-D5 intersection [27], with right and left moving excitations as opposed to KK black holes in which the set of dualities we applied makes this kind of description more involved.

Moreover, the three-charge 5D black holes possess an AdS₃ (BTZ) near-horizon geometry, which ensures that not only the entropy but also the mass doesn't get renormalized when going from weak to strong coupling. This could be a crucial point in order to reproduce the superradiant bound (2.1.22) from the microscopic side, since it involves an energy.

Therefore, in the next chapter we consider D1-D5-P extremal black holes with an ergosphere to perform a quantitative analysis of our microscopic model for superradiance emission.

3.3.2 4D vs 5D perspectives

The charges Q and P , or alternatively the corresponding integers N_0 and N_6 , have a neat geometrical interpretation from the five-dimensional point of view: N_0 is the number of units of quantized momentum in the compact fifth direction, and N_6 is the degree of the fibration of this internal S^1 on the orbital S^2 's. So when $N_6 > 0$ the horizon topology in 5D is S^3/\mathbb{Z}_{N_6} . If the horizon size is much smaller than the compact radius, the black hole can be regarded as an MP black hole at the tip of a Taub-NUT geometry [46]. We elaborate in detail on this in appendix A, and mention here only some salient features.

The MP black hole generically has angular momenta J_1, J_2 in two independent rotation planes. The KK electric charge Q is proportional to the self-dual component of the angular momentum, $\mathcal{J} = J_1 + J_2$, aligned with the KK fiber, and J to the anti-self-dual component $\bar{\mathcal{J}} = J_1 - J_2$, off the KK direction. In the extremal limit, the MP black hole entropy reduces to (3.0.2), which can be written as

$$S = \pi \sqrt{|\mathcal{J}^2 - \bar{\mathcal{J}}^2|}. \quad (3.3.1)$$

Both the slowly and the fastly rotating extremal KK black holes lead, in the decompactification limit, to extremal MP black holes, the former with $\mathcal{J}^2 > \bar{\mathcal{J}}^2$, the latter with $\mathcal{J}^2 < \bar{\mathcal{J}}^2$. From a purely 5D (decompactified) viewpoint, this distinction is obviously arbitrary. However, we have found that the brane configurations describing each of these two regimes are rather different. The point is that the symmetry between \mathcal{J} and $\bar{\mathcal{J}}$ is broken once we put the MP black hole at a certain orientation within Taub-NUT. There is a choice to be made of which of the 5D angular momenta is going to correspond to the four-dimensional J and which to Q . So the two microscopic configurations actually describe two different ways to embed the extremal MP black holes within Taub-NUT, and in this sense they describe different black holes.

One might then ask how it can be that the MP black hole in Taub-NUT is capable of superradiating when $\mathcal{J}^2 < \bar{\mathcal{J}}^2$, but not when $\mathcal{J}^2 > \bar{\mathcal{J}}^2$. It turns out that, as we show in detail in appendix B, superradiance *is* possible in both situations but is interpreted differently in each case. Consider an incident wave in the KK black hole background with dependence

$$\Psi \sim e^{iky + in\phi - i\omega t}, \quad (3.3.2)$$

on the Killing directions, y being the coordinate along the KK circle. The wavenumber k is KK electric charge from the 4D viewpoint. We find that the necessary condition for superradiant amplification is

$$k < \omega < n\Omega_H + 2G_4k\Phi_E, \quad (3.3.3)$$

where Ω_H is the 4D horizon angular velocity and Φ_E is the KK electric potential. From the 5D viewpoint, $2G_4\Phi_E$ is the velocity at which the 5D horizon is rotating in the y direction relative to static asymptotic observers.

The conventional rotational superradiance of fastly-rotating KK black holes corresponds to amplification of neutral ($k = 0$) waves with $\omega < n\Omega_H$. We show in appendix B that this is indeed possible for scalar fields. This is the process whose microscopic dual is suggested in the previous section.

On the other hand, slowly spinning extremal black holes have $\Omega_H = 0$ so they show no rotational superradiance. But they can produce superradiant amplification of waves with KK electric charge k . In appendix B we show that this indeed happens and is always allowed since these black holes have $2G_4\Phi_E > 1$. This process, however, is not so naturally described in the dual CFT system, since it requires either the emission of 4D charge and hence changing the central charge of the CFT, or altering the direction in which the branes wrap T^6 , which is not seen by the CFT.

Chapter 4

Microscopic Theory of Black Hole Superradiance

The microscopic string theory of black holes provides an accurate statistical counting of the Bekenstein-Hawking entropy [30, 47–50] and a microscopic picture of Hawking radiation [29, 51–54] at least for some classes of black holes. In this chapter we address how this microscopic theory also accounts for a characteristic phenomenon of rotating black holes: the black hole superradiance. We shall follow mostly the suggestion advanced in Chapter 3, making it more precise and quantitative.

Superradiance is a phenomenon associated to the presence of an ergoregion around the black hole [13, 14, 45, 55–59]. Since the Killing vector that defines the energy measured by asymptotic observers becomes spacelike within the ergosurface, it follows that in the ergoregion there can exist excitations with negative energy relative to infinity. So if we scatter a wave off the black hole, this wave can excite negative energy modes that may subsequently fall into the horizon. To an asymptotic observer this will appear as a positive energy flux coming out of the horizon, and the scattered wave can emerge with higher amplitude than the impinging wave: this is known as superradiant scattering. If an incident wave $\Phi \sim f(r, \theta)e^{-i\omega t + im\phi}$, with energy $\omega > 0$ and angular momentum number m , scatters off a black hole with horizon angular velocity Ω_H , the requirement that a negative-energy flux crosses the horizon towards the future is

$$0 < \omega < m\Omega_H. \quad (4.0.1)$$

Only modes satisfying this condition can undergo superradiant amplification.

Superradiant scattering can be regarded as stimulated emission, and, just like the latter (classical) process is related by detailed balance to (quantum) spontaneous emission, rotating black holes are also known to spontaneously emit superradiant modes within the range (4.0.1), in a process closely related to Hawking radiation. These carry away energy, but also angular momentum off the black hole. In our microscopic picture it is convenient to first describe the process of spontaneous superradiant emission, and then infer the stimulated emission.

When the black hole temperature is different from zero it is difficult to disentangle spontaneous superradiant emission from thermal Hawking radiation—in fact both become part of one and the same phenomenon. Since we are interested only in the microphysics behind the presence of an ergoregion and the existence of superradiant modes (4.0.1), we will investigate the spontaneous emission from an extremal, *i.e.*, zero-temperature, rotating black hole, for which thermal Hawking radiation is absent. Since the black hole has a ‘cold’ ergoregion, we refer to it as an *ergo-cold black hole*. This will allow us to isolate superradiance: only modes that satisfy (4.0.1) will be emitted. Note, however, that after the emission of superradiant quanta begins, the angular momentum will be reduced below its maximal value and the black hole will be driven away from extremality, so thermal Hawking radiation will promptly set in. It is the onset of the decay that will give us more neatly the microscopic basis of the superradiant bound (4.0.1).

There have been previous papers dealing with emission rates from rotating black holes and the microscopic calculations that match them [43, 45, 52, 60] (see [61, 62] for a review), in some cases discussing, more or less directly, aspects of superradiance. Typically, these papers have computed the absorption cross sections for a non-extremal black hole and for its microscopic finite-temperature dual. Even if these results exhibit essential agreement between both sides, we feel that the long calculations involved, and the mixing with thermal Hawking radiation, hide some very simple microphysics behind (4.0.1). We hope to clarify the microscopic origin of the ergoregion and provide a simple interpretation of the superradiant modes in it.

In Section 3.3, we already introduced a picture for these phenomena in terms of opposite chirality excitations in a CFT, which can collide and emit a closed string mode to the bulk, in analogy to the microscopic description of Hawking radiation. As mentioned there, in order to perform a more quantitative analysis it is convenient to investigate this mechanism in the context of the D1-D5-P system. The advantages are that this system can be described with a well known effective string model, namely a 1+1 conformal field theory on a specific sigma model. This CFT is dual to an AdS_3 geometry, and the metric of the black hole near the horizon is the BTZ black hole. In the extremal limit, these black holes exhibit an attractor mechanism that fixes both the entropy and the energy as a function only of conserved charges and independently of moduli. These quantities are therefore not renormalized when interpolating between the gravitational description (the BH) and the perturbative field theory description.

A salient conclusion of our analysis is a clear understanding of the bound (4.0.1) as essentially a consequence of Fermi-Dirac statistics for the microscopic degrees of freedom that give the black hole its angular momentum.

4.1 Microphysics of cold ergoregions

We begin by introducing the microscopic picture of superradiance and then provide a simple derivation and interpretation of the bound (4.0.1) for the ergo-cold black hole.

4.1.1 Qualitative microscopic origin of the ergoregion

Our basic picture applies to any black hole that admits an ‘effective string’ description, *i.e.*, to which AdS₃/CFT₂ duality applies¹, but for definiteness we focus, for the most part, on the D1-D5-P system, which describes a class of near-supersymmetric five-dimensional black holes. We shall begin by reviewing in qualitative terms the microscopic picture of several kinds of D1-D5-P black holes.

The D1 and D5-branes form a bound state whose low-energy dynamics is described by a 1+1-dimensional field theory along their common worldvolume directions (the other four directions wrap a small T^4 or $K3$). It is a non-chiral conformal field theory (CFT) with (4, 4) supersymmetry, *i.e.*, both the left- and right-moving sectors are supersymmetric. Supersymmetry itself will not play any essential role in our discussion, but the existence of fermionic excitations in at least one of the two chiral sectors is important. For large numbers N_1 , N_5 , of D1 and D5 branes, the central charge of both sectors is $c = 6N_1N_5$. The CFT can have left- and right-moving excitations, with levels L_0 and \bar{L}_0 , corresponding to open string excitations propagating along the worldvolume of the branes. These give rise to a linear momentum P .

When the spatial direction along this D1-D5-P system is compactified on a circle of size $2\pi R$ (much larger than the other compact directions), we obtain a five-dimensional configuration. Typically, the state corresponding to a black hole has both sectors populated by thermal ensembles of excitations with temperatures T_L and T_R . If the two sectors interact only very weakly, the total entropy, energy and momentum are $S = S_L + S_R$, $E = P_L + P_R$ and $P = P_L - P_R$, with quantized momenta $P_{L,R} = N_{L,R}/R$. Since $T_{L,R}^{-1} = (\partial S_{L,R}/\partial P_{L,R}) = 2(\partial S_{L,R}/\partial E)_P$, it follows that the actual temperature $T_H^{-1} = (\partial S/\partial E)_P$ of the entire configuration is

$$T_H^{-1} = \frac{1}{2} (T_L^{-1} + T_R^{-1}) . \quad (4.1.1)$$

If any of the two sectors is in a ground state (either T_L or T_R vanish), the temperature of the entire system vanishes.

The simplest black hole corresponds to a thermal ensemble of excitations in only one of the two sectors, say the right-moving one. Supersymmetry of the left sector is then preserved, and $T_L = T_H = 0$. This is the static supersymmetric extremal black hole of ref. [47]. If both sectors are excited, then generically the system has $T_H \neq 0$. An open string excitation from the left sector can combine with an open string from the right sector, and form a closed string that propagates away into the bulk of spacetime. This is the microscopic counterpart of Hawking emission at temperature T_H [48, 63].

To include rotation, we take into account that the fermionic excitations of the left and right sectors are charged under the R-symmetry group $SU(2)_L \times SU(2)_R$ of the supersymmetric CFT.

¹And even to some that may not, like in the previous chapter, although in this case the bound (4.0.1) is recovered only up to numerical factors.

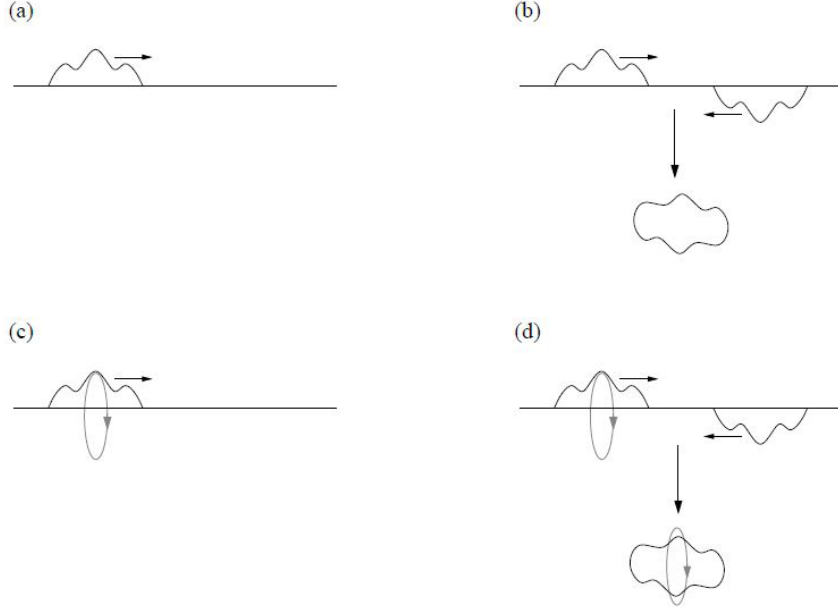


Figure 4.1: Four different kinds of black hole in the ‘effective string’ picture. The excitations of the two chiral sectors, with levels L_0 (left-moving) and \bar{L}_0 (right-moving), correspond to open strings attached to the brane bound state. (a) *Supersymmetric static black hole*: $L_0 = 0$, $\bar{L}_0 = N_R$: only the right-moving sector is excited. (b) *Near-supersymmetric static black hole*: $L_0 = N_L > 0$, $\bar{L}_0 = N_R > 0$. Left and right-moving excitations can annihilate to emit a closed string: this is Hawking radiation. (c) *Supersymmetric rotating black hole*: $L_0 = 0$, $\bar{L}_0 = N_R - 6J_R^2/c > 0$. The coherent polarization of right-moving fermions yields a macroscopic (self-dual) angular momentum J_R . In the absence of left-moving open strings, there cannot be any radiation of closed strings, hence there is no Hawking nor superradiant emission. (d) *Ergo-cold black hole*: $L_0 > 0$, and $\bar{L}_0 = N_R - 6J_R^2/c = 0$ with $N_R > 0$. The right-moving sector is a Fermi sea of polarized fermionic excitations, so the temperature vanishes. Open strings in this sector can interact with those in the left sector and emit closed strings that carry angular momentum: *the black hole possesses a superradiant ergosphere*. The superradiant bound on modes (4.0.1) is directly related to the energy of the Fermi level, and thus is a consequence of Fermi-Dirac statistics for the excitations of the CFT.

These R-symmetries generate the five-dimensional spatial rotation group $SO(4) \simeq SU(2)_L \times SU(2)_R$. So the R-charge corresponds to spacetime angular momentum, J_L or J_R , respectively for left and right fermions. If many of these fermions are coherently polarized we obtain a macroscopically large angular momentum. This projection into definite polarization shifts the levels as

$$L_0 = N_L - \frac{6J_L^2}{c} \quad \bar{L}_0 = N_R - \frac{6J_R^2}{c}, \quad (4.1.2)$$

and in particular the total entropy and temperature are reduced.

Observe now that there are two distinct ways of achieving an extremal ($T_H = 0$) rotating black hole. In the first one we set, say, $N_L = 0 = J_L$ (so half of the supersymmetry is preserved), $\bar{L}_0 > 0$, and some of the right-moving fermions polarized to give $J_R \neq 0$ [64]. Since only one of the two sectors is excited, the left and right-moving open strings cannot combine to emit a closed string. This fits nicely with the property that the horizon of the corresponding black hole remains static relative to asymptotic observers: since $\Omega_L = \Omega_R = 0$ there is no ergosphere nor superradiant emission, even if $J_R \neq 0$.

The second, less studied way to achieve a zero-temperature rotating black hole is by having the right-moving sector contain only polarized fermions that fill energy levels up until the Fermi level. This occurs when

$$N_R = \frac{6J_R^2}{c}. \quad (4.1.3)$$

This is a ground state, $\bar{L}_0 = 0$, at fixed J_R , with zero entropy and at zero-temperature. The left-moving sector is assumed to be thermally excited, with $L_0 > 0$: this provides for the entropy. Both sectors can carry angular momentum, so, in contrast to the supersymmetric case, the total angular momentum need not be self-dual nor anti-self-dual. More importantly, even if the system is at zero temperature, both left and right moving open strings are present and can annihilate to emit a closed string. Since the right-moving open string necessarily carries spin, so will also the emitted radiation. This is, qualitatively, what we expect from superradiant emission. In fact, the corresponding black hole possesses an ergosphere and superradiant emission is present. So we have found a qualitative microscopic picture for the superradiance from the ergo-cold black hole.

4.1.2 Microscopic derivation of the superradiant frequency bound

We can be more quantitative and recover the superradiant frequency bound from this microscopic picture. In five spacetime dimensions the black hole can rotate in two independent planes and if we label the rotation angles on these planes by ϕ and ψ then the bound (4.0.1) is generalized to

$$0 < \omega < m_\phi \Omega_\phi + m_\psi \Omega_\psi, \quad (4.1.4)$$

where $\Omega_{\phi,\psi}$ are the horizon angular velocities on each rotation plane, and $m_{\phi,\psi}$ the corresponding angular momentum (“magnetic”) quantum numbers. We may instead use the left and right Euler

angles $\psi_{L,R} = \phi \mp \psi$, in terms of which the bound is

$$0 < \omega < m_L \Omega_L + m_R \Omega_R, \quad (4.1.5)$$

with $m_{L,R} = \frac{1}{2}(m_\phi \mp m_\psi)$ and $\Omega_{L,R} = \Omega_\phi \mp \Omega_\psi$. This is slightly more convenient, since as we saw above these angles diagonalize the R-charges (*i.e.*, target-space spins) of the left and right-moving fermions of the CFT.

The ergo-cold black hole described above has $\Omega_R \neq 0$ and $\Omega_L = 0$ (although J_L need not vanish). So the bound is

$$0 < \omega < m_R \Omega_R, \quad (4.1.6)$$

i.e., m_L does not limit the frequencies. We wish to derive eq. (4.1.6) from our microscopic picture.

To begin with, we can easily obtain that at zero-temperature only one of Ω_L, Ω_R , can be different from zero. The two sectors of the CFT have negligible interaction, so $S(E, P, J_L, J_R) = S_L(E_L, J_L) + S_R(E_R, J_R)$. For each sector we have a chemical potential $\mu_{L,R}$ associated to the respective R-charges, *i.e.*, $J_{L,R}$, through

$$\frac{\mu_{L,R}}{T_{L,R}} = - \left(\frac{\partial S_{L,R}}{\partial J_{L,R}} \right)_{E_{L,R}}. \quad (4.1.7)$$

The angular velocities of the total system are in turn

$$\frac{\Omega_{L,R}}{T_H} = - \left(\frac{\partial S(E, P, J_L, J_R)}{\partial J_{L,R}} \right)_{E,P}, \quad (4.1.8)$$

where T_H is the total system's temperature (4.1.1). Hence

$$\Omega_{L,R} = \frac{T_H}{T_{L,R}} \mu_{L,R}, \quad (4.1.9)$$

and in the extremal limit in which $T_R \rightarrow 0$,

$$\Omega_R \rightarrow 2\mu_R, \quad \Omega_L \rightarrow 0. \quad (4.1.10)$$

As we explained above, for the ergo-cold black hole we take the right sector of the CFT to be populated by polarized fermions filling up to the Fermi level, so their number density distribution is a step function

$$\rho(\epsilon, j_R) = \Theta(j_R \mu_R - \epsilon). \quad (4.1.11)$$

Here ϵ is the energy and j_R the R-charge of the fermion, *i.e.*, spin in $SU(2)_R$, which in general can be $\pm 1/2$. We assume that in the state (4.1.11) they are all polarized with $j_R = +1/2$, to achieve maximum angular momentum, see (4.1.3). Using the chemical potential μ_R introduced above, the Fermi energy is

$$\epsilon_{\text{Fermi}} = \frac{\mu_R}{2} = \frac{\Omega_R}{4}. \quad (4.1.12)$$

In this state it is possible to have a collision of left and right-moving open strings creating a closed string massless scalar mode. Our aim is to show that if this scalar has frequency ω and angular momentum numbers ℓ , m_R and m_L , then ω must lie in the range (4.1.6). In order for the scalar to escape to infinity its energy must be positive, so we need only derive the upper bound in (4.1.6).

The interaction vertex involves bosonic and fermionic open strings from each sector, in either the initial or final states. But the spin of the scalar is provided only by fermions. For a given ℓ the angular momentum of the scalar is in the $(\ell/2, \ell/2)$ representation of $SU(2)_L \times SU(2)_R$, *i.e.*, $|m_L|, |m_R| \leq \ell/2$, so we need ℓ fermionic open strings from each sector to match the spin quantum numbers of the scalar. A minimal scalar at s-wave ($\ell = 0$) couples to an operator of conformal dimension $(1, 1)$, typically of the form $\partial_+ X \partial_- X$, *i.e.*, one boson from each sector. Then, at the ℓ^{th} partial wave it will couple to this boson pair and to the ℓ fermion pairs. Additional bosons may be involved, but then the amplitudes are suppressed by higher powers of the coupling and the frequency, although we need not assume their absence.

For our system, the right-sector open strings in the initial-state in the interaction can only be fermionic with $j_R = +1/2$. The fermions in the final state can have either $j_R = \pm 1/2$: we take the numbers of each kind of these to be n_{\pm} , so the number of initial fermions from the right sector is $\ell - n_+ - n_-$. The balance of angular momentum in the interaction is then

$$\frac{1}{2}(\ell - n_+ - n_-) = m_R + \frac{1}{2}n_+ - \frac{1}{2}n_-, \quad (4.1.13)$$

i.e., the closed string is emitted with

$$m_R = \frac{\ell}{2} - n_+. \quad (4.1.14)$$

We will not need to consider any specific properties of the left-moving modes in our analysis.

Both the left and right sectors contribute an equal amount $\omega/2$ to the energy of the emitted closed string — otherwise the latter would carry the difference as a net momentum: this more general case will be dealt with later below. The energy-budget of the interaction in the right sector is then

$$\omega_R^{(f)\text{in}} = \frac{\omega}{2} + \omega_R^{(f)\text{out}} + \omega_R^{(b)}, \quad (4.1.15)$$

where f and b denote fermionic and bosonic open strings. In the lhs of this equation we have the energy of the $\ell - n_+ - n_-$ initial fermions. Since their energy levels are bounded above by the Fermi energy (4.1.12), we have

$$\omega_R^{(f)\text{in}} \leq (\ell - n_+ - n_-)\epsilon_{\text{Fermi}} = (\ell - n_+ - n_-)\frac{\Omega_R}{4}. \quad (4.1.16)$$

As for the final fermions, the energies of the n_- fermions with $j_R = -1/2$ are not constrained other than to be positive: they may fill states with less or more energy than ϵ_{Fermi} . But the n_+ fermions

with $j_R = +1/2$ must have energies above the Fermi level, since in the initial configuration the levels below ϵ_{Fermi} are all filled with positive-spin fermions. This sets a lower bound

$$\omega_R^{(f)\text{out}} > n_+ \frac{\Omega_R}{4}. \quad (4.1.17)$$

The energy of the bosonic open strings is only constrained to be positive, $\omega_R^{(b)} > 0$. Then, eq. (4.1.15), together with (4.1.14), (4.1.16) and (4.1.17), yields the inequality

$$\omega < m_R \Omega_R - \frac{n_-}{2} \Omega_R \leq m_R \Omega_R, \quad (4.1.18)$$

which reproduces exactly the superradiant bound (4.1.6) derived for the rotating black hole². Note that this result follows essentially from Pauli's exclusion principle for the polarized fermions in the initial state: *the superradiant bound on frequencies is a consequence of Fermi-Dirac statistics for the carriers of angular momentum in the dual CFT.*

Note that at least one bosonic open string must appear in the right-sector in the final state, so the system will not remain extremal after it begins to radiate. This is also just like we anticipated from the supergravity side.

The left-moving fermions, which can contribute arbitrarily to m_L , have not played any role in this derivation. This is in accord with the fact that when $\Omega_L = 0$ (even if $J_L \neq 0$), m_L does not appear in the macroscopically-derived bound (4.1.4).

4.1.3 Four-dimensional black holes

This analysis applies almost immediately to the four-dimensional black holes described by a dual chiral $(0, 4)$ CFT. Only the right sector is supersymmetric so the R-symmetry consists of a single $SU(2)$ group. This corresponds to the four-dimensional rotation group $SU(2) \simeq SO(3)$. Again, non-BPS extremal rotating black holes exist, with four charges, that possess an ergosphere and the accompanying superradiant modes satisfying (4.0.1). The dual microscopic state is essentially the same as above: the right sector is filled up to $\epsilon_{\text{Fermi}} = \Omega_H/4$ with fermions with $j = +1/2$, while the left sector is in a thermal ensemble and accounts for the entropy. The emission of a closed string massless scalar with quantum numbers (ω, ℓ, m) involves 2ℓ right-sector fermions since now $|m| \leq \ell$. So (4.1.14) is replaced by

$$m = \ell - n_+. \quad (4.1.19)$$

There is also one boson from the right sector in the final state of the interaction. From the left sector the only requirement is an operator of conformal dimension $\Delta_L = 1 + \ell$. Following the

²The bound is as close as possible to saturation when $n_- = 0$, the boson energy $\omega_R^{(b)}$ is minimal (set by the gap $\sim 1/N_1 N_5 R$), and all fermions are the closest possible to the Fermi energy (*i.e.*, within $\sim 1/N_1 N_5 R$ of it). If $n_- > 0$ then this closest value to the bound cannot be achieved.

steps above we find

$$\omega < m\Omega_H - \frac{n_-}{2}\Omega_H \leq m\Omega_H. \quad (4.1.20)$$

Thus eq. (4.0.1) has been derived microscopically for this ergo-cold black hole.

4.1.4 Other systems with ergoregion

It seems likely that the basic features of our microscopic picture are also valid for any other gravitating object with a cold ergoregion. The most familiar of these is the extremal Kerr black hole. Ref. [52] exhibited in a striking way how the absorption rates from a Kerr black hole contained hints of a CFT description. That this CFT must contain fermions as the carriers of angular momentum seems difficult to dispense with, if one wants to account for superradiant emission. Indeed, the results presented in Chapter 3 together with those in [30] provide a microscopic model for the extremal five-dimensional Myers-Perry black holes. A microscopic model for the extremal Kerr black hole has been proposed too [50]. These black holes are mapped, through symmetries and dualities, to four-dimensional black holes of the kind we have discussed in Section 4.1.3. So the presence of superradiant emission in these neutral black holes is understood, at least qualitatively, in the same terms we have discussed: a filled Fermi sea in one sector of the dual CFT. The quantitative recovery of the superradiant bound is nevertheless not expected, since these neutral black holes suffer non-trivial renormalizations of their masses and energy levels (though not of their entropies) as a function of the coupling.

Systems with cold ergoregions which are not U-dual to these black holes are perhaps of more interest to test the applicability of our ideas about the microphysics of superradiance. An instance of this are the extremal rotating black rings with a dipole, in particular those in which the dipole charge corresponds to a fundamental string and the extremal limit is singular. The microscopic description of this dipole ring has been described recently in [65], and argued to possess the right properties to fit our picture for a superradiating system: a zero-temperature sector with angular momentum carriers, which can interact with excitations from another sector and emit a spinning closed string into the bulk.

All these ergo-cold black holes provide, in a sense, cleaner laboratories for the study of quantum emission from a black hole, closely similar to Hawking radiation, than do non-extremal black holes. Since one of their sectors is in a ground state, they are in a purer, less mixed state than non-extremal systems. But still, their other sector is in a mixed, thermal ensemble. Therefore it would be very interesting to consider states of the CFT such that both sectors are in pure states but nevertheless they can interact and decay by bulk emission. One such example is provided by the non-supersymmetric smooth supergravity solitons with D1-D5-P charges in [66]. On the microscopic side, they correspond to non-chiral spectral flows of the Neveu-Schwarz ground state to non-BPS states in the Ramond sector. The states have both sectors containing only spin-carrying fermions. So we see that an interaction between the two sectors will result into

the emission of a spinning bulk scalar. Following the overall picture proposed in this chapter, superradiance is naturally expected. Indeed, these supergravity solitons have ergoregions (but not horizons) that have been shown to exhibit a superradiant instability [67]. A correspondence between the two pictures of the decay of precisely this type has been worked out in detail very recently in [68], and conforms to the overall ideas we have proposed.

4.1.5 No superradiant emission of linear momentum

We can also consider the emission of closed strings that carry away some of the momentum P of the D1-D5-P system. This is also of interest, as the momentum corresponds to one of the three charges of the black hole and there is a charge-ergoregion associated to it. From the six-dimensional perspective, the horizon of the black string is moving with velocity V_H along the string direction y , and the superradiance bound for a mode $\sim \exp(-i\omega t + ipy + im_L\psi_L + im_R\psi_R)$ is modified to

$$p < \omega < m_L\Omega_L + m_R\Omega_R + pV_H. \quad (4.1.21)$$

In the non-BPS extremal rotating limit that we study, the black hole has $\Omega_L \rightarrow 0$. For a generic D1-D5-P black hole the velocity is $|V_H| \leq 1$, but we are particularly interested in the decoupling limit in which the D1 and D5 charges of the black hole are much larger than its momentum or the energy above the BPS bound. In this limit, the ergo-cold black hole has $V_H \rightarrow 1$, so the bound becomes

$$0 < \omega - p < m_R\Omega_R. \quad (4.1.22)$$

We can easily derive this again from microscopic considerations. First note that the first law of thermodynamics gives

$$\frac{V_H}{T_H} = - \left(\frac{\partial S}{\partial P} \right)_E. \quad (4.1.23)$$

Reasoning as we did when deriving (4.1.1) for a two-sector system, we find

$$V_H = \frac{T_H}{2} (T_R^{-1} - T_L^{-1}) = \frac{T_L - T_R}{T_L + T_R}, \quad (4.1.24)$$

so $V_H \rightarrow 1$ when $T_R \rightarrow 0$. Also observe that in any case $|V_H| \leq 1$.

The left and right-moving open strings that interact to emit a closed string of frequency ω and momentum p do not in this case have the same energy, but instead

$$\epsilon_{L,R} = \frac{\omega \pm p}{2}. \quad (4.1.25)$$

We can follow now the same arguments for the right-sector dynamics that we used above, only changing $\omega/2 \rightarrow \epsilon_R$. Hence we obtain

$$\omega - p < m_R\Omega_R. \quad (4.1.26)$$

In order to complete the derivation of (4.1.22) we need only notice that if the closed string is to arrive at infinity as an on-shell, propagating state, it must satisfy $\omega > 0$ and $\omega^2 - p^2 \geq 0$, *i.e.*, $\omega \geq |p| \geq p$.

This implies that there cannot be any superradiant emission of linear momentum (*i.e.*, P charge in five dimensions) unless angular momentum is radiated as well. This is in spite of the fact that in the black hole geometry there is a momentum ergoregion, even in the absence of rotation. From the supergravity point of view, the reason for this difference between the emission of linear and angular momentum is that in the former case the contribution to the effective potential for scalar propagation coming from the momentum does not fall off at infinity but creates an asymptotic potential barrier of height p , so if $\omega < |p|$ the wave is asymptotically exponentially suppressed.

Put another way, in a KK reduction to five dimensions the scalar has mass $|p|$ and a propagating wave at infinity must satisfy $\omega > |p|$. So a would-be superradiant momentum mode, satisfying $\omega < pV_H$, cannot escape to infinity since $V_H \leq 1$: if emitted, it gets reflected back off to the black hole by the effective potential. In contrast, the centrifugal potential barriers fall off faster at large distances: the spin does not affect the dispersion relation of the wave at infinity. From the microscopic perspective, there is a possible interaction vertex for the emission of a scalar with linear momentum and zero angular momentum: take an initial state with only a left-moving boson, and a final state with a right-moving boson and a bulk scalar. However, in this case the scalar would have $\omega < |p|$ and therefore could only exist as a virtual excitation³.

4.1.6 Superradiant amplification, extremal and non-extremal

We have obtained a microscopic picture for the spontaneous emission of superradiant scalars off an extremal non-BPS rotating black hole — the ergo-cold black hole. It is clear now that, if there is an incident flux of this scalar field on the black hole, then those modes that satisfy the bound (4.0.1) will undergo stimulated emission. This is simply the familiar phenomenon that the amplitude to emit a boson is amplified by a factor $\sqrt{N+1}$ if the final state already contains N bosons. This is, superradiant amplification follows conventionally from the relation between Einstein's A and B coefficients. For a classical incident wave, *i.e.*, with large bosonic occupation number N , the stimulated emission is then a classical process.

In more detail, in our system at zero temperature we have argued that superradiant modes, and only them, can be emitted and have a finite decay rate $\Gamma_{\ell m}(\omega)$. Moreover, the system cannot absorb any superradiant mode: if in the argument that lead to the superradiant bound (4.1.6) we change the scalar from the final to the initial state, *i.e.*, $\omega \rightarrow -\omega$, $m_R \rightarrow -m_R$, we see that absorption of this scalar can only happen when $\omega > m_R \Omega_R$. So, for an incident flux \mathcal{F}_{in} , detailed

³An alternative interpretation is in terms of charge superradiance: an extremal Reissner-Nordstrom black hole can spontaneously emit particles of charge e and mass m only if $|e| > m$ [69]. In our case, the 5D mass and KK electric charge of the particles are both equal to p .

balance yields a total absorption cross section of superradiant modes $\sigma_{\ell m}(\omega) = -\Gamma_{\ell m}(\omega)/\mathcal{F}_{\text{in}} < 0$.

The absorption cross section determines the ratio between the outgoing and ingoing fluxes as

$$\frac{\mathcal{F}_{\text{out}}}{\mathcal{F}_{\text{in}}} = 1 - \frac{\omega^3}{(\ell + 1)^2 4\pi} \sigma_{\ell m}, \quad (4.1.27)$$

(this is the relation in five dimensions, see [54] for generic dimension). Superradiant modes, and only them, have $\sigma_{\ell m} < 0$, and therefore yield $\mathcal{F}_{\text{out}} > \mathcal{F}_{\text{in}}$, as desired.

This argument shows that the extremal rotating system that we study exhibits classical stimulated amplification for those modes that it can spontaneously decay into, *i.e.*, modes that satisfy (4.1.6). What happens away from extremality? In this case, the system can spontaneously emit modes of any frequency by the microscopic dual of Hawking radiation. Why, then, is there superradiant amplification only for modes that satisfy (4.1.6)? The reason is known: the first law, applied to an emission process from the black hole with $\delta E = -\omega$ and $\delta J = -m$, states that

$$\frac{\kappa}{8\pi G} \delta \mathcal{A}_H = -(\omega - m\Omega_H). \quad (4.1.28)$$

Then, the classical stimulated emission of a mode with $\omega > m\Omega_H$ would violate the area law $\delta \mathcal{A}_H \geq 0$ [57]. So, classically, the emission of such non-superradiant modes is strictly forbidden, while microscopically it is allowed but statistically suppressed by a factor

$$e^{\delta S} = e^{-(\omega - m\Omega_H)/T_H}. \quad (4.1.29)$$

This is of course the Boltzmann factor for Hawking radiation.

Sometimes the existence of the superradiant frequency bound (4.0.1) is presented as a consequence of the area law. But we see that the latter is important only in constraining the classical, macroscopic process. Entropic considerations did not play any role in our microscopic analysis, which nevertheless shows that the superradiant bound on modes holds strictly at the microscopic level for emission at zero temperature.

4.2 Emission rates: supergravity analysis

The preceding analysis has provided a qualitative origin of the superradiant ergoregion in rotating black holes at zero temperature. We have also given a quantitative elementary derivation of the superradiant frequency bound. A more precise match between the two descriptions is obtained when one considers the actual emission rates.

To do so, in this section we carry out the supergravity computation of absorption cross sections and Hawking and superradiant emission rates for a minimal scalar. We consider the most general case where the black hole has all charges and rotations turned on, and the scalar has generic quantum numbers for the frequency, spins, and linear momentum along the S^1 string direction. At the end of the section we particularize to the ergo-cold black hole in order to isolate the effects of the ergosphere.

4.2.1 The D1-D5-P family of black holes

The D1-D5-P black hole solutions belong to type IIB supergravity compactified to five dimensions on $T^4 \times S^1$. The T^4 is assumed to be much smaller than the S^1 so we view the system as a six-dimensional black string. The most general solution is described by eight parameters: a parameter M_0 that measures deviation away from supersymmetry; two spin parameters for rotation in two orthogonal planes, a_1, a_2 ; three ‘boost’ parameters, $\delta_1, \delta_5, \delta_p$, which fix the D1-brane, D5-brane and momentum charges, respectively; and two moduli: the radius R of the S^1 , and the volume V of the T^4 . We choose units such that the five-dimensional Newton constant is $G_5 = G_{10}/2\pi RV \equiv \pi/4$.

The metric of the six-dimensional black string is [43, 70, 71]

$$\begin{aligned}
ds^2 = & -\frac{f}{\sqrt{H_1 H_5}}(dt^2 - dy^2) + \frac{M_0}{\sqrt{H_1 H_5}}(s_p dy - c_p dt)^2 \\
& + \sqrt{H_1 H_5} \left(\frac{r^2 dr^2}{(r^2 + a_1^2)(r^2 + a_2^2) - M_0 r^2} + d\theta^2 \right) \\
& + \left(\sqrt{H_1 H_5} - (a_2^2 - a_1^2) \frac{(H_1 + H_5 - f) \cos^2 \theta}{\sqrt{H_1 H_5}} \right) \cos^2 \theta d\psi^2 \\
& + \left(\sqrt{H_1 H_5} + (a_2^2 - a_1^2) \frac{(H_1 + H_5 - f) \sin^2 \theta}{\sqrt{H_1 H_5}} \right) \sin^2 \theta d\phi^2 \\
& - \frac{M_0}{\sqrt{H_1 H_5}} (a_1 \cos^2 \theta d\psi + a_2 \sin^2 \theta d\phi)^2 \\
& - \frac{2M_0 \cos^2 \theta}{\sqrt{H_1 H_5}} [(a_1 c_1 c_5 c_p - a_2 s_1 s_5 s_p) dt + (a_2 s_1 s_5 c_p - a_1 c_1 c_5 s_p) dy] d\psi \\
& - \frac{2M_0 \sin^2 \theta}{\sqrt{H_1 H_5}} [(a_2 c_1 c_5 c_p - a_1 s_1 s_5 s_p) dt + (a_1 s_1 s_5 c_p - a_2 c_1 c_5 s_p) dy] d\phi, \quad (4.2.1)
\end{aligned}$$

where we use the notation $c_i \equiv \cosh \delta_i$, $s_i \equiv \sinh \delta_i$, and

$$\begin{aligned}
f(r) &= r^2 + a_1^2 \sin^2 \theta + a_2^2 \cos^2 \theta, \quad H_i(r) = f(r) + M_0 s_i^2, \quad \text{with } i = 1, 5, \\
g(r) &= (r^2 + a_1^2)(r^2 + a_2^2) - M_0 r^2. \quad (4.2.2)
\end{aligned}$$

The dilaton and 2-form RR gauge potential will not be needed and can be found in [71]. We assume without loss of generality⁴

$$a_1 \geq a_2 \geq 0. \quad (4.2.3)$$

Depending on the value of the parameters, the geometry can describe a black hole, a naked singularity, a smooth soliton or a conical singularity [66]. The black hole family of solutions is described by the range $M_0 \geq (a_1 + a_2)^2$ and has horizons at $g(r) = 0$,

$$r_{\pm}^2 = \frac{1}{2} (M_0 - a_1^2 - a_2^2) \pm \frac{1}{2} \sqrt{(M_0 - a_1^2 - a_2^2)^2 - 4a_1^2 a_2^2}. \quad (4.2.4)$$

⁴The simultaneous exchange $a_1 \rightarrow -a_1$, $\delta_p \rightarrow -\delta_p$, $y \rightarrow -y$ and $\psi \rightarrow -\psi$ is a symmetry of the solution. The same is true for $a_2 \rightarrow -a_2$, $\delta_p \rightarrow -\delta_p$, $y \rightarrow -y$ and $\phi \rightarrow -\phi$. So the solutions with $a_1 a_2 \leq 0$ are physically equivalent to the solutions with $a_1 a_2 \geq 0$. For definiteness we assume the latter.

We are particularly interested in the existence of an ergoregion, whose properties were discussed in [66]. The norm of the Killing vector ∂_t ,

$$|\partial_t|^2 = -\frac{f - M_0 c_p^2}{\sqrt{H_1 H_5}}, \quad (4.2.5)$$

becomes spacelike for $f(r) < M_0 c_p^2$. This defines a six-dimensional ergoregion, which includes not only the effects of rotation but also of the linear motion of the string. As we mentioned above, and will prove below, the latter does not actually contribute to superradiance. It is therefore more convenient to consider the vector $\zeta = \partial_t + \tanh \delta_p \partial_y$ such that, upon dimensional reduction (so linear momentum becomes charge), its orbits define static asymptotic observers in the five-dimensional black hole geometry, and whose causal character is therefore associated to the rotation ergosphere. Specifically, its norm

$$|\zeta|^2 = -\frac{f - M_0}{\sqrt{H_1 H_5}}, \quad (4.2.6)$$

becomes spacelike for $f(r) < M_0$ so a rotational ergosphere appears at $f(r) = M_0$.

The ADM mass M , the angular momenta (J_ϕ, J_ψ) and the gauge charges (Q_1, Q_5, Q_p) are

$$\begin{aligned} M &= \frac{M_0}{2} [\cosh(2\delta_1) + \cosh(2\delta_5) + \cosh(2\delta_p)], \\ J_\phi &= M_0 (a_2 c_1 c_5 c_p - a_1 s_1 s_5 s_p), \\ J_\psi &= M_0 (a_1 c_1 c_5 c_p - a_2 s_1 s_5 s_p), \\ Q_i &= M_0 s_i c_i, \quad i = 1, 5, p. \end{aligned} \quad (4.2.7)$$

The horizon angular velocities $\Omega_{\phi, \psi}$ along the Cartan angles of $SO(4)$, ϕ and ψ , are more conveniently written in terms of the Euler left and right rotations in $U(1)_L \times U(1)_R \subset SU(2)_L \times SU(2)_R \simeq SO(4)$,

$$\Omega_{\phi, \psi} = \frac{1}{2} (\Omega_R \pm \Omega_L), \quad \Omega_{R,L} = \frac{2\pi}{\beta_H} \frac{a_2 \pm a_1}{[M_0 - (a_2 \pm a_1)^2]^{1/2}}. \quad (4.2.8)$$

Following [60], from the surface gravities of the inner and outer horizons κ_\pm we introduce the temperatures $\beta_{L,R} = 1/T_{L,R}$

$$\beta_{R,L} = \frac{2\pi}{\kappa_+} \pm \frac{2\pi}{\kappa_-}, \quad \frac{1}{\kappa_\pm} = \frac{M_0}{2} \left[\frac{c_1 c_5 c_p + s_1 s_5 s_p}{[M_0 - (a_2 + a_1)^2]^{1/2}} \pm \frac{c_1 c_5 c_p - s_1 s_5 s_p}{[M_0 - (a_2 - a_1)^2]^{1/2}} \right]. \quad (4.2.9)$$

Observe that the Hawking temperature of the outer horizon is related to $T_{L,R}$ as in (4.1.1). Similarly, from the areas of the inner and outer horizons we introduce $S_{L,R}$ such that

$$S = S_L + S_R, \quad S_{R,L} = \pi M_0 (c_1 c_5 c_p \mp s_1 s_5 s_p) [M_0 - (a_2 \pm a_1)^2]^{1/2}. \quad (4.2.10)$$

The horizon of the black string is also moving relative to asymptotic observers that follow orbits of ∂_t . We can compute the linear velocities for both the inner and outer horizons

$$V_{\pm} = \frac{\pi M_0}{\beta_H} \left[\frac{c_1 c_5 s_p + s_1 s_5 c_p}{[M_0 - (a_2 + a_1)^2]^{1/2}} \pm \frac{c_1 c_5 s_p - s_1 s_5 c_p}{[M_0 - (a_2 - a_1)^2]^{1/2}} \right], \quad (4.2.11)$$

and introduce

$$V_{R,L} = -\frac{\beta_H}{\beta_{R,L}} (V_+ \pm V_-). \quad (4.2.12)$$

In terms of these, the velocity of the outer horizon, V_+ , which we also denote as V_H , is

$$V_H = -\frac{T_H}{2} \left(\frac{V_L}{T_L} + \frac{V_R}{T_R} \right). \quad (4.2.13)$$

These velocities become much simpler in the decoupling limit where the D1 and D5 boosts are very large so the system is near-supersymmetric, the numbers of anti-D1 and anti-D5 branes are suppressed, and we can make contact with the dual CFT. In this regime we approximate $c_{1,5} \simeq s_{1,5} \simeq e^{\delta_{1,5}}/2$ and we find that

$$V_{L,R} \rightarrow \pm 1, \quad (4.2.14)$$

which is microscopically interpreted as the fact that the momentum excitations are chiral and massless⁵. Observe that in this regime we recover eq. (4.1.24), which we had derived from the microscopic two-sector system. The role that the inner horizon plays in defining the microscopic magnitudes associated to the two chiral sectors, emphasized in [60], is very intriguing and not well understood.

During the remainder of this section we will not need to restrict ourselves to this near-supersymmetric regime. But our main interest lies in extremal rotating black hole solutions. These correspond to degenerate horizons, which appear when the two roots r_{\pm} coincide. From (4.2.4) we identify two possibilities:

- The BPS black hole.

Obtained by taking the limit $M_0 \rightarrow 0$, $a_{1,2} \rightarrow 0$, keeping the mass, angular momenta and charges finite, which requires $\delta_{1,5,p} \rightarrow \infty$. In this limit

$$T_R \rightarrow 0, \quad T_L \neq 0, \quad S_R \rightarrow 0, \quad S_L \neq 0, \quad \Omega_{L,R} \rightarrow 0, \quad -V_R, V_L \rightarrow V_H \rightarrow 1. \quad (4.2.15)$$

Also, $J_{\phi} + J_{\psi} \rightarrow 0$, the BPS bound is saturated, the solution is supersymmetric, and the timelike Killing vector that becomes null at the horizon is globally defined, so there is no ergoregion. This is also clear from (4.2.6). This is the BMPV black hole.

⁵We are taking left velocities and momenta as positive.

- The ergo-cold black hole.

Obtained in the limit

$$M_0 \rightarrow (a_1 + a_2)^2, \quad (4.2.16)$$

in which $T_H \rightarrow 0$ but now keeping $\Omega_R \neq 0$. Since $M_0 \neq 0$ the BPS bound is not saturated and supersymmetry is absent. In this limit,

$$T_R \rightarrow 0, T_L \neq 0, \quad S_R \rightarrow 0, S_L \neq 0, \quad \Omega_L \rightarrow 0, \Omega_R \neq 0, \quad -V_R \rightarrow V_H, \quad (4.2.17)$$

while V_L takes no particular value (unless we take the decoupling limit) and the conserved charges M , Q_i and $J_{\psi,\phi}$ are unconstrained other than by the extremality condition. The horizon does rotate relative to asymptotic observers, and there is an ergosphere, determined by $f(r) = (a_1 + a_2)^2$; see (4.2.6). Observe that in contrast to the BMPV solution, J_ϕ and J_ψ are independent of each other.

The BMPV black hole has been thoroughly studied, and it will only serve us to emphasize the differences with the ergo-cold black hole, which is our system of choice for the study of superradiance.

4.2.2 Absorption cross section and emission rate

We consider a minimal scalar field, typically a graviton with polarization in the internal T^4 in the compactification of the IIB theory to six dimensions. The field satisfies the massless Klein-Gordon equation in the general three-charge black string geometry,

$$\partial_\mu (\sqrt{-g} g^{\mu\nu} \partial_\nu \Phi) = 0. \quad (4.2.18)$$

Introducing the ansatz

$$\Phi = \exp[-i\omega t + ipy + im_\psi \psi + im_\phi \phi] \chi(\theta) h(r), \quad (4.2.19)$$

and the separation constant Λ , the wave equation can be separated. The angular equation is

$$\frac{1}{\sin 2\theta} \frac{d}{d\theta} \left(\sin 2\theta \frac{d\chi}{d\theta} \right) + \left[\Lambda - \frac{m_\psi^2}{\cos^2 \theta} - \frac{m_\phi^2}{\sin^2 \theta} + (\omega^2 - p^2)(a_1^2 \sin^2 \theta + a_2^2 \cos^2 \theta) \right] \chi = 0. \quad (4.2.20)$$

This angular equation (plus regularity requirements) is a Sturm-Liouville problem, and the solutions are higher-dimensional spin-weighted spheroidal harmonics. We can label the corresponding eigenvalues Λ with an index ℓ , $\Lambda(\omega) = \Lambda_\ell(\omega)$ and therefore the wavefunctions form a complete set over the integer ℓ . In the general case, the problem consists of two coupled second order differential equations: given some boundary conditions, one has to compute simultaneously both values of ω and Λ that satisfy these boundary conditions. However, for vanishing a_i^2 we get the

(five-dimensional) flat space result, $\Lambda = \ell(\ell + 2)$, and the associated angular functions are given by Jacobi polynomials. For non-zero, but small $(\omega^2 - p^2)a_i^2$ we have

$$\Lambda = \ell(\ell + 2) + \mathcal{O}(a_i^2(\omega^2 - p^2)). \quad (4.2.21)$$

The integer ℓ is constrained to be $\ell \geq |m_\phi| + |m_\psi|$, and can only take even (odd) values when $|m_\phi| + |m_\psi|$ is even (odd) [72]—this follows from the fact that the scalar ℓ^{th} wave is in the $(\ell/2, \ell/2)$ of $SU(2)_R \times SU(2)_L$. The angular coordinates ϕ, ψ are periodic with period 2π so m_ϕ, m_ψ must take integer values. Our waves have positive frequency $\omega > 0$.

The radial wave equation can be written in a form that is particularly appropriate to find its solutions. Introduce the new radial coordinate

$$x = \frac{r^2 - \frac{1}{2}(r_+^2 + r_-^2)}{r_+^2 - r_-^2}, \quad (4.2.22)$$

which maps $r = (r_-, r_+, \infty) \leftrightarrow x = (-1/2, 1/2, \infty)$. Introduce also

$$m_{L,R} = \frac{1}{2}(m_\phi \mp m_\psi). \quad (4.2.23)$$

The radial wave equation is then

$$\begin{aligned} \partial_x \left[\left(x - \frac{1}{2} \right) \left(x + \frac{1}{2} \right) \partial_x h \right] + \frac{1}{4} [(\omega^2 - p^2)(r_+^2 - r_-^2)x - (\Lambda - U)] h \\ + \frac{1}{4} \left[\frac{\Sigma_+^2}{(x - \frac{1}{2})} - \frac{\Sigma_-^2}{(x + \frac{1}{2})} \right] h = 0, \end{aligned} \quad (4.2.24)$$

where we defined

$$\begin{aligned} \Sigma_\pm &= \frac{\omega}{\kappa_\pm} \mp m_L \frac{\Omega_L}{\kappa_+} - m_R \frac{\Omega_R}{\kappa_+} - p \frac{V_\pm}{\kappa_+}, \\ U &= (\omega^2 - p^2) \left[\frac{1}{2}(r_+^2 + r_-^2) + M_0(s_1^2 + s_5^2) \right] + (\omega c_p + p s_p)^2 M_0. \end{aligned} \quad (4.2.25)$$

Equation (4.2.24) was first written (though in a much less compact form) in [73]. For $p = 0$ there is no dynamics associated to the sixth direction and (4.2.24) reduces to the wave equation studied in [60] for the scattering of a neutral scalar off the five-dimensional D1-D5-P black hole.

Near-region wave equation and solution

In the near-region, the term $p^2(r_+^2 - r_-^2)x$ is suppressed and the radial wave equation reduces to

$$\partial_x \left[\left(x - \frac{1}{2} \right) \left(x + \frac{1}{2} \right) \partial_x h \right] + \frac{1}{4} \left[-(\Lambda - U) + \frac{\Sigma_+^2}{(x - \frac{1}{2})} - \frac{\Sigma_-^2}{(x + \frac{1}{2})} \right] h = 0. \quad (4.2.26)$$

To find the analytical solution of this equation, define the new radial coordinate,

$$z = x + \frac{1}{2}, \quad r = (r_-, r_+, \infty) \leftrightarrow x = (-1/2, 1/2, \infty) \leftrightarrow z = (0, 1, \infty), \quad (4.2.27)$$

and introduce the new wavefunction

$$h = z^{-i\frac{1}{2}\Sigma_-} (z-1)^{-i\frac{1}{2}\Sigma_+} F. \quad (4.2.28)$$

The near-region radial wave equation can then be written as

$$z(1-z)\partial_z^2 F + \left[(1-i\Sigma_-) - [2-i(\Sigma_+ + \Sigma_-)]z \right] \partial_z F + \left[i\frac{1}{4}(\Sigma_+ + \Sigma_-)[2-i(\Sigma_+ + \Sigma_-)] + (\Lambda - U) \right] F = 0, \quad (4.2.29)$$

which is a standard hypergeometric equation [74], $z(1-z)\partial_z^2 F + [c - (a+b+1)z]\partial_z F - abF = 0$, with

$$a = \xi - \frac{i}{2}(\Sigma_+ + \Sigma_-), \quad b = 1 - \xi - \frac{i}{2}(\Sigma_+ + \Sigma_-), \quad c = 1 - i\Sigma_-, \quad (4.2.30)$$

where we defined

$$\xi = \frac{1}{2} \left(1 + \sqrt{1 + \Lambda - U} \right). \quad (4.2.31)$$

Its most general solution in the neighborhood of $z = 1$ (*i.e.*, $r = r_+$) is $A_H^{in} z^{-b} F(b, b-c+1, a+b-c+1, \frac{z-1}{z}) + A_H^{out} z^{a-c} (z-1)^{c-a-b} F(c-a, 1-a, c-a-b+1, \frac{z-1}{z})$. Using (4.2.28), one finds that the solution of the near-region equation is

$$h = A_H^{in} \left(x - \frac{1}{2} \right)^{-i\frac{1}{2}\Sigma_+} \left(x + \frac{1}{2} \right)^{-\xi + i\frac{1}{2}\Sigma_+} F \left(b, b-c+1, a+b-c+1, \frac{x-\frac{1}{2}}{x+\frac{1}{2}} \right) + A_H^{out} \left(x - \frac{1}{2} \right)^{+i\frac{1}{2}\Sigma_+} \left(x + \frac{1}{2} \right)^{-\xi} F \left(c-a, 1-a, c-a-b+1, \frac{x-\frac{1}{2}}{x+\frac{1}{2}} \right). \quad (4.2.32)$$

The first term represents an ingoing wave at the horizon $x = \frac{1}{2}$, while the second term represents an outgoing wave at the horizon. The computation of the absorption cross-section is a classical problem where outgoing waves at the horizon are forbidden, so we set $A_H^{out} = 0$. Furthermore, we need the large r , $x \rightarrow \infty$ behavior of the ingoing near-region solution. We use the $z \rightarrow 1-z$ transformation law for the hypergeometric function [74],

$$F \left(b, b-c+1, a+b-c+1, \frac{x-\frac{1}{2}}{x+\frac{1}{2}} \right) = \frac{\Gamma(a+b-c+1)\Gamma(a-b)}{\Gamma(a-c+1)\Gamma(a)} F \left(b, b-c+1, -a+b+1, \frac{1}{x+\frac{1}{2}} \right) + \left(x + \frac{1}{2} \right)^{a-b} \frac{\Gamma(a+b-c+1)\Gamma(-a+b)}{\Gamma(b)\Gamma(b-c+1)} F \left(a-c+1, a, a-b+1, \frac{1}{x+\frac{1}{2}} \right), \quad (4.2.33)$$

the property $F(a, b, c, 0) = 1$, and $x \pm \frac{1}{2} \sim x$. The large x behavior of the ingoing near-horizon solution is then

$$h \sim A_H^{in} \left[\frac{\Gamma[1 - i\Sigma_+] \Gamma[1 - 2\xi]}{\Gamma[1 - \xi - i\frac{1}{2}(\Sigma_+ - \Sigma_-)] \Gamma[1 - \xi - i\frac{1}{2}(\Sigma_+ + \Sigma_-)]} x^{-\xi} + \frac{\Gamma[1 - i\Sigma_+] \Gamma[1 - 2\xi]}{\Gamma[\xi - i\frac{1}{2}(\Sigma_+ - \Sigma_-)] \Gamma[\xi - i\frac{1}{2}(\Sigma_+ + \Sigma_-)]} x^{\xi-1} \right]. \quad (4.2.34)$$

Far-region wave equation and solution

In the far-region, the terms $(x \pm \frac{1}{2})^{-1}$ are suppressed, and $x \pm \frac{1}{2} \sim x$. The radial wave equation can be written as

$$\partial_x^2(xh) + \left[\frac{(\omega^2 - p^2)(r_+^2 - r_-^2)}{4x} - \frac{\Lambda - U}{4x^2} \right] (xh) = 0. \quad (4.2.35)$$

The most general solution of this equation is a linear combination of Bessel functions [74],

$$h = x^{-1/2} \left[A_\infty^+ J_{2\xi-1}(\mu x^{1/2}) + A_\infty^- J_{1-2\xi}(\mu x^{1/2}) \right], \quad (4.2.36)$$

where ξ was defined in (4.2.31) and

$$\mu = [(\omega^2 - p^2)(r_+^2 - r_-^2)]^{1/2}. \quad (4.2.37)$$

We want to study the scattering process so we require real μ *i.e.*, $\omega > |p|$. Using the asymptotic properties of the Bessel function [74], we find that for small $\mu x^{1/2}$ the far-region solution has the behavior

$$h \sim A_\infty^+ \frac{(\mu/2)^{2\xi-1}}{\Gamma(2\xi)} x^{\xi-1} + A_\infty^- \frac{(\mu/2)^{1-2\xi}}{\Gamma(2-2\xi)} x^{-\xi}. \quad (4.2.38)$$

while for large $\mu x^{1/2}$ it reduces to

$$h \sim \frac{1}{2} \sqrt{\frac{2}{\pi\mu}} x^{-3/4} \left\{ \left[A_\infty^+ e^{-i\pi(-\xi+1/4)} + A_\infty^- e^{-i\pi(\xi-3/4)} \right] e^{-i\mu\sqrt{x}} + \left[A_\infty^+ e^{i\pi(-\xi+1/4)} + A_\infty^- e^{i\pi(\xi-3/4)} \right] e^{i\mu\sqrt{x}} \right\}. \quad (4.2.39)$$

The first term represents an incoming wave while the second term describes an outgoing solution.

Matching the near-region and the far-region solutions

There is an intermediate region for x where the approximations in both the near and far regions can be simultaneously satisfied. In this overlapping region we can match the large x behavior of

the near-region solution to the small x behavior of the far-region solution. This allows to fix the amplitude ratios. Matching (4.2.34) with (4.2.38) yields then

$$\begin{aligned}\frac{A_H^{in}}{A_\infty^+} &= \left(\frac{\mu}{2}\right)^{2\xi-1} \frac{\Gamma\left[\xi - i\frac{1}{2}(\Sigma_+ - \Sigma_-)\right] \Gamma\left[\xi - i\frac{1}{2}(\Sigma_+ + \Sigma_-)\right]}{\Gamma(2\xi)\Gamma(2\xi-1)\Gamma[1-i\Sigma_+]}, \\ \frac{A_\infty^-}{A_\infty^+} &= \left(\frac{\mu}{2}\right)^{2(2\xi-1)} \frac{\Gamma(2-2\xi)\Gamma(1-2\xi)}{\Gamma(2\xi)\Gamma(2\xi-1)} \frac{\Gamma\left[\xi - i\frac{1}{2}(\Sigma_+ - \Sigma_-)\right] \Gamma\left[\xi - i\frac{1}{2}(\Sigma_+ + \Sigma_-)\right]}{\Gamma\left[1-\xi - i\frac{1}{2}(\Sigma_+ - \Sigma_-)\right] \Gamma\left[1-\xi - i\frac{1}{2}(\Sigma_+ + \Sigma_-)\right]}.\end{aligned}\tag{4.2.40}$$

The first relation will be needed to compute the absorption cross section. In the second relation we note the presence of the factor $\mu^{2\xi-1}$, where μ is defined in (4.2.37). We want $\xi \in \mathbb{R}$ which implies $2\xi - 1 > 0$. Therefore, for $\mu \ll 1$, *i.e.*, for low frequency scattering or for near-supersymmetric solutions (decoupling limit), one has $|A_\infty^-| \ll |A_\infty^+|$. This regime allows to considerably simplify (4.2.39).

Absorption cross-section, Hawking and superradiant emission rate

The radial flux associated with our radial wave equation is

$$\mathcal{F} = \frac{1}{2i} \left(h^* \frac{g(r)}{r} \partial_r h - h \frac{g(r)}{r} \partial_r h^* \right).\tag{4.2.41}$$

The incoming flux from infinity \mathcal{F}_{in} is computed using (4.2.39). Near the decoupling regime $|A_\infty^-| \ll |A_\infty^+|$, this yields

$$\mathcal{F}_{in} = -\frac{r_+^2 - r_-^2}{2\pi} |A_\infty^+|^2,\tag{4.2.42}$$

where the minus sign signals incoming flux. On the other hand, use of the ingoing contribution of (4.2.32) yields for the absorbed flux at the horizon,

$$\mathcal{F}_{abs} = -\Sigma_+(r_+^2 - r_-^2) |A_H^{in}|^2.\tag{4.2.43}$$

The absorption probability is the ratio of the above fluxes,

$$1 - |S_\ell|^2 = \frac{\mathcal{F}_{abs}}{\mathcal{F}_{in}},\tag{4.2.44}$$

and the absorption cross-section of the ℓ^{th} partial wave is

$$\sigma_{\ell,p,m_{R,L}} = \frac{4\pi}{\omega^3} (\ell+1)^2 (1 - |S_\ell|^2).\tag{4.2.45}$$

In general, the factor multiplying the absorption probability depends on the spacetime dimension through the codimension of the absorbing object (see, *e.g.*, [54]). So for a six-dimensional black

string we use the same factor as for a five-dimensional black hole. Collecting the results, the absorption cross-section is

$$\sigma_{\ell,p,m_{R,L}} = \frac{4\pi(\ell+1)^2}{\omega^3} \beta_H \varpi \left[\frac{1}{4}(\omega^2 - p^2)(r_+^2 - r_-^2) \right]^{2\xi-1} \left| \frac{\Gamma\left(\xi - i\frac{\beta_L \varpi_L}{2\pi}\right) \Gamma\left(\xi - i\frac{\beta_R \varpi_R}{2\pi}\right)}{\Gamma(2\xi) \Gamma(2\xi - 1) \Gamma\left(1 - i\frac{\beta_H \varpi}{2\pi}\right)} \right|^2, \quad (4.2.46)$$

where we defined

$$\varpi = \omega - pV_H - m_L \Omega_L - m_R \Omega_R, \quad \varpi_{L,R} = \frac{1}{2}(\omega + pV_{L,R}) - m_{L,R} \Omega_{L,R} \frac{\beta_H}{\beta_{L,R}}. \quad (4.2.47)$$

Observe in the latter equation the presence of $\Omega_{L,R} \frac{\beta_H}{\beta_{L,R}}$, which correspond to the chemical potentials $\mu_{L,R}$ of the microscopic two-sector system (4.1.9).

By detailed balance, the decay rate is the absorption cross-section divided by the thermal Bose-Einstein occupation number,

$$\Gamma_{\ell,p,m_{R,L}} = \frac{\sigma_{\ell,p,m_{R,L}}}{e^{\beta_H \varpi} - 1}. \quad (4.2.48)$$

The matching (4.2.40) was performed in the low frequency regime of waves with wavelength much larger than the typical size of the black hole. This is actually the regime of relevance when comparing to the microscopic dual, in which the excitations near the horizon are (almost) decoupled from the asymptotic region, and we only allow a little leakage of energy between the two regions. The latter corresponds to coupling the dual CFT to a bulk scalar. Using (4.2.21) and (4.2.25) this is the range of parameters where

$$U \ll \Lambda \simeq \ell(\ell+2) \quad \Rightarrow \quad \xi \simeq \frac{\ell+2}{2}. \quad (4.2.49)$$

In particular, since ξ is integer or half-integer, the relations [74]

$$\begin{aligned} |\Gamma(n - iz)|^2 &= \Gamma(n - iz)\Gamma(n + iz), & \Gamma(n \pm iz) &= \Gamma(1 \pm iz) \prod_{j=1}^{n-1} (j^2 + z^2), \\ |\Gamma(1 - iz)|^2 &= \frac{\pi z}{\sinh(\pi z)}, & \left| \Gamma\left(\frac{1}{2} - iz\right) \right|^2 &= \frac{\pi}{\cosh(\pi z)}, \end{aligned} \quad (4.2.50)$$

allow to express the absorption cross-section (4.2.46) in terms of Bose-Einstein or Fermi-Dirac thermal factors.

We have to distinguish the cases of even and odd angular quantum number ℓ . For even ℓ , (4.2.46), (4.2.48), (4.2.50) give the decay rate,

$$\begin{aligned} \text{Even } \ell: \quad \Gamma_{\ell,p,m_{R,L}} &= \frac{4\pi}{(\ell!)^4} \left[(\omega^2 - p^2) \frac{\mathcal{A}_H^{(5)}}{4\pi} \right]^{\ell+1} \frac{\varpi_L \varpi_R}{\omega^3} \frac{\beta_L \beta_R}{\beta_H} \left(e^{\beta_L \varpi_L} - 1 \right)^{-1} \left(e^{\beta_R \varpi_R} - 1 \right)^{-1} \\ &\times \prod_{j=1}^{\ell/2} \left[j^2 + \left(\frac{\beta_L \varpi_L}{2\pi} \right)^2 \right] \left[\left(\frac{j}{\beta_H} \right)^2 + \left(\frac{\beta_R \varpi_R}{2\pi \beta_H} \right)^2 \right], \end{aligned} \quad (4.2.51)$$

where we have used $r_+^2 - r_-^2 = \mathcal{A}_H^{(5)}/(4G_5\beta_H)$ with $\mathcal{A}_H^{(5)}$ the area of the five-dimensional black hole, and in our units $G_5 = \pi/4$.

For odd ℓ , the decay rate is

$$\begin{aligned} \text{Odd } \ell : \quad \Gamma_{\ell,p,m_{R,L}} &= \frac{2(2\pi)^3}{(\ell!)^4} \left[(\omega^2 - p^2) \frac{\mathcal{A}_H^{(5)}}{4\pi} \right]^{\ell+1} \frac{1}{\omega^3} \left(e^{\beta_L \varpi_L} + 1 \right)^{-1} \left(e^{\beta_R \varpi_R} + 1 \right)^{-1} \\ &\times \prod_{j=1}^{(\ell+1)/2} \left[\left(j - \frac{1}{2} \right)^2 + \left(\frac{\beta_L \varpi_L}{2\pi} \right)^2 \right] \left[\left(\frac{2j-1}{2\beta_H} \right)^2 + \left(\frac{\beta_R \varpi_R}{2\pi\beta_H} \right)^2 \right]. \end{aligned} \quad (4.2.52)$$

As observed in [52], for even ℓ there appear left and right bosonic thermal factors (4.2.51) while for odd ℓ they are fermionic thermal factors. This is already a hint of the microscopic degrees of freedom responsible for the radiation—taking into account that the bosonic factors can emerge as effective ones from even numbers of fermions [53, 75].

4.2.3 Superradiant emission rate from the ergo-cold black hole

These emission rates contain effects of Hawking radiation as well as superradiance. As explained in the introduction, in order to eliminate the former we take an extremal, zero temperature limit, while at the same time we want to preserve the superradiant ergoregion.

In the case of the supersymmetric BMPV black hole, neither thermal nor superradiant emission are present. In the limit to this solution

$$\lim_{\beta_R \rightarrow \infty} \varpi_R = \frac{\omega}{2} > 0, \quad (4.2.53)$$

and the positivity of ϖ_R implies that the right thermal factor $(e^{\beta_R \varpi_R} \pm 1)^{-1} \rightarrow 0$, so $\Gamma_{\ell m} = 0$. This is as it should be, since this a BPS state. The absorption cross section is positive for any quantum numbers of the wave, so stimulated emission cannot occur either.

The ergo-cold black hole is obtained in the limit in which $\beta_R \rightarrow \infty$ while Ω_R remains finite. In this case

$$\begin{aligned} \lim_{\beta_R \rightarrow \infty} \varpi_L &= \frac{1}{2} (\omega + pV_L) - m_L \frac{\pi(a_2 - a_1)\sqrt{a_1 a_2}}{\beta_L}, \\ \lim_{\beta_R \rightarrow \infty} \varpi_R &= \frac{1}{2} (\omega - pV_H - m_R \Omega_R). \end{aligned} \quad (4.2.54)$$

Now ϖ_R can take negative values, so the decay rates do not vanish for all modes but contain a factor of a step function

$$\lim_{\beta_R \rightarrow \infty} \left(e^{\beta_R \varpi_R} \pm 1 \right)^{-1} = \mp \Theta(-\varpi_R), \quad (4.2.55)$$

so the emission decay rate is

$$\begin{aligned}
\text{Even } \ell : \quad \Gamma_{\ell,p,m_{R,L}} &= \Theta(-\varpi_R) \frac{8\pi^2}{(\ell!)^4} \left[(\omega^2 - p^2) \frac{\mathcal{A}_H^{(5)}}{4\pi^2} \right]^{\ell+1} \frac{\beta_L \varpi_L |\varpi_R|^{\ell+1}}{\omega^3 (e^{\beta_L \varpi_L} - 1)} \prod_{j=1}^{\ell/2} \left[j^2 + \left(\frac{\beta_L \varpi_L}{2\pi} \right)^2 \right], \\
\text{Odd } \ell : \quad \Gamma_{\ell,p,m_{R,L}} &= \Theta(-\varpi_R) \frac{2(2\pi)^3}{(\ell!)^4} \left[(\omega^2 - p^2) \frac{\mathcal{A}_H^{(5)}}{4\pi^2} \right]^{\ell+1} \frac{|\varpi_R|^{\ell+1}}{\omega^3 (e^{\beta_L \varpi_L} + 1)} \\
&\quad \times \prod_{j=1}^{(\ell+1)/2} \left[\left(j - \frac{1}{2} \right)^2 + \left(\frac{\beta_L \varpi_L}{2\pi} \right)^2 \right]. \tag{4.2.56}
\end{aligned}$$

Thus we have derived the superradiant bound (4.1.21). The ergo-cold black hole can only emit modes that satisfy $\varpi_R < 0$. The absorption cross section is positive or negative depending on whether ϖ_R is positive or negative, so when $\varpi_R < 0$, and only then, superradiant amplification occurs.

We can also see that there cannot be any spinless, pure momentum superradiance. An oscillating wave near infinity must have $\omega > |p|$. Technically, this follows from the reality requirement of quantities like (4.2.37) or (4.2.56). Physically, $\omega^2 - p^2 > 0$ for a wave propagating in the asymptotically flat region. According to (4.2.54), spinless superradiant modes require $\omega < pV_H$. But (4.2.12) gives at extremality $V_H = \frac{c_1 c_5 s_p + s_1 s_5 c_p}{c_1 c_5 c_p + s_1 s_5 s_p}$ so $|V_H| \leq 1$ and $|pV_H| \leq |p|$. Then, none of these superradiant momentum modes can exist as propagating waves at infinity: if emitted by the black hole, they will be reflected back to it before getting to the asymptotic region. This is a general feature present in black string backgrounds [76, 77].

4.3 Microscopic description

4.3.1 The dual CFT state

The CFT state dual to the ergo-cold black hole is most easily identified by analyzing the solution in the decoupling limit. This is a low energy limit, keeping the energies finite in string units, which is obtained taking $\alpha' \rightarrow 0$ and $\delta_{1,5} \rightarrow \infty$ while keeping $r(\alpha')^{-1}$, $M(\alpha')^{-2}$, $a_{1,2}(\alpha')^{-1}$, and $Q_{1,5}(\alpha')^{-1}$ fixed. For the general black hole geometry, this has been shown to result in a twisted fibration of S^3 over the BTZ black hole [43]. The CFT states dual to the extremal black holes we have been studying can be identified using the map introduced in [78]. This yields the R-charges (j, \bar{j}) and conformal dimensions (h, \bar{h}) of the CFT state in terms of parameters of the supergravity solution. Introducing the AdS₃ curvature radius ℓ_3 , BTZ black hole mass M_3 ,

$$\begin{aligned}
\ell_3^2 &= \sqrt{Q_1 Q_5}, \\
M_3 &= \frac{R^2}{\ell^4} \left[(M - a_1^2 - a_2^2) (c_p^2 + s_p^2) + 4a_1 a_2 s_p c_p \right], \tag{4.3.1}
\end{aligned}$$

and central charge $c = 3\ell_3/2$, the following values are obtained for the two extremal rotating black holes:

- BMPV black hole:

$$\begin{aligned} j &= \frac{c}{6} \frac{R}{\ell_3^4} J_L, & h &= \frac{c}{24} \left(1 + 2M_3 + \frac{4R^2}{\ell_3^8} J_L^2 \right), \\ \bar{j} &= 0, & \bar{h} &= \frac{c}{24}. \end{aligned} \tag{4.3.2}$$

- Ergo-cold black hole:

$$\begin{aligned} j &= \frac{c}{6} \frac{R}{\ell_3^4} J_L, & h &= \frac{c}{24} \left(1 + 2M_3 + \frac{4R^2}{\ell_3^8} J_L^2 \right), \\ \bar{j} &= \frac{c}{6} \frac{R}{\ell_3^4} J_R, & \bar{h} &= \frac{c}{24} \left(1 + \frac{4R^2}{\ell_3^8} J_R^2 \right). \end{aligned} \tag{4.3.3}$$

To interpret these results we note that the conformal dimensions receive contributions of three kinds,

$$h = h_0 + l_0 + \frac{6j^2}{c}, \quad \bar{h} = \bar{h}_0 + \bar{l}_0 + \frac{6\bar{j}^2}{c}. \tag{4.3.4}$$

Here $(h_0, \bar{h}_0) = (c/24, c/24)$ correspond to the energy of the Ramond ground-state. On top of this, the left sector has in both cases an excitation energy given by the Virasoro level $l_0 = \ell_3 M_3/8$: this is the energy of its thermal excitations, which give the system a Cardy entropy

$$S_L = 2\pi\sqrt{cl_0/6}. \tag{4.3.5}$$

Additionally, the left sector contains some polarized fermions, which yield a charge j and an energy $6j^2/c$.

The right sector in both black holes is at zero level, $\bar{l}_0 = 0$, so they are at vanishing temperature. But there is a crucial difference between the two states: whereas in the BMPV black hole this sector is in the Ramond ground state, in the ergo-cold black hole it is filled with polarized fermions, giving charge \bar{j} and additional energy $6\bar{j}^2/c$ that lifts the system above the BPS state. This is the microscopic picture that we are advocating for this black hole.

4.3.2 Emission rate and absorption cross section

A coupling of the schematic form

$$S_{\text{int}} \propto \int dt dx \partial^\ell \Phi(t, x, \vec{x}=0) \mathcal{O}(t, x), \tag{4.3.6}$$

(t, x are worldsheet coordinates and \vec{x} are directions transverse to the string) describes the interaction of the ℓ^{th} partial wave of the bulk scalar Φ with an operator $\mathcal{O}(t, x)$ of the CFT of

conformal dimension $(1 + \ell/2, 1 + \ell/2)$. We build the latter out of a pair of bosons $\partial_{\pm}X$, and ℓ pairs of left and right fermions $\psi_L\bar{\psi}_R$. This coupling gives a decay rate of the CFT into a scalar mode with quantum numbers ω , $m_{R,L}$ and p , of the form

$$\Gamma_{\ell,p,m_{R,L}}(\omega) = \mathcal{V} \int dx^+ dx^- e^{-i\varpi_R x^- - i\varpi_L x^+} \mathcal{G}(t - i\varepsilon, x), \quad (4.3.7)$$

where $x^{\pm} = t \pm x$, the Green's function is

$$\mathcal{G}(t, x) = \langle \mathcal{O}^{\dagger}(t, x) \mathcal{O}(0) \rangle, \quad (4.3.8)$$

with the $i\varepsilon$ prescription in (4.3.7) corresponding to emission, \mathcal{V} is a factor from the interaction vertex to be discussed below, and

$$\varpi_{L,R} = \frac{1}{2} (\omega \pm p) - m_{L,R} \mu_{L,R}, \quad (4.3.9)$$

account for the presence of left and right sectors with chiral momenta $(\omega \pm p)/2$ and chemical potentials $\mu_{L,R}$ for the R-charges $m_{R,L}$, given by (4.1.9). These $\varpi_{L,R}$ coincide with those defined for supergravity in (4.2.47) if we take the decoupling limit in which $V_{L,R} \rightarrow \pm 1$.

Superradiant bound

We can easily derive from these formulas the bound on decay frequencies for the CFT state dual to the black hole (4.3.3). For this state, the left sector is at temperature T_L so the left-chirality operator $\mathcal{O}_L(x^+)$ gives in (4.3.8) a thermal two-point function periodic in imaginary time,

$$\langle \mathcal{O}_L^{\dagger}(x^+) \mathcal{O}_L(0) \rangle_{T_L} \sim \left(\frac{\pi T_L}{\sinh(\pi T_L x^+)} \right)^{2+\ell}. \quad (4.3.10)$$

The right sector is at zero-temperature, and so the boson gives the two point function $\partial_- X(x^-) \partial_- X(0) \sim 1/(x^-)^2$ and each fermion gives $\psi(x^-) \psi(0) \sim 1/x^-$, so

$$\langle \mathcal{O}_R^{\dagger}(x^-) \mathcal{O}_R(0) \rangle_0 \sim \left(\frac{1}{x^-} \right)^{2+\ell}, \quad (4.3.11)$$

and the integration over the right sector in the decay rate (4.3.7) gives a factor

$$\int dx^- e^{-i\varpi_R x^-} \left(\frac{1}{x^- - i\varepsilon} \right)^{2+\ell}. \quad (4.3.12)$$

This contour integral vanishes for $\varpi_R > 0$, so

$$\Gamma_{\ell,p,m_{R,L}}(\omega) \propto \Theta(-\varpi_R). \quad (4.3.13)$$

This bound on frequencies coincides with the one we derived from the supergravity side, (4.2.54), (4.2.56), in the extremal limit where $\mu_R \rightarrow \Omega_R/2$ (4.1.10), and in the decoupling limit in which $V_H \rightarrow 1$. We feel, nevertheless, that the derivation we gave in Section 4.1 is physically more transparent.

Absorption cross section: general case

It is actually possible to compute the absorption cross section for the more general case where both sectors are at temperatures T_L and T_R so we can compare it with the general results we obtained from the supergravity side. We follow [52, 61, 62] but discuss the general case with non-vanishing $\mu_{L,R}$ and p . The Green's function (4.3.8) now has thermal correlation functions from both sectors,

$$\mathcal{G}(t, x) = (-1)^\ell C_{\mathcal{O}} \left(\frac{\pi T_L}{\sinh(\pi T_L x^+)} \right)^{2+\ell} \left(\frac{\pi T_R}{\sinh(\pi T_R x^-)} \right)^{2+\ell}, \quad (4.3.14)$$

where $C_{\mathcal{O}} = C_{\mathcal{O}_+} C_{\mathcal{O}_-} = \frac{Q_1 Q_5}{4\pi^2}$ accounts for the normalization factors of the operators [62]. The CFT absorption cross-section is the difference between absorption and emission rates divided by the flux \mathcal{F} . Then

$$\begin{aligned} \sigma_{\ell, p, m_{R,L}}^{CFT} &= \frac{2\pi R}{\mathcal{F}} \mathcal{V} \int dx^+ dx^- e^{-i(\varpi_R x^- + \varpi_L x^+)} [\mathcal{G}(t - i\epsilon, x) - \mathcal{G}(t + i\epsilon, x)] \\ &= \mathcal{V} \frac{2\pi R C_{\mathcal{O}}}{\mathcal{F}} \frac{(2\pi T_L)^{1+\ell} (2\pi T_R)^{1+\ell}}{\Gamma(2+\ell)^2} \sinh\left(\frac{\varpi_H}{2T_H}\right) \\ &\quad \left| \Gamma\left(\frac{\ell+2}{2} + i\frac{\varpi_L}{2\pi T_L}\right) \Gamma\left(\frac{\ell+2}{2} + i\frac{\varpi_R}{2\pi T_R}\right) \right|^2. \end{aligned} \quad (4.3.15)$$

Here ϖ_H is exactly the same quantity that we introduced in the supergravity analysis in (4.2.47), with V_H given in terms of $T_{L,R}$ as in (4.1.24). The precise form of the factor \mathcal{V} requires an explicit derivation of the interaction vertex from string theory, but there are several features that can be deduced heuristically [53]. The $Q_1 Q_5$ flavors of fermions in the long string yield a factor $(Q_1 Q_5)^\ell$ for the ℓ fermion pairs entering the interaction. We must also divide it by $(\ell!)^2$ to account for the fact that we are overcounting possibilities since the ℓ fermions in each sector are indistinguishable. Additionally, it must at least contain the ℓ factors of momentum from the derivatives in the vertex. Each of the left and right fermions contribute, respectively, with $(\omega \mp p)/2$ to this factor, yielding a total

$$\mathcal{V} = \left[\frac{1}{4}(\omega^2 - p^2) \right]^\ell \frac{(Q_1 Q_5)^\ell}{(\ell!)^2} \hat{\mathcal{V}}_\ell, \quad (4.3.16)$$

where there remains an undetermined ℓ -dependent factor $\hat{\mathcal{V}}_\ell$. The flux \mathcal{F} measures the frequency or energy flow per unit cross section. For a scalar of frequency ω and vanishing momentum $p = 0$ the canonically normalized flux of the incident field is $\mathcal{F} = \omega$. However, if it has momentum p , then in the frame of the string the frequency is increased by a Lorentz factor $(1 - p^2/\omega^2)^{-1/2}$, while the cross section is Lorentz-contracted by $(1 - p^2/\omega^2)^{1/2}$. Therefore, in (4.3.15) the flux is

$$\mathcal{F} = \frac{\omega}{1 - p^2/\omega^2}. \quad (4.3.17)$$

The final result is then

$$\begin{aligned} \sigma_{\ell,p,m_{R,L}}^{CFT} &= \frac{\pi \hat{\mathcal{V}}_\ell}{(\ell!(\ell+1)!)^2} \frac{1}{\omega} \left(\frac{\omega^2 - p^2}{4} \right)^\ell (4\pi^2 T_L T_R Q_1 Q_5)^{\ell+1} \sinh \left(\frac{\varpi_H}{2T_H} \right) \\ &\times \left| \Gamma \left(\frac{\ell+2}{2} + i \frac{\varpi_L}{2\pi T_L} \right) \Gamma \left(\frac{\ell+2}{2} + i \frac{\varpi_R}{2\pi T_R} \right) \right|^2. \end{aligned} \quad (4.3.18)$$

In order to compare this with the result from supergravity, we must restrict the latter to the decoupling limit. In this regime

$$\mathcal{A}_H \rightarrow 4\pi^3 \frac{T_L T_R}{T_H} Q_1 Q_5, \quad (4.3.19)$$

while the velocities all become light-like, (4.2.14), so $\varpi_{L,R}$ and ϖ_H are identical quantities in both sides of the correspondence. In this case (4.3.18) is such that

$$\sigma_{\ell,p,m_{R,L}}^{CFT} = (\ell+1)^2 \hat{\mathcal{V}}_\ell \sigma_{\ell,p,m_{R,L}}^{\text{sugra}}. \quad (4.3.20)$$

So the decay rates agree remarkably well, and it would only remain to check that a computation from first principles of $\hat{\mathcal{V}}_\ell$ yields a perfect match. Taking the limit $T_R \rightarrow 0$ we find the decay via superradiant emission of the ergo-cold black hole (4.2.56).

Chapter 5

Conclusions

The inclusion of rotation gives rise to physics that allows a more precise and detailed understanding of the microscopic string theory of black holes. In this thesis we have focused on two models of particular interest: one is based on the D0-D6 system and the other on the D1-D5-P system. The former is interesting because, through its connection to M-theory, it yields a statistical-mechanics description of neutral black holes. The latter allows us to have better control over the microscopic conformal field theory and yields a cleaner picture of the origin of superradiance.

We extended the microscopic analysis of extremal dyonic Kaluza-Klein (D0-D6) black holes to cover the regime of fast rotation in addition to slow rotation. Fastly rotating black holes, in contrast to slow ones, have non-zero angular velocity and possess ergospheres, so they are more similar to the Kerr black hole. The D-brane model reproduces their entropy exactly, but the mass gets renormalized from weak to strong coupling, in agreement with recent macroscopic analyses of rotating attractors. We discussed how the microscopic model accounts for the fact that fastly rotating extremal KK black holes possess an ergosphere and exhibit superradiance while slow ones don't.

In addition, we showed in full generality how Myers-Perry black holes are obtained as a limit of Kaluza-Klein black holes, and discussed the slow and fast rotation regimes and superradiance in this context. A, perhaps surprising, consequence of our analysis is that both slowly and fastly-rotating KK black holes provide microscopic accounts of the entropy formula of MP black holes, even if they correspond to rather different microscopic states. As we discussed, this does not pose any problem, since the microscopic theory always retains a memory of how the 5D black hole is embedded within Taub-NUT.

For a more detailed and quantitative study of black hole superradiance from the stringy microscopic side, we moved to the D1-D5-P system. In order to disentangle superradiance from finite-temperature effects, we considered an extremal, rotating D1-D5-P black hole that has an ergosphere and is not supersymmetric.

We explained how the microscopic dual accounts for the superradiant ergosphere of this black

hole. The bound $0 < \omega < m\Omega_H$ on superradiant mode frequencies was argued to be a consequence of Fermi-Dirac statistics for the spin-carrying degrees of freedom in the dual CFT.

We also computed the superradiant emission rates from both sides of the correspondence, and showed their agreement. This is an extension of previous analyses of radiation from the D1-D5-P black holes studied at length in [43, 60]. We generalized their results to include momentum for the bulk scalar.

It would be interesting to extend our picture for superradiance to the smooth SUGRA solitons with D1-D5-P charges which correspond to CFT states such that both sectors are in pure states.

Another issue to be investigated would be the absence of fermionic superradiance emission by the previously considered systems with ergoregion.

Appendices

Appendix A

Myers-Perry from Kaluza-Klein: General case

From a five-dimensional standpoint, KK black holes with non-zero magnetic charge can be regarded as black holes sitting at the tip of a Taub-NUT space, at least as long as the black hole size is much smaller than the compact radius. This was noted, in a particular case, in ref. [46], which showed that in a limit of large fifth-dimensional radius the *static* ($J = 0$) dyonic Kaluza-Klein black holes reduce to five-dimensional Myers-Perry black holes with *self-dual* angular momentum. This corresponds to the case where the rotation of the MP black hole is aligned exactly along the Kaluza-Klein direction. In this appendix we consider the most general case: the KK black hole has non-vanishing four-dimensional angular momentum J , which corresponds to the anti-self-dual component of the angular momentum of the MP black hole. We keep parameters in the KK solution arbitrary, in particular we do not confine ourselves to extremal limits. Hence we are able to recover the general MP solution.

A.1 Limiting procedure

We write the solution in essentially the form given in [33], and use the results therein for the physical parameters¹. In five-dimensional form,

$$ds^2 = \frac{H_q}{H_p}(dy + \mathbf{A})^2 - \frac{\Delta_\theta}{H_q}(dt + \mathbf{B})^2 + H_p \left(\frac{dr^2}{\Delta} + d\theta^2 + \frac{\Delta}{\Delta_\theta} \sin^2 \theta d\phi^2 \right), \quad (\text{A.1.1})$$

¹Here, and in (A.1.21) below, our sign choices for the rotation parameters are such that positive α , a , and b correspond to positive rotation.

where

$$H_p = r^2 + \alpha^2 \cos^2 \theta + r(p - 2m) + \frac{p}{p+q} \frac{(p-2m)(q-2m)}{2} + \frac{p}{2m(p+q)} \sqrt{(q^2 - 4m^2)(p^2 - 4m^2)} \alpha \cos \theta, \quad (\text{A.1.2})$$

$$H_q = r^2 + \alpha^2 \cos^2 \theta + r(q - 2m) + \frac{q}{p+q} \frac{(p-2m)(q-2m)}{2} - \frac{q}{2m(p+q)} \sqrt{(q^2 - 4m^2)(p^2 - 4m^2)} \alpha \cos \theta, \quad (\text{A.1.3})$$

$$\Delta_\theta = r^2 + \alpha^2 \cos^2 \theta - 2mr, \quad (\text{A.1.4})$$

$$\Delta = r^2 + \alpha^2 - 2mr, \quad (\text{A.1.5})$$

$$\mathbf{A} = - \left[2Q \left(r + \frac{p-2m}{2} \right) - \sqrt{\frac{q^3(p^2 - 4m^2)}{4m^2(p+q)}} \alpha \cos \theta \right] H_q^{-1} dt - \left[2P(H_q + \alpha^2 \sin^2 \theta) \cos \theta - \sqrt{\frac{p(q^2 - 4m^2)}{4m^2(p+q)^3}} [(p+q)(pr - m(p-2m)) + q(p^2 - 4m^2)] \alpha \sin^2 \theta \right] H_q^{-1} d\phi, \quad (\text{A.1.6})$$

$$\mathbf{B} = \frac{\sqrt{pq}(pq + 4m^2)r - m(p-2m)(q-2m)}{2m(p+q)\Delta_\theta} \alpha \sin^2 \theta d\phi. \quad (\text{A.1.7})$$

The (four-dimensional) physical parameters are

$$2G_4M = \frac{p+q}{2}, \quad (\text{A.1.8})$$

$$G_4J = \frac{\sqrt{pq}(pq + 4m^2)}{4(p+q)} \frac{\alpha}{m}, \quad (\text{A.1.9})$$

$$Q^2 = \frac{q(q^2 - 4m^2)}{4(p+q)}, \quad (\text{A.1.10})$$

$$P^2 = \frac{p(p^2 - 4m^2)}{4(p+q)}. \quad (\text{A.1.11})$$

Solutions with black hole horizons have $q \geq 2m$, $p \geq 2m$, $m \geq |\alpha|$.

For regularity, the coordinate y must be periodically identified as

$$y \sim y + 2\pi R, \quad R = \frac{4P}{N_6}, \quad (\text{A.1.12})$$

for integer N_6 . As usual, $\phi \sim \phi + 2\pi$. From a five-dimensional viewpoint the KK electric charge is momentum along the y -direction and so is quantized as

$$Q = \frac{2G_4N_0}{R}, \quad (\text{A.1.13})$$

for integer N_0 . In the string theory embedding, N_0 and N_6 correspond to the numbers of D0 and D6 branes introduced in (3.1.5), and $R = g$ in string units.

We take a limit where the magnetic charge P grows to infinity while Q , J and the black hole size remain finite. This has the effect of effectively decompactifying the fifth direction. To perform this, we send $p \rightarrow \infty$, and also send $r, m, \alpha, q \rightarrow 0$, and $y \rightarrow \infty$ in such a way that pr , pm , $p\alpha$, pq , y/p , remain finite. It is convenient to introduce new finite parameters μ , a , b , and finite radial and angular coordinates, ρ and ψ , through

$$pq = \frac{\mu}{4}, \quad (\text{A.1.14})$$

$$p\alpha = \frac{1}{8} (\mu - (a+b)^2)^{1/2} (a-b), \quad (\text{A.1.15})$$

$$pm = \frac{1}{8} [\mu(\mu - (a+b)^2)]^{1/2}, \quad (\text{A.1.16})$$

$$pr = \frac{1}{4} \left[\rho^2 - \frac{1}{2} (\mu - a^2 - b^2 - \sqrt{\mu(\mu - (a+b)^2)}) \right], \quad (\text{A.1.17})$$

$$\psi = \frac{y}{p}, \quad \text{with } \psi \sim \psi + \frac{4\pi}{N_6}. \quad (\text{A.1.18})$$

The angles (ψ, ϕ, θ) are Euler angles for (a topological) S^3/\mathbb{Z}_{N_6} . It is also convenient to use

$$\tilde{\psi} = \frac{\psi + \phi}{2}, \quad \tilde{\phi} = \frac{\psi - \phi}{2}, \quad \tilde{\theta} = \frac{\theta}{2}, \quad (\text{A.1.19})$$

with

$$(\tilde{\psi}, \tilde{\phi}) \sim \left(\tilde{\psi} + \frac{2\pi}{N_6}, \tilde{\phi} + \frac{2\pi}{N_6} \right) \sim (\tilde{\psi}, \tilde{\phi} + 2\pi). \quad (\text{A.1.20})$$

After lengthy algebra, in the limit $p \rightarrow \infty$ the metric (A.1.1) becomes

$$ds^2 = -dt^2 + \frac{\mu}{\Sigma} \left(dt - a \sin^2 \tilde{\theta} d\tilde{\psi} - b \cos^2 \tilde{\theta} d\tilde{\phi} \right)^2 + \Sigma \left(\frac{d\rho^2}{\tilde{\Delta}} + d\tilde{\theta}^2 \right) + (\rho^2 + a^2) \sin^2 \tilde{\theta} d\tilde{\psi}^2 + (\rho^2 + b^2) \cos^2 \tilde{\theta} d\tilde{\phi}^2, \quad (\text{A.1.21})$$

with

$$\Sigma = \rho^2 + a^2 \cos^2 \tilde{\theta} + b^2 \sin^2 \tilde{\theta}, \quad (\text{A.1.22})$$

$$\tilde{\Delta} = \frac{(\rho^2 + a^2)(\rho^2 + b^2) - \mu\rho^2}{\rho^2}. \quad (\text{A.1.23})$$

This is the general five-dimensional MP black hole, with independent rotation parameters a and b [16]. When $N_6 > 1$ the orbifold identification (A.1.18) implies that the solution is not globally asymptotically flat, but instead the spatial geometry asymptotes to $\mathbb{R}^4/\mathbb{Z}_{N_6}$. In this case the MP black hole sits at the tip of a conical space.

A.2 Relations between physical parameters

The 4D and 5D Newton constants are as usual related by

$$G_4 = \frac{G_5}{2\pi R}, \quad (\text{A.2.24})$$

with R given in (A.1.12).

The 4D mass, given by (A.1.8), is dominated in the limit $p \rightarrow \infty$ by the magnetic KK monopole mass. This is identified as

$$\mathcal{M}_{KK} = \frac{P}{2G_4}, \quad (\text{A.2.25})$$

and diverges as $p \rightarrow \infty$. The finite limiting difference between the total 4D mass and the KK monopole mass corresponds exactly to the 5D mass,

$$M - \mathcal{M}_{KK} \rightarrow \frac{3\pi}{8N_6 G_5} \mu = M_{(5)}. \quad (\text{A.2.26})$$

According to this equation, we can regard the 5D mass as the excitation energy above the KK monopole background. The N_6 in the denominator comes from integration over the \mathbb{Z}_{N_6} -orbifolded S^3 .

Consider the following two Killing vectors of the KK black hole geometry,

$$\zeta_{(1),(2)} = 2P\partial_y \pm \partial_\phi. \quad (\text{A.2.27})$$

Their associated conserved charges are²

$$J_{1,2} = \frac{PQ}{G_4} \pm J = \frac{N_0 N_6}{2} \pm J, \quad (\text{A.2.28})$$

which are independent of R and therefore remain invariant as $p \rightarrow \infty$. In this limit

$$\zeta_{(1)} \rightarrow \partial_{\tilde{\psi}}, \quad \zeta_{(2)} \rightarrow \partial_{\tilde{\phi}}, \quad (\text{A.2.29})$$

so J_1 and J_2 become the angular momenta of the MP black hole in the directions $\tilde{\psi}$ and $\tilde{\phi}$,

$$J_1 \rightarrow \frac{\pi\mu a}{4G_5 N_6}, \quad J_2 \rightarrow \frac{\pi\mu b}{4G_5 N_6}. \quad (\text{A.2.30})$$

So, from (A.2.28), the electric charge, which is the component of the rotation aligned with the KK direction y , corresponds to the 5D self-dual angular momentum \mathcal{J}

$$N_0 = \frac{J_1 + J_2}{N_6} = \frac{\mathcal{J}}{N_6}, \quad (\text{A.2.31})$$

and the 4D angular momentum,

$$J = \frac{J_1 - J_2}{2} = \frac{\tilde{\mathcal{J}}}{2}, \quad (\text{A.2.32})$$

is the 5D anti-self-dual angular momentum $\tilde{\mathcal{J}}$. This is a $U(1)$ charge in the $SU(2) \subset SO(4)/\mathbb{Z}_{N_6}$ that remains unbroken by the compactification. It is the component of the rotation of the MP black hole that lies away from the compactification direction.

²Our definitions of $J_{1,2}$ differ from [30] by a factor of N_6 .

It can also be checked, with some work, that the entropy measured from the area in four dimensions agrees in the limit with the entropy of the MP black hole,

$$\begin{aligned} S &= \frac{\mathcal{A}_{\text{KKbh}}}{4G_4} = \frac{\pi\sqrt{pq}}{G_4} \left[m + \frac{pq + 4m^2}{2m(p+q)} \sqrt{m^2 - \alpha^2} \right] \\ &\rightarrow \frac{2\pi^2}{4G_5 N_6} \mu \rho_+ = \frac{\mathcal{A}_{\text{MPbh}}}{4G_5}, \end{aligned} \quad (\text{A.2.33})$$

(with ρ_+ the outer horizon radius).

A.3 The two extremal limits

There are two different extremal limits for KK black holes, which correspond to two different classes of extremal limit for the MP black holes:

- Slowly-rotating extremal KK black holes are the limit of (A.1.1) where $\alpha, m \rightarrow 0$ with finite $|\alpha|/m < 1$. This implies $G_4|J| < |PQ|$.

In the decompactification limit to the MP black hole, this corresponds to

$$\mu = (a + b)^2 \quad \text{with } ab > 0, \quad (\text{A.3.34})$$

which is

$$M_{(5)}^3 = \frac{27\pi}{32G_5 N_6} \mathcal{J}^2, \quad \text{with } |\mathcal{J}| > |\bar{\mathcal{J}}|. \quad (\text{A.3.35})$$

- Fastly-rotating extremal KK black holes have $|\alpha| = m > 0$, so $G_4|J| > |PQ|$. In the decompactification limit this is

$$\mu = (a - b)^2 \quad \text{with } ab < 0, \quad (\text{A.3.36})$$

i.e.,

$$M_{(5)}^3 = \frac{27\pi}{32G_5 N_6} \bar{\mathcal{J}}^2, \quad \text{with } |\bar{\mathcal{J}}| > |\mathcal{J}|. \quad (\text{A.3.37})$$

The mass bound (3.1.1) translates into a bound on $M_{(5)}$ in terms of \mathcal{J} ,

$$M_{(5)}^3 = \frac{27\pi}{32G_5 N_6} \mathcal{J}^2, \quad (\text{A.3.38})$$

which is obviously saturated at extremal slow-rotation, (A.3.35), and never saturated at fast rotation, (A.3.37). From a purely 5D viewpoint the distinction is arbitrary. It is only when we put the solution at a certain orientation within Taub-NUT that the symmetry between \mathcal{J} and $\bar{\mathcal{J}}$ is broken.

Finally, since

$$J_1 J_2 = \frac{(N_0 N_6)^2}{4} - J^2, \quad (\text{A.3.39})$$

we can write the entropy as

$$S = 2\pi\sqrt{|J_1 J_2|}, \tag{A.3.40}$$

independently of R . The two extremal cases above correspond to $J_1 J_2 > 0$ and $J_1 J_2 < 0$, respectively.

Appendix B

Ergospheres and superradiance in extremal KK-Black Holes

Let us first consider a general necessary condition for superradiant scattering, which follows from the second law of black hole thermodynamics. From the 4D point of view, we must have

$$T_H dS = dM - \Phi_E dQ - \Phi_M dP - \Omega_H dJ > 0, \quad (\text{B.0.1})$$

(the condition is still valid in the extremal limit where $T_H \rightarrow 0$). We only consider processes where the topology of the 5D solution remains fixed, so $dP = 0$.

Consider a scalar field Ψ in the black hole background (A.1.1), satisfying

$$\square_{(5)} \Psi = 0, \quad (\text{B.0.2})$$

with the form

$$\Psi = \psi_{\omega kn}(r, \theta) e^{iky + in\phi - i\omega t}. \quad (\text{B.0.3})$$

Here k is interpreted as KK electric charge and is quantized in units of $1/R$. From a 4D viewpoint it also gives a rest mass, so if the charged wave is to propagate to infinity it must satisfy $\omega > |k|$.

It can easily be shown that absorption of this field by the black hole results in a change in black hole parameters such that

$$\frac{\delta J}{\delta M} = \frac{n}{\omega}, \quad \frac{\delta Q}{\delta M} = 2G_4 \frac{k}{\omega}. \quad (\text{B.0.4})$$

Then (B.0.1) requires

$$\delta M \left(1 - \frac{n}{\omega} \Omega_H - 2G_4 \frac{k}{\omega} \Phi_E \right) > 0. \quad (\text{B.0.5})$$

Since we are considering a process of energy extraction, $\delta M < 0$, the only way for this to hold is that

$$\omega < n\Omega_H + 2G_4 k \Phi_E. \quad (\text{B.0.6})$$

- For the slowly-rotating extremal solution the four dimensional horizon has $\Omega_H = 0$ and hence what we have is a charge ergosphere. We can only extract energy by discharging the black hole. The electric potential for these black holes is

$$2G_4\Phi_E = \sqrt{\frac{p+q}{q}} > 1, \quad (\text{B.0.7})$$

so the charge-superradiance condition can be satisfied.

- The fastly-rotating extremal solution has both non-zero angular velocity and electric potential on the horizon,

$$\Omega_H = \frac{1}{\sqrt{pq}}, \quad (\text{B.0.8})$$

and

$$2G_4\Phi_E = \sqrt{\frac{q^2 - 4m^2}{q(p+q)}} < 1. \quad (\text{B.0.9})$$

Rotational superradiance of neutral ($k = 0$) waves is obviously possible. Bearing in mind that $\omega > k$ for a wave to escape, then it is not possible to extract energy by simply discharging the black hole ($k > 0, n = 0$), but it seems possible to do so by simultaneous extraction of angular momentum and charge.

Note that (B.0.6) is necessary, but not sufficient, for superradiance to be possible. Next we perform a detailed analysis of scalar wave propagation to find, in particular illustrative cases, that superradiance indeed happens when this is satisfied. We consider extremal black holes with non-zero magnetic charge, but set to zero either J or Q , to obtain simple examples of slowly and fastly rotating black holes.

B.1 $Q \neq 0, J = 0$ extremal black hole

This is the static (in 4D) limit of slowly rotating black holes, obtained taking $\alpha = 0$ and then $m \rightarrow 0$. The horizon is at $r = 0$ and from a 5D viewpoint it is moving along y . Indeed, the horizon is generated by orbits of the Killing vector

$$\xi = \frac{\partial}{\partial t} + v_H \frac{\partial}{\partial y}, \quad (\text{B.1.10})$$

where

$$v_H = \sqrt{\frac{p+q}{q}}. \quad (\text{B.1.11})$$

So the horizon is rotating at velocity v_H relative to asymptotic static observers that follow orbits of ∂_t . The vector ∂_t becomes spacelike for $r < r_e = \frac{1}{2} \left(q - p + \sqrt{q^2 + p^2} \right)$, so there is an ergosphere,

which from the 4D viewpoint is a charge ergosphere. The velocity v_H is actually the same as the KK electric potential $2G_4\Phi_E$. The fact that $v_H > 1$ does not result in any causal pathology.

We now analyze if there are massless scalar superradiant modes in this background. The equation (B.0.2) is separable for the *ansatz*

$$\Psi = \frac{f(r)}{\chi(r)} \Theta(\theta) e^{in\phi + iky - i\omega t}, \quad (\text{B.1.12})$$

where

$$\chi(r) = [(2qr^2 + 2pr(q+r) + p^2(q+2r)) (2qr(q+r) + p(q^2 + 2qr + 2r^2))]^{1/4}. \quad (\text{B.1.13})$$

For the angular part we get

$$\frac{1}{\sin\theta} \frac{d}{d\theta} \left(\sin\theta \frac{d\Theta}{d\theta} \right) + \left(\lambda_{lnk} + \frac{1}{\sin^2\theta} \left(pk \sqrt{\frac{p}{p+q}} + n \cos\theta \right)^2 \right) \Theta = 0, \quad (\text{B.1.14})$$

where λ_{lnk} is a separation constant.

For the radial part we obtain

$$\frac{d^2 f}{dr_*^2} + V(r) f = 0, \quad (\text{B.1.15})$$

where we have defined the ‘tortoise’ radial coordinate r_* as

$$\frac{dr_*}{dr} = \frac{1}{2r^2(p+q)} (p^3 q^3 + 4p^2 q^2 (p+q)r + 6pq(p+q)^2 r^2 + 4(p+q)^3 r^3 + 4(p+q)^2 r^4)^{1/2}, \quad (\text{B.1.16})$$

and whose asymptotic behaviour is

$$\begin{cases} r_* \sim r & \text{for } r \rightarrow \infty, \\ r_* \sim -\frac{1}{r} & \text{for } r \rightarrow 0. \end{cases} \quad (\text{B.1.17})$$

For the analysis of superradiance, we follow the approach of [14], which only requires the asymptotic behavior of (B.1.15). Near the horizon

$$V(r) \simeq \omega_H^2 + O(r) \quad (r \rightarrow 0), \quad (\text{B.1.18})$$

with

$$\omega_H = \omega - v_H k. \quad (\text{B.1.19})$$

Near infinity

$$V(r) \simeq \omega_\infty^2 + O(1/r) \quad (r \rightarrow \infty), \quad (\text{B.1.20})$$

where $\omega_\infty^2 = \omega^2 - k^2$. Then

$$f(r) \sim \begin{cases} e^{-i\omega_\infty r_*} + R e^{i\omega_\infty r_*} & r \rightarrow \infty, \\ T e^{-i\omega_H r_*} & r \rightarrow 0, \end{cases} \quad (\text{B.1.21})$$

is a wave of unitary amplitude travelling from infinity and then splitting into a transmitted wave of amplitude T that goes into the horizon, and a reflected wave of amplitude R which goes back to infinity. If (B.1.21) corresponds to a solution of (B.1.15) so does its complex conjugate

$$f^*(r) \sim \begin{cases} e^{i\omega_\infty r_*} + R^* e^{-i\omega_\infty r_*} & r \rightarrow \infty, \\ T^* e^{i\omega_H r_*} & r \rightarrow 0. \end{cases} \quad (\text{B.1.22})$$

These two solutions are linearly independent, and the theory of ordinary differential equations tells us that their wronskian $W = f f'^* - f'^* f$ must be independent of r . Near infinity this is $W = 2i\omega_\infty(|R|^2 - 1)$, and near the horizon $W = -2i\omega_H|T|^2$. Equating these we get

$$|R|^2 = 1 - \frac{\omega_H}{\omega_\infty}|T|^2. \quad (\text{B.1.23})$$

A wave travelling from and to infinity ($\omega > |k|$) will undergo superradiant amplification ($|R| > 1$) if $\omega_H < 0$, *i.e.*,

$$k < \omega < v_H k. \quad (\text{B.1.24})$$

This can be always fulfilled since $v_H > 1$. Since these black holes have $\Omega_H = 0$, it reproduces correctly the condition (B.0.6).

B.2 $Q = 0, J \neq 0$ extremal black hole

This is a particular case of extremal fastly rotating black holes. It is obtained taking $|\alpha| = m$ and $q = 2m$. The latter sets $Q = 0$.

Now the horizon is at $r = m$. The ergosphere is a squashed sphere given by $r = m(1 + \sin \theta)$, which touches the horizon at $\theta = 0$. The Killing horizon generator is

$$\xi = \frac{\partial}{\partial t} + \Omega_H \frac{\partial}{\partial \phi}, \quad (\text{B.2.25})$$

where

$$\Omega_H = \frac{1}{\sqrt{2mp}}. \quad (\text{B.2.26})$$

The procedure to study superradiance is as in the previous section. For simplicity we consider a field without any dependence on y , so in 4D terms this is an electrically neutral ($k = 0$) scalar field. Since the background is also neutral, the only effect of having $k \neq 0$ would be to give a 4D mass to the field.

The Klein-Gordon equation is separable for an *ansatz* of the form

$$\Psi = \frac{f(r)}{\chi(r)} \Theta(\theta) e^{in\phi - i\omega t} \quad (\text{B.2.27})$$

with

$$\chi(r) = [(m^2 + r^2)(m^2 - 2mr + r(p+r))]^{1/4}. \quad (\text{B.2.28})$$

The angular equation is

$$\frac{1}{\sin \theta} \frac{d}{d\theta} \left(\sin \theta \frac{d\Theta}{d\theta} \right) + \left(\lambda_{ln} + m^2 \omega^2 \cos^2 \theta - \frac{n^2}{\sin^2 \theta} \right) \Theta = 0, \quad (\text{B.2.29})$$

which is the equation for spheroidal harmonics. The radial equation takes again the form (B.1.15), but with a different $V(r)$ and a different ‘tortoise’ coordinate, now defined as

$$\frac{dr_*}{dr} = \frac{1}{(r-m)^2} [(m^2 + r^2) (m^2 - 2mr + r(p+r))]^{1/2}, \quad (\text{B.2.30})$$

and with the asymptotic behavior

$$\begin{cases} r_* \sim r & \text{for } r \rightarrow \infty, \\ r_* \sim -\frac{1}{r-m} & \text{for } r \rightarrow m. \end{cases} \quad (\text{B.2.31})$$

The potential goes as

$$V(r) \rightarrow \begin{cases} \omega^2 & \text{for } r \rightarrow \infty, \\ (\omega - \Omega_H n)^2 & \text{for } r \rightarrow m. \end{cases} \quad (\text{B.2.32})$$

In this case we have no potential barrier near infinity from the KK masses. Arguing as before, we get superradiant modes for

$$0 < \omega < \Omega_H n. \quad (\text{B.2.33})$$

B.3 $Q \neq 0$, $J \neq 0$, fastly rotating extremal black hole

The generalization from the previous section to fastly rotating black holes with $Q \neq 0$ ($\alpha = m$, $q > 2m$) is straightforward but very cumbersome, so we do not provide here the full calculation. The result one obtains is the natural generalization of the electrically neutral case: (B.2.33) is still valid, now with the general value (B.0.8) for Ω_H . Since we are considering neutral fields, $k = 0$, this is in perfect agreement with (B.0.6).

Appendix C

The near-horizon signature of superradiance

It is natural to expect that the near-horizon geometry of the black hole, which encodes in a dual manner the CFT description, contains information about the possibility or not of superradiance. In the dual CFT, superradiance refers to an interaction between the CFT and a bulk scalar. The latter appears when the near-horizon geometry is not fully decoupled from asymptotic infinity and therefore disappears in the strict decoupling limit. Nevertheless, it would seem natural that the near-horizon geometry could still encode a signature that anticipates the existence of superradiant phenomena in the full geometry. An effect of this kind was identified in [45] for the extremal Kerr black hole, which is the simplest example of an ergo-cold black hole. From the study of scalar propagation in the near-horizon geometry, they could indeed identify an effect that signals superradiance in the Kerr solution. In this appendix we show how this same effect is present in our ergo-cold black hole, but not in the BMPV solution.

C.1 Near-horizon geometry

Take the black hole solutions of the D1-D5-P system described in (4.2.1). To obtain their near-horizon geometry we introduce

$$r^2 = r_+^2 + \varepsilon\rho, \quad \tau = \gamma\frac{t}{\varepsilon}, \quad (\text{C.1.1})$$

where γ is a constant to be defined later, and we take the $\varepsilon \rightarrow 0$ limit. To avoid divergencies of the type $1/\varepsilon$ and $1/\varepsilon^2$, this coordinate transformation must be accompanied by a shift in the circle and angular directions,

$$y = \tilde{y} + V_H \frac{t}{\varepsilon}, \quad \phi = \tilde{\phi} + \Omega_\phi \frac{t}{\varepsilon}, \quad \psi = \tilde{\psi} + \Omega_\psi \frac{t}{\varepsilon}, \quad (\text{C.1.2})$$

where $\Omega_\phi, \Omega_\psi, V_H$ represent the horizon angular velocities defined in (4.2.8), (4.2.13). With the shift (C.1.2), the Killing vector $\partial/\partial t$ becomes tangent to the horizon, *i.e.*, the new coordinates co-rotate with the horizon. Next, we just write the near-horizon limit of the extreme black hole metrics (in the end of this appendix we comment on the non-extreme cases), since the near-horizon dilaton and RR fields are not important for our discussion.

- Near-horizon geometry of the BPS black hole.

In this case one has $\Omega_{\phi,\psi} = 0$ and $\gamma = \ell_3^2 \sqrt{Q_p}/2$ and one gets (dropping the \sim in the angular coordinates),

$$ds_{NH}^2 = \frac{\ell_3^2}{4} \left(-\rho^2 d\tau^2 + \frac{d\rho^2}{\rho^2} \right) + \ell_3^2 (d\theta^2 + \sin^2 \theta d\phi^2 + \cos^2 \theta d\psi^2) + \frac{Q_p}{\ell_3^2} \left(dy + \frac{\ell_3^2 \rho}{2\sqrt{Q_p}} d\tau \right)^2 + \frac{2J_\phi}{\ell_3^2} dy (\sin^2 \theta d\phi + \cos^2 \theta d\psi), \quad (\text{C.1.3})$$

where $\ell_3^2 = \sqrt{Q_1 Q_5}$.

- Near-horizon geometry of the ergo-cold black hole.

One has $\Omega_\phi = \Omega_\psi$. We restrict our attention to the simplest case with $a_1 = a_2$. This case contains all the features that are crucial for our study and does not lose any important information, while avoiding non-insightful factors.

One gets, with $\gamma = -[2a^3(c_1 c_5 c_p + s_1 s_5 s_p)]^{-1}$ (and dropping the \sim in the angular coordinates),

$$ds_{NH}^2 = \frac{K_0}{4} \left(-\rho^2 d\tau^2 + \frac{d\rho^2}{\rho^2} \right) + K_0 d\theta^2 + K (\sin^2 \theta d\phi + \cos^2 \theta d\psi + P \rho d\tau)^2 + K_0 \sin^2 \theta (d\phi + P \rho d\tau)^2 + K_0 \cos^2 \theta (d\psi + P \rho d\tau)^2 + K_y [dy + K_{ty} \rho d\tau + P_{\phi y} (\sin^2 \theta d\phi + \cos^2 \theta d\psi)]^2, \quad (\text{C.1.4})$$

where $K_0, K, P, K_y, K_{ty}, K_{\phi y}$ are constants given in terms of the black hole parameters $a, \delta_{1,5,p}$ by

$$\begin{aligned} K_0 &= 2a^2 \sqrt{\cosh(2\delta_1) \cosh(2\delta_5)}, & K &= \frac{2a^2 [1 - 2\text{sech}(2\delta_p)(s_1 s_5 c_p - c_1 c_5 s_p)^2]}{\sqrt{\cosh(2\delta_1) \cosh(2\delta_5)}}, \\ P &= -\frac{1 + \cosh(2\delta_1) \cosh(2\delta_5) + \cosh(2\delta_1) \cosh(2\delta_p) + \cosh(2\delta_5) \cosh(2\delta_p)}{8(s_1 s_5 s_p + c_1 c_5 c_p)^2}, \\ K_y &= \frac{\cosh(2\delta_p)}{\sqrt{\cosh(2\delta_1) \cosh(2\delta_5)}}, \\ P_{\phi y} &= -2a(s_1 s_5 c_p - c_1 c_5 s_p) \text{sech}(2\delta_p), & P_{ty} &= -a(s_1 s_5 c_p + c_1 c_5 s_p) \text{sech}(2\delta_p). \end{aligned} \quad (\text{C.1.5})$$

When $a_1 \neq a_2$, there are overall θ -dependent multiplicative factors both on the AdS_2 and fibred S^3 parts of the metric. They play no fundamental role in the analysis that we do next.

The key observation in (C.1.4) is that the cross terms between the time coordinate τ and the angular coordinates ϕ, ψ , are linear in the radial coordinate ρ in the case of the black hole with ergoregion. On the other hand, when the ergoregion is absent, the radial dependence in the cross terms is also not present. This feature plays an important role in the near-horizon superradiant analysis that we do next.

C.2 The Bardeen-Horowitz signature of superradiance

In this section we identify and justify the superradiant signature in a near-horizon geometry. We refer to this as the Bardeen-Horowitz signature, since the feature that we will describe was first identified by these authors in the extremal Kerr solution [45]. We will initially focus our analysis on the near-horizon geometry (C.1.4) of the ergo-cold black hole. We will single out the factor responsible for superradiance in this case. Then we will observe that this factor is absent when the ergoregion is not present, and in particular in the BPS case.

Take (C.1.4). The following analysis gets simplified if we carry dimensional reduction along y (again we will take waves with no momentum along the T^4 , so this plays no role in the discussion). This yields ¹

$$ds_{NH(5)}^2 = \frac{K_0}{4} \left(-\rho^2 d\tau^2 + \frac{d\rho^2}{\rho^2} \right) + K_0 d\theta^2 + K(\sin^2 \theta d\phi + \cos^2 \theta d\psi + P\rho d\tau)^2 + K_0 \sin^2 \theta (d\phi + P\rho d\tau)^2 + K_0 \cos^2 \theta (d\psi + P\rho d\tau)^2. \quad (\text{C.2.6})$$

This five-dimensional metric is of the form $AdS_2 \times S^3$. We can introduce global AdS_2 coordinates to cover the entire spacetime [45],

$$\rho = \sqrt{1+x^2} \cos T + x, \quad \tau = \frac{\sqrt{1+x^2} \sin T}{\rho}, \quad (\text{C.2.7})$$

whose ranges are $-\infty < T < \infty$, $-\infty < x < \infty$. To avoid new crossed terms between S^3 and AdS_2 coordinates, we have to shift ϕ and ψ [45],

$$\phi, \psi = \tilde{\phi}, \tilde{\psi} + P \log \left[\frac{\cos T + x \sin T}{1 + \sqrt{1+x^2} \sin T} \right]. \quad (\text{C.2.8})$$

In these global coordinates the metric (C.2.6) reads,

$$ds_{NH(5)}^2 = \frac{K_0}{4} \left(-(1+x^2)dT^2 + \frac{dx^2}{1+x^2} \right) + K_0 d\theta^2 + K(\sin^2 \theta d\tilde{\phi} + \cos^2 \theta d\tilde{\psi} + Px dT)^2 + K_0 \sin^2 \theta (d\tilde{\phi} + Px dT)^2 + K_0 \cos^2 \theta (d\tilde{\psi} + Px dT)^2. \quad (\text{C.2.9})$$

¹We absorb a factor of K_y^{-1} in the lhs that comes from the KK dilaton (which being constant plays no role): $ds_{NH(5)}^2 \equiv K_y^{-1} ds_{NH(5)}^2$. There is also a gauge field which is irrelevant for our purposes, and whose components are $A_\tau = K_{ty}\rho$, $A_\phi = K_{\phi y} \sin^2 \theta$, $A_\psi = K_{\psi y} \cos^2 \theta$.

We now study the Klein-Gordon equation in this near-horizon background (C.2.9). Introducing the *ansatz*

$$\Phi = e^{-i(wT - m\tilde{\phi} - n\tilde{\psi})} \Theta(\theta) X(x), \quad (\text{C.2.10})$$

the wave equation separates and yields

$$\begin{aligned} \frac{1}{\sin 2\theta} \frac{d}{d\theta} \left[\sin 2\theta \frac{d\Theta}{d\theta} \right] + \left[\Lambda - \frac{m^2}{\sin^2 \theta} - \frac{n^2}{\cos^2 \theta} \right] \Theta &= 0, \\ \frac{d}{dx} \left[(1+x^2) \frac{dX}{dx} \right] + \frac{1}{4} \left[\frac{4[w + (m+n)Px]^2}{1+x^2} + \frac{K}{K+K_0} (m+n)^2 - \Lambda \right] X &= 0, \end{aligned} \quad (\text{C.2.11})$$

where K_0 , K and P are defined in (C.1.5).²

The radial equation presents an important feature. Indeed, apart from the contribution coming from the piece $(m+n)Px$, this radial equation is very similar to the equation describing perturbations in a pure AdS_2 background [45]. That is, in (C.2.11) we have $[w + (m+n)Px]^2$ instead of w^2 that is present in the pure AdS_2 case. The origin of this factor can be easily traced back and found to be due to the presence of the terms $P\rho d\tau$ in (C.1.4); see discussion at the end of Section C.1. We next discuss the implications of this property for the near-horizon signature of superradiance.

In a WKB approximation the effective wavenumber for traveling waves obeying (C.2.11), $k = -\frac{i}{X} \frac{dX}{dx}$, is

$$k = \pm \frac{1}{4\sqrt{1+x^2}} \left[\frac{4[w + (m+n)Px]^2}{1+x^2} + \frac{K}{K+K_0} (m+n)^2 - \Lambda \right]^{1/2}, \quad (\text{C.2.12})$$

from which follows the associated group velocity,

$$\frac{dw}{dk} = \pm \frac{4(1+x^2)^{3/2}}{w + (m+n)Px} \left[\frac{[w + (m+n)Px]^2}{1+x^2} + \frac{K}{K+K_0} (m+n)^2 - \Lambda \right]^{1/2}. \quad (\text{C.2.13})$$

On the other hand, the phase velocity of the waves is w/k . As first observed in [45], in the context of the Kerr geometry, here the group and phase velocities can have opposite signs. For positive $(m+n)P$ this occurs when $x < \frac{w}{(m+n)P}$, while for negative $(m+n)P$ this is true when $x > \frac{w}{(m+n)P}$. An original argument from Press and Teukolsky [13], concludes that this defines the near-horizon superradiant regime. Indeed, the opposite sign between group and phase velocities of a wave in the vicinity of a horizon is responsible for the fundamental origin of superradiance. Classically, only ingoing waves are allowed to cross the horizon. The quantity that defines the physical direction of a wave is its group velocity rather than its phase velocity. So the classical absorption of incident waves is described by imposing a negative group velocity as a boundary condition. Note however that in the near-horizon superradiant regime above mentioned, the associated phase velocity is

²The separation constant is exactly $\Lambda = \ell(\ell + 2)$ (this is a consequence of working with the $a_1 = a_2$ case), and poses a bound on the other angular quantum numbers: $\ell \geq |m| + |n|$.

positive and so waves appear as outgoing to an inertial observer at spatial infinity. Thus, energy is in fact being extracted, *i.e.*, superradiance is active [13].

At this point, we make a contact with the other extreme case and with the discussion in the end of Section C.1. For the BPS black hole, there is no radial dependence in the cross terms between the time and angular coordinates in its near-horizon geometry (C.1.3). As a consequence, there is no linear term in the frequency in the wave equation associated with this background. But this implies that group and phase velocities always have the same sign in this background. Thus there is no available room for a superradiant regime in the near-horizon geometries of extreme black holes without ergoregion. Finally note that in a general non-extreme black hole the situation is quite similar to the ergo-cold black hole in what concerns the issue discussed in this appendix.

Bibliography

- [1] R. Emparan and A. Maccarrone, “Statistical description of rotating Kaluza-Klein black holes,” *Phys. Rev. D* **75** (2007) 084006, [arXiv:hep-th/0701150].
- [2] O. J. C. Dias, R. Emparan and A. Maccarrone, “Microscopic theory of black hole superradiance,” *Phys. Rev. D* **77** (2008) 064018, arXiv:0712.0791 [hep-th].
- [3] S. M. Carroll, “Spacetime and geometry,” *Addison-Wesley (2003)* 513p
- [4] R. M. Wald, “General Relativity,” *Chicago, Usa: Univ. Pr. (1984)* 491p
- [5] K. Schwarzschild, “On the gravitational field of a mass point according to Einstein’s theory,” (S. Antoci, A. Loinger Trans.) arXiv:physics/9905030 [physics.hist-ph].
- [6] P. K. Townsend, “Black Holes: Lecture notes,” [arXiv:gr-qc/9707012].
- [7] S. W. Hawking, “Particle Creation by Black Holes,” *Commun. Math. Phys.* **43** (1975) 199 [Erratum.ibid. **46** (1976) 206].
- [8] J. D. Bekenstein, “Black holes and entropy,” *Phys. Rev. D* **7** (1973) 2333.
- [9] S. F. Ross, “Black hole thermodynamics,” [arXiv:hep-th/0502195].
- [10] H. Reissner, “Über die Eigengravitation des elektrischen Feldes nach der Einstein’schen Theorie,” *Ann. Physik.* **50** (1916) 106;
G. Nordström, “On the Energy of the Gravitational Field in Einstein’s Theory,” *Proc. Kon. Ned. Akad. Wet.* **20** (1918) 1238.
- [11] R. P. Kerr, “Gravitational field of a spinning mass as an example of algebraically special metrics,” *Phys. Rev. Lett.* **11** (1963) 237
- [12] R. Penrose and R. M. Floyd, “Extraction of Rotational Energy from a Black Hole,” *Nature-Phys. Sci.* **229** (1971) 177.

- [13] W. H. Press, S. A. Teukolsky, “Perturbations of a rotating black hole. II. Dynamical stability of the Kerr metric,” *Astrophys. J.* **185** (1973) 649;
W. H. Press, S. A. Teukolsky, “Perturbations of a rotating black hole. III - Interaction of the hole with gravitational and electromagnetic radiation,” *Astrophys. J.* **193** (1974) 443.
- [14] A.A. Starobinsky, “Amplification of waves during reflection from a rotating black hole,” *Sov. Phys. JETP* **37**, 28 (1973);
A.A. Starobinsky and S.M. Churilov, “Amplification of electromagnetic and gravitational waves scattered by a rotating black hole,” *Sov. Phys. JETP* **38**, 1 (1973).
- [15] F. R. Tangherlini, “Schwarzschild Field in n Dimensions and the Dimensionality of Space Problem,” *Nuovo Cimento* **27** (1963) 636.
- [16] R. C. Myers and M. J. Perry, “Black Holes In Higher Dimensional Space-Times,” *Annals Phys.* **172**, 304 (1986).
- [17] R. Emparan and H. S. Reall, “A rotating black ring in five dimensions,” *Phys. Rev. Lett.* **88** (2002) 101101 [arXiv:hep-th/0110260]; for a review, see “Black rings,” *Class. Quant. Grav.* **23** (2006) R169 [arXiv:hep-th/0608012].
- [18] P. Figueras, “A Black ring with a rotating 2-sphere,” *JHEP* **0507** (2005) 039 [arXiv:hep-th/0505244];
T. Mishima and H. Iguchi, “New axisymmetric stationary solutions of five-dimensional vacuum Einstein equations with asymptotic flatness,” *Phys. Rev. D* **73** (2006) 044030 [arXiv:hep-th/0504018];
H. Elvang and P. Figueras, “Black Saturn,” *JHEP* **0705** (2007) 050 [arXiv:hep-th/0701035];
H. Elvang, R. Emparan and P. Figueras, “Phases of five-dimensional black holes,” *JHEP* **0705** (2007) 056 [arXiv:hep-th/0702111].
- [19] R. Emparan, T. Harmark, V. Niarchos and N. A. Obers, “World-Volume Effective Theory for Higher-Dimensional Black Holes,” *Phys. Rev. Lett.* **102** (2009) 191301 arXiv:0902:0427 [hep-th].
- [20] T. Kaluza, “On the Problem of Unity in Physics,” *Sitzungsber. Preuss. Akad. Wiss. Berlin (Math. Phys.)* **1921** (1921) 966;
O. Klein, “Quantum Theory and Five-Dimensional Theory of Relativity. (In German and English),” *Z. Phys.* **37** (1926) 895
- [21] For an introductory review on Kaluza-Klein Black Holes, see: G. T. Horowitz and T. Wiseman, “General black holes in Kaluza-Klein theory,” arXiv:1107.5563 [gr-qc].

- [22] D. J. Gross and M. J. Perry “Magnetic Monopoles in Kaluza-Klein Theories,” Nucl. Phys. B **226** (1983) 29;
R. D. Sorkin, “Kaluza-Klein Monopole,” Phys. Rev. Lett. **51** (1983) 87
- [23] T. Ortín, “Gravity and Strings,” *Cambridge, UK: Univ. Pr. (2004) 684p*
- [24] M. B. Green, J. H. Schwarz and E. Witten, “Superstring Theory,” Two Vols., *Cambridge, UK: Univ. Pr. (1987) 469+596 p*
- [25] K. Becker, M. Becker and J. H. Schwarz, “String theory and M-theory,” *Cambridge, UK: Univ. Pr. (2007) 739p*
- [26] For a review, see: A. W. Peet, “TASI lectures on black holes in string theory,” in *TASI 99: Strings, Branes and Gravity* eds. J. Harvey, S. Kachru and E. Silverstein (World Scientific, Singapore, 2001) [arXiv:hep-th/0008241].
- [27] A. Strominger and C. Vafa, “Microscopic Origin of the Bekenstein-Hawking Entropy,” Phys. Lett. B **379** (1996) 99 [arXiv:hep-th/9601029].
- [28] K. Goldstein, K. Iizuka, R. P. Jena, S. P. Trivedi, “Non-supersymmetric attractors,” Phys. Rev. D **72** (2005) 124021 [arXiv:hep-th/0507096];
P. K. Tripathy and S. P. Trivedi, “Non-supersymmetric attractors in string theory,” JHEP **0603** (2006) 022 [arXiv:hep-th/0511117];
A. Dabholkar, A. Sen, S. P. Trivedi, “Black hole microstates and attractor without supersymmetry,” JHEP **0701** (2007) 096 [arXiv:hep-th/0611143].
- [29] S. R. Das and S. D. Mathur, “Comparing decay rates for black holes and D-branes,” Nucl. Phys. B **478**, 561 (1996) [arXiv:hep-th/9606185].
- [30] R. Emparan and G. T. Horowitz, “Microstates of a neutral black hole in M theory,” Phys. Rev. Lett. **97** (2006) 141601 [arXiv:hep-th/0607023].
- [31] W. I. Taylor, “Adhering 0-branes to 6-branes and 8-branes,” Nucl. Phys. B **508** (1997) 122 [arXiv:hep-th/9705116].
- [32] D. Rasheed, “The Rotating dyonic black holes of Kaluza-Klein theory,” Nucl. Phys. B **454**, 379 (1995) [arXiv:hep-th/9505038].
- [33] F. Larsen, “Rotating Kaluza-Klein black holes,” Nucl. Phys. B **575** (2000) 211 [arXiv:hep-th/9909102].
- [34] D. Astefanesei, K. Goldstein, R. P. Jena, A. Sen and S. P. Trivedi, “Rotating attractors,” JHEP **0610** (2006) 058 [arXiv:hep-th/0606244].

- [35] A. Dabholkar, A. Sen and S. Trivedi, “Black hole microstates and attractor without supersymmetry,” arXiv:hep-th/0611143.
- [36] D. Astefanesei, K. Goldstein and S. Mahapatra, “Moduli and (un)attractor black hole thermodynamics,” arXiv:hep-th/0611140.
- [37] F. Larsen, “Kaluza-Klein black holes in string theory,” arXiv:hep-th/0002166.
- [38] J. M. Maldacena and A. Strominger, “Statistical Entropy of Four-Dimensional Extremal Black Holes,” Phys. Rev. Lett. **77**, 428 (1996) [arXiv:hep-th/9603060];
C. V. Johnson, R. R. Khuri and R. C. Myers, “Entropy of 4D Extremal Black Holes,” Phys. Lett. B **378**, 78 (1996) [arXiv:hep-th/9603061].
- [39] J. M. Maldacena, A. Strominger and E. Witten, “Black hole entropy in M-theory,” JHEP **9712** (1997) 002 [arXiv:hep-th/9711053].
- [40] G. T. Horowitz, D. A. Lowe and J. M. Maldacena, “Statistical Entropy of Nonextremal Four-Dimensional Black Holes and U-Duality,” Phys. Rev. Lett. **77**, 430 (1996) [arXiv:hep-th/9603195].
- [41] V. Balasubramanian and F. Larsen, “On D-Branes and Black Holes in Four Dimensions,” Nucl. Phys. B **478**, 199 (1996) [arXiv:hep-th/9604189].
- [42] M. Cvetič and D. Youm, “Entropy of Non-Extreme Charged Rotating Black Holes in String Theory,” Phys. Rev. D **54** (1996) 2612 [arXiv:hep-th/9603147].
- [43] M. Cvetič and F. Larsen, “Near horizon geometry of rotating black holes in five dimensions,” Nucl. Phys. B **531** (1998) 239 [arXiv:hep-th/9805097];
M. Cvetič and F. Larsen, “Statistical entropy of four-dimensional rotating black holes from near-horizon geometry,” Phys. Rev. Lett. **82** (1999) 484 [arXiv:hep-th/9805146].
- [44] For a review, see P. Kraus, “Lectures on black holes and the AdS(3)/CFT(2) correspondence,” arXiv:hep-th/0609074.
- [45] J. M. Bardeen and G. T. Horowitz, “The extreme Kerr throat geometry: A vacuum analog of AdS(2) x S(2),” Phys. Rev. D **60**, 104030 (1999) [arXiv:hep-th/9905099].
- [46] N. Itzhaki, “D6 + D0 and five dimensional spinning black hole,” JHEP **9809** (1998) 018 [arXiv:hep-th/9809063].
- [47] A. Strominger and C. Vafa, “Microscopic Origin of the Bekenstein-Hawking Entropy,” Phys. Lett. B **379** (1996) 99 [arXiv:hep-th/9601029].

- [48] G. T. Horowitz and A. Strominger, “Counting States of Near-Extremal Black Holes,” *Phys. Rev. Lett.* **77**, 2368 (1996) [arXiv:hep-th/9602051].
- [49] J. C. Breckenridge, D. A. Lowe, R. C. Myers, A. W. Peet, A. Strominger and C. Vafa, “Macroscopic and Microscopic Entropy of Near-Extremal Spinning Black Holes,” *Phys. Lett. B* **381** (1996) 423 [arXiv:hep-th/9603078].
- [50] G. T. Horowitz and M. M. Roberts, “Counting the Microstates of a Kerr Black Hole,” arXiv:0708.1346 [hep-th].
- [51] S. R. Das and S. D. Mathur, “Interactions involving D-branes,” *Nucl. Phys. B* **482** (1996) 153 [arXiv:hep-th/9607149].
- [52] J. M. Maldacena and A. Strominger, “Universal low-energy dynamics for rotating black holes,” *Phys. Rev. D* **56** (1997) 4975 [arXiv:hep-th/9702015].
- [53] S. D. Mathur, “Absorption of angular momentum by black holes and D-branes,” *Nucl. Phys. B* **514** (1998) 204 [arXiv:hep-th/9704156].
- [54] S. S. Gubser, “Can the effective string see higher partial waves?,” *Phys. Rev. D* **56** (1997) 4984 [arXiv:hep-th/9704195].
- [55] Ya.B. Zel’dovich, *Pis’ma Zh. Eksp. Teor. Fiz.* **14**, 270 (1971) [*JETP Lett.* **14**, 180 (1971)];
Ya.B. Zel’dovich, “Amplification of cylindrical electromagnetic waves reflected from a rotating body,” *Zh. Eksp. Teor. Fiz* **62**, 2076 (1972) [*Sov. Phys. JETP* **35**, 1085 (1972)].
- [56] C. W. Misner, “Interpretation of gravitational-wave observations,” *Phys. Rev. Lett.* **28**, 994 (1972).
- [57] J. D. Bekenstein, “Extraction of energy and charge from a black hole,” *Phys. Rev. D* **7** (1973) 949.
- [58] W. G. Unruh, “Second quantization in the Kerr metric,” *Phys. Rev. D* **10**, 3194 (1974);
“Absorption cross-section of small black holes,” *Phys. Rev. D* **14**, 3251 (1976).
- [59] V. Cardoso, O. J. C. Dias, J. P. S. Lemos and S. Yoshida, “The black hole bomb and super-radiant instabilities,” *Phys. Rev. D* **70** (2004) 044039 [Erratum-*ibid.* *D* **70** (2004) 049903] [arXiv:hep-th/0404096].
- [60] M. Cvetič and F. Larsen, “General rotating black holes in string theory: Greybody factors and event horizons,” *Phys. Rev. D* **56** (1997) 4994 [arXiv:hep-th/9705192].
- [61] S. S. Gubser, “Dynamics of D-brane black holes,” arXiv:hep-th/9908004.

- [62] J. R. David, G. Mandal and S. R. Wadia, “Microscopic formulation of black holes in string theory,” *Phys. Rept.* **369** (2002) 549 [arXiv:hep-th/0203048].
- [63] C. G. Callan and J. M. Maldacena, “D-brane Approach to Black Hole Quantum Mechanics,” *Nucl. Phys. B* **472** (1996) 591 [arXiv:hep-th/9602043].
- [64] J. C. Breckenridge, R. C. Myers, A. W. Peet and C. Vafa, “D-branes and spinning black holes,” *Phys. Lett. B* **391** (1997) 93 [arXiv:hep-th/9602065].
- [65] J.J. Blanco-Pillado, R. Emparan and A. Iglesias, “Fundamental Plasmid Strings and Black Rings,” arXiv:0712.0611 [hep-th].
- [66] V. Jejjala, O. Madden, S.F. Ross and G. Titchener, “Non-supersymmetric smooth geometries and D1-D5-P bound states,” *Phys. Rev. D* **71**, 1240030 (2005), hep-th/0504181.
- [67] V. Cardoso, O. J. C. Dias, J. L. Hovdebo and R. C. Myers, “Instability of non-supersymmetric smooth geometries,” *Phys. Rev. D* **73** (2006) 064031 [arXiv:hep-th/0512277].
- [68] B. D. Chowdhury and S. D. Mathur, “Radiation from the non-extremal fuzzball,” arXiv:0711.4817 [hep-th].
- [69] G. W. Gibbons, “Vacuum Polarization And The Spontaneous Loss Of Charge By Black Holes,” *Commun. Math. Phys.* **44** (1975) 245.
- [70] M. Cvetič and D. Youm, “General Rotating Five Dimensional Black Holes of Toroidally Compactified Heterotic String,” *Nucl. Phys. B* **476**, 118 (1996) [arXiv:hep-th/9603100];
D. Youm, “Black holes and solitons in string theory,” *Phys. Rept.* **316**, 1 (1999) [arXiv:hep-th/9710046].
- [71] S. Giusto, S. D. Mathur, and A. Saxena, “Dual geometries for a set of 3-charge microstates,” *Nucl. Phys. B* **701**, 357 (2004) [arXiv:hep-th/0405017].
- [72] E. Berti, V. Cardoso and M. Casals, “Eigenvalues and eigenfunctions of spin-weighted spheroidal harmonics in four and higher dimensions,” *Phys. Rev. D* **73** (2006) 024013 [Erratum-ibid. *D* **73** (2006) 109902] [arXiv:gr-qc/0511111].
- [73] V. Cardoso, O. J. C. Dias and R. C. Myers, “On the gravitational stability of D1-D5-P black holes,” *Phys. Rev. D* **76** (2007) 105015 [arXiv:0707.3406 [hep-th]].
- [74] M. Abramowitz and A. Stegun, *Handbook of mathematical functions*, (Dover Publications, New York, 1970).
- [75] C. G. Callan, S. S. Gubser, I. R. Klebanov and A. A. Tseytlin, “Absorption of fixed scalars and the D-brane approach to black holes,” *Nucl. Phys. B* **489** (1997) 65 [arXiv:hep-th/9610172].

- [76] V. Cardoso and J. P. S. Lemos, “New instability for rotating black branes and strings,” *Phys. Lett. B* **621** (2005) 219 [arXiv:hep-th/0412078].
- [77] O. J. C. Dias, “Superradiant instability of large radius doubly spinning black rings,” *Phys. Rev. D* **73** (2006) 124035 [arXiv:hep-th/0602064].
- [78] V. Balasubramanian, J. de Boer, E. Keski-Vakkuri, and S. F. Ross, “Supersymmetric conical defects: Towards a string theoretic description of black hole formation,” *Phys. Rev. D* **64**, 064011 (2001), [arXiv:hep-th/0011217].
J. M. Maldacena and L. Maoz, “De-singularization by rotation,” *JHEP* **12**, 055 (2002), hep-th/0012025.